Universidade do Porto
FEUP Faculdade de Engenharia

CATALYTIC GENERATION AND STORAGE OF HYDROGEN FROM HYDROLYSIS OF SODIUM-BOROHYDRIDE UNDER PRESSURE

APPLICATION IN A HYDROGEN/OXYGEN FUEL CELL

by

Maria Josefina Figueira Ferreira

A dissertation submitted to the Department of Chemical Engineering
and to the Department of Mechanical Engineering,
Faculty of Engineering from University of Porto, Portugal,
in conformity with the requirements for the degree of
Master in Fundamentals and Applications of Fluid Mechanics

This dissertation was supervised by
Dr. Alexandra Maria Pinheiro da Silva Ferreira Rodrigues Pinto,
CEFT, Department of Chemical Engineering,
Faculty of Engineering of the University of Porto, Portugal

November 2009

To my son,

Luís

To the memory of my dearly loved grandfather,

José da Silva

PREFACE

This dissertation on hydrogen generation from catalytic hydrolysis of sodium borohydride has grown out from the necessity of finishing my Master course in Fundamentals and Applications of Fluid Mechanics, started on the year 2003, at FEUP. After a gap of four years, in early September 2007, I had the privilege of speaking with Dr. Carlos T. Pinho, the Head of the Master course, who offered me the opportunity of working on EDEN's Project (http://www.h2eden.com) – Task PR07.33.01 – *Hydrogen generation via chemical hydrides*, on a 8.5 months scholarship, funded by the Agência de Inovação S.A. of Portugal. This was my first experience on the interesting field of *clean energies*! Dr. Alexandra Pinto, the scientific leader of Task PR07.33.01, with whom I've been working since 15 of October 2007, gently accepted my invitation to be the supervisor of this dissertation and I am deeply thankful for that.

Hydrogen generation and storage from chemical hydrides, specifically from sodium borohydride, to fuel hydrogen/oxygen fuel cells is a vast and rapidly evolving research field since the late 1990s. This dissertation does not provide an exhaustive review; my ambition was to write a text that describes one year and half of intensive experimental work and that shows my delight in understanding the catalysed hydrolysis reaction of sodium borohydride ($NaBH_4$), thus closing the *old* objective of finishing my Master course.

The start of this investigation turned out to be a hard work, because my previous experience on the subject was scarce; but I have been fortunate in having a supervisor who gave me all the support and freedom as the research evolved. Beginning with the aim of "producing and simultaneously storing molecular hydrogen due to solubility's effects in the remaining solution after $NaBH_4$ hydrolysis completion in a batch reactor" (see Pinto *et al.*, Int. J. Hydrogen Energy, 31 (2006) 1341-47), the work progresses following three main lines of kinetic experiments: *alkali*, *alkali free* and *less Polar Organic Polymeric Solutions* (*l*POPS) hydrolysis of sodium borohydride under pressure. Therefore, three main individual chapters where written, in which the experimental results are shown and

compared with published work. In this dissertation, most chapters start with a specific related literature review, and the need for a separate chapter of literature background in the mainly body text was not felt. In this sense, the information in each individual chapter can be understood without the need to read the precedents ones. It is my hope that the readers understand the lines beneath this dissertation and recognize the importance, which is particularly high in portable applications, of producing hydrogen via sodium borohydride hydrolysis, with the goal of feeding a polymer electrolyte membrane (PEM) fuel cell on demand.

At last, a final word for *Hydrogen*: being the simplest and the most abundant atom both on the Universe and in Earth and having the highest energy to weight ratio (12.24×10^4 kJ/kg) of all the energy sources known today, are not prime reasons to change energetic paradigm?

M. Josefina F. Ferreira

ABSTRACT

Ferreira, M.J.F., University of Porto, Faculty of Engineering, November 2009. *Catalytic generation and storage of hydrogen from hydrolysis of sodium borohydride solutions under pressure – application in a hydrogen/oxygen fuel cell*. Supervisor: Dr. Alexandra M.F.R. Pinto.

The present dissertation aimed at studying the catalytic generation and storage of hydrogen from hydrolysis of sodium borohydride solutions under pressure. The catalytic hydrolysis of sodium borohydride ($NaBH_4$) was studied under pressure, up to 2.6 MPa, using a reused ruthenium nickel based powered catalyst, in three batch reactors with internal volumes of 0.645, 0.369 and 0.228 *l*, made of stainless-steel and positioned vertically. Three different types of sodium borohydride hydrolysis were considered, two of them in the presence of an inhibitor (sodium hydroxide), namely, *alkali* hydrolysis and also *less Polar Organic Polymeric Solutions (lPOPS)*, and the other in absence of sodium hydroxide, designated by *alkali free* hydrolysis. The effects of temperature, sodium borohydride concentration, sodium hydroxide concentration, catalyst concentration and system pressure, on the hydrogen gas generation rate, were investigated. Particular importance was given to the effects of reactor bottom geometry on hydrogen generation yields, rates and induction times. Two different geometries were adopted for this purpose - a flat and a conical bottom shapes. The reactor with the conical shape significantly increases the reaction rates and decreases the lag time. Successive loadings of reactant solution with and without magnetic stirring were also presented to evaluate the capability of generating H_2 without recharging the reactor with fresh catalyst.

A detailed characterization of ruthenium nickel based catalyst after 200 reutilizations is presented in terms of textural properties and of morphology. The results reveal some deterioration of the catalyst which leads to slower rates and lower hydrogen yields, but with similar lag time values.

Analysis of reaction by-product by X-Ray Diffractometry revealed the presence of sodium metaborate in *alkali* hydrolysis and anhydrous borates in *lPOPS* hydrolysis. The formation of anhydrous borates is particularly important because it increases the gravimetric hydrogen storage density.

During the entire experimental studies, the hydrogen generated by the catalytic hydrolysis of sodium borohydride was used to fuel a PEM fuel cell available at the CEFT research Laboratory to evaluate the capabilities of an integrated solution/application.

RESUMO

Ferreira, M.J.F., Universidade do Porto, Faculdade de Engenharia, Novembro 2009. *Produção e contentorização de hidrogénio a partir da reacção de hidrólise catalizada de borohidreto de sódio sobre pressão – aplicação numa célula de combustível a hidrogénio/.oxigénio* Supervisora: Professora Doutora Alexandra M.F.R. Pinto.

O objectivo principal desta dissertação foi o estudo detalhado da produção e contentorização de hidrogénio a partir da reacção de hidrólise catalizada de borohidreto de sódio sobre pressão A hidrólise catalisada de borohidreto de sódio foi estudada sobre pressão, até 2.6 MPa, recorrendo a um catalisador em pó à base de níquel, impregnado com ruténio, não suportado, em três reactores de aço inox, com funcionamento por partidas e posicionamento vertical, com volumes internos 0.645, 0.369 and 0.228 *l*, respectivamente. Três tipos de hidrólise foram considerados – duas delas ocorrem na presença de um inibidor alcalino (hidróxido de sódio) e são designadas como hidrólise *alcalina* e como hidrólise de solução orgânica menos polar (*lPOPS)*; a terceira ocorre sem a presença deste inibidor e é designada por hidrólise sem hidróxido. Os efeitos da temperatura, concentração do borohidreto de sódio, concentração de hidróxido de sódio, concentração de catalizador e pressão do sistema, na taxa de geração de hidrogénio molecular foram investigados. Foi dada particular atenção aos efeitos da geometria do fundo do reactor no rendimento, taxa e tempo de indução reacional. Duas geometrias diferentes para o fundo do reactor foram selecionadas com este propósitio: uma plana e a outra cónica. Alimentações sucessivas de solução reagente com e sem agitação magnética foram usadas para avaliar a actividade do catalizador.

O catalizador de ruténio à base de níquel após 200 re-utilizações foi caracterizado em termos de textura e morfologia. Os resultados revelaram alguma deterioração do catalizador, traduzindo-se em taxas de produção de hidrogénio e rendimentos de reacção mais baixos, mantendo-se no entanto os tempos de indução.

A análise do produto da reação por difracção de raios X revelou a presença de metaborato de sódio na hidrólise *alcalina* e de boratos de sódio anidridos na hidrólise de solução orgânica menos polar (*lPOPS).*

O hidrogénio gerado por hidrólise catalítica de borohidreto de sódio foi usado para alimentar uma célula de combustível de membrana de permuta cateónica, disponível no laboratório do CEFT, para analisar a possibilidade de soluções/aplicações integradas.

ACKNOWLEDGEMENTS

I would like to acknowledge the friends and colleagues at Department of Chemical Engineering at FEUP for their help during this work. In particular, I would like to mention:

Dr. Alexandra M. P. S. F. R. Pinto for her supervision.
Dr. Carlos T. Pinho for the opportunity of introducing me to the very interesting theme of 'the clean energies, through the conception of 8.5 months scholarship (15Out07 to 30Jun08) of the EDEN's Project – INEGI Collaboration, financed by ADI of Portugal, under which a great part of this work was carried out.
Dr. Carmen Rangel, from INETI, for catalyst conception and supplying.
Dr. Luís Gales, from IBMC-ICBAS, for his active collaboration in performing the XRD analysis.
Dr. Carlos P. M. de Sá, from CEMUP, for working on XPS-SEM/EDS catalyst characterization, after 200 times of being reused.
Dr. João B. L. Moreira de Campos, for the payment of XPS-SEM/EDS analysis.
Dr. Manuel Fernando R. Pereira, from LCM-DEQ-FEUP, for working on N_2 adsorption isotherms (BET) catalyst characterization, after 200 times of being reused.
Eng. Luís Carlos Matos for helping with the data acquisition system.
Special thanks to members of CEFT-DEQ-FEUP for laboratory facilities.

I also would like to express my thankfulness to my husband, Pedro Ribeiro, for his constructive criticisms.

LIST OF CONTENTS

DEDICATION III

PREFACE V

ABSTRACT VII

RESUMO IX

ACKNOWLEDGEMENTS XI

LIST OF CONTENTS XIII

LIST OF FIGURES XVII

LIST OF TABLES XXI

NOMENCLATURE XXIII

1 INTRODUCTION 1

1.1 General introduction / 1

1.1.1 Hydrogen as energy carrier / 1

1.1.2 Chemical hydrides as H_2 carrier: the particular case of $NaBH_4$ / 4

1.2 Hydrogen/oxygen fuel cell / 7

1.2.1 Polymer Electrolyte Membrane Fuel Cell (PEMFC) / 8

1.2.2 The "MicroBoro Bus" – a didactic demonstration prototype / 10

1.3 Objectives and organization of the dissertation / 11

1.4 Conclusions / 13

1.5 References / 13

2 EXPERIMENTAL TECHNIQUES AND APPARATUS 15

2.1 Introduction / 15

2.2 Materials / 15

2.2.1 Sodium borohydride / 15

2.2.2 Nickel based bimetallic catalyst / 16

2.3 Apparatus for kinetic studies / 19

2.3.1 Reactor design / 19

2.3.2 Experimental rig / 21

2.4 General plan for sodium borohydride hydrolysis experiments / 22

2.4.1 *Alkali* hydrolysis / 22

2.4.1.1 Successive loadings of reactant solution / 23

2.4.2 *Alkali free* hydrolysis / 23

2.4.3 *Less Polar Organic Polymeric Solutions (lPOPS)* hydrolysis / 24

2.5 Reaction products analysis / 25

2.5.1 Molecular hydrogen / 25

2.5.2 Sodium borates by-products / 25

2.6 Conclusions / 26

2.7 References / 26

3 ALKALI HYDROLYSIS **27**
Results for sodium borohydride kinetic experiments
3.1 Introduction / 27
3.2 Experimental procedure / 32
3.2.1 Effect of reactor temperature on hydrogen generation rate / 32
3.2.2 Effect of $NaBH_4$ concentration on hydrogen generation rate / 33
3.2.3 Effect of NaOH concentration on hydrogen generation rate / 33
3.2.4 Effect of pressure on hydrogen generation rate / 33
3.2.5 Effect of reactor bottom shape on hydrogen generation rate / 34
3.2.6 Effect of successive loadings on catalyst activity/ 34
3.2.6.1 Effect of agitation on hydrogen reaction rate / 35
3.3 Results and discussion / 35
3.3.1 Effect of reactor temperature on hydrogen generation rate / 35
3.3.2 Effect of $NaBH_4$ concentration on hydrogen generation rate / 36
3.3.3 Effect of NaOH concentration on hydrogen generation rate / 37
3.3.4 Effect of pressure on hydrogen generation rate / 37
3.3.5 Effect of reactor bottom shape on hydrogen generation rate / 38
3.3.6 Effect of successive loadings on catalyst activity / 39
3.3.6.1 Effect of agitation on hydrogen reaction rate / 42
3.4 Reaction by-product characterization / 43
3.4.1 Materials and methods / 43
3.4.2 Results and discussion / 43
3.5 Conclusions / 44
3.6 References / 45

4 ALKALI FREE HYDROLYSIS **49**
Results for sodium borohydride kinetic experiments
4.1 Introduction / 49
4.2 Experimental procedure / 51
4.3 Results and discussion / 52
4.3.1 Effect of $H_2O/NaBH_4$ (mol/mol) on H_2 generation yield / 53
4.3.2 Effect of catalyst/$NaBH_4$ (g/g) on H_2 generation rate / 56
4.3.3 Effect of pressure on hydrogen generation yield and rate / 56
4.3.4 Effect of reactor bottom shape on hydrogen generation / 58
4.3.5 Effect of temperature on hydrogen generation rate / 60
4.3.6 Gravimetric and volumetric densities / 61
4.4 Reaction by-product characterization / 63
4.4.1 Materials and methods / 63
4.4.2 Results and discussion / 64
4.5 Conclusions / 64
4.6 References / 65

5 *less* POLAR ORGANIC POLYMERIC SOLUTIONS HYDROLYSIS **67**
Results for sodium borohydride kinetic experiments
5.1 Introduction / 67
5.2 Experimental procedure / 69
5.3 Results and discussion / 69
5.4 Reaction by-product characterization / 72
5.5 Conclusions / 75
5.6 References / 76

6 NICKEL BASED BIMETALLIC CATALYST CHARACTERIZATION **77**
Results after 200 reutilizations
6.1 Introduction / 77
6.2 Catalyst characterization / 78
6.2.1 Textural properties / 78
6.2.2 Morphology / 81
6.2.3 XPS analysis / 84
6.3 Catalyst activity analysis after 200 reutilizations / 88
6.4 Conclusions / 89
6.5 References / 90

7 CONCLUSION **93**
7.1 Conclusions / 93
7.2 Suggestions for future work / 96

LIST OF FIGURES

CHAPTER 1

Figure 1.1. Volumetric and gravimetric capacities for several possible H_2 storage technologies. [1.3] / 3

Figure 1.2. Status of hydrogen storage technologies. Capacities for both materials-only basis and total system are shown [1.9]. / 5

Figure 1.3. The first fuel cell, by William Grove (1839). / 7

Figure 1.4. (A) Schematic of a typical H_2/O_2 PEMFC [1.13]. (B) Nafion® Polymer Electrolyte Membrane Structure and Characteristics. / 9

Figure 1.5. Front view and top view of the "MicroBoro Bus" (A – connection to the H_2 generator and storage tank; B- gas-washing bottle; C- PEMFC single cell). / 10

CHAPTER 2

Figure 2.1. Photograph of the nickel based bimetallic catalyst in the form of a finely divided black powder. / 16

Figure 2.2. Photo Scanning electron microscope view of the synthesized catalyst powder (a) and associated elemental analysis EDAX (b). / 17

Figure 2.3. Nitrogen adsorption/desorption isotherms. / 18

Figure 2.4. Photograph of the main batch reactor with the two separate filling pieces used to change the internal free volume for $NaBH_4$ hydrolysis reactions. / 19

Figure 2.5. Schematic view of the reactors inside: reactor LG – flat bottom, and reactors MR and SR – conical bottom, with mention of the internal available free volume. / 20

Figure 2.6. Global picture of the experimental setup used for the kinetics studies of hydrogen production via catalytic hydrolysis of sodium borohydride, under pressure. (1) batch reactor; (2a-2b) data acquisition system; (3) "MicroBoro bus" with a PEM fuel cell; (4) thermostatic bath and (5) refrigeration unit. / 21

Figure 2.7. Survey picture of the: (a) main reaction vessel / LR; (b) accessories fixed on the outside lid of the reactor: 1- reactor inlet bore valve, 2- syringe, 3- pressure probe, 4- Bourdon manometer and 5- reactor exhaustion needle valve; (c) ascendant view of the inside lid of the reactor: 1- needle of the syringe, 2- "T.Bottom" k thermocouple and 3- "T.Top" k thermocouple; (d) top view of the inside lid of the reactor showing the left 'holes' after connecting the some accessories; (e) syringe with needle (150 mm length). / 22

CHAPTER 3

Figure 3.1. Hydrogen generation plot with a $NaBH_4$ concentration of 10%, an inhibitor concentration of 3%, at different temperatures. The reactions, for 20 cm^3 of reactant solution, were performed in the MR batch reactor (369 cm^3) with a proportion of Ru-Ni based catalyst/$NaBH_4$: 0.4 g/g. / 35

Figure 3.2. Hydrogen generation plot with an inhibitor concentration of 3%, at 27 ºC, and with different $NaBH_4$ concentrations. The reactions where performed in LR batch reactor (646 cm^3) with a proportion of Ru-Ni based catalyst/$NaBH_4$: 0.4 g/g. / 36

Figure 3.3. Hydrogen generation with a $NaBH_4$ concentration of 10%, at 25 ºC, with different NaOH concentrations. The reactions, for 10 cm^3 of reactant solution, were performed in LR batch reactor (646 cm^3) with a proportion of Ru-Ni based catalyst/$NaBH_4$: 0.4 g/g. / 37

Figure 3.4. Hydrogen generation with a $NaBH_4$ concentration of 10 wt%, an inhibitor concentration of 7wt%, at 45 ºC, for the three design reactors: LR (646 cm^3), MR (369 cm^3) and SR (229 cm^3). The reactions, for 20 cm^3 of reactant solution, were performed with a proportion of Ru-Ni based catalyst/$NaBH_4$: 0.4 g/g. / 38

Figure 3.5. Hydrogen generation plots with a $NaBH_4$ concentration of 10%, an inhibitor concentration of 7%, at ≈ 26 ºC, for two batch reactors with different bottom shape. The reactions, for 10 cm^3 of reactant solution, were performed with a proportion of Ru-Ni based catalyst/$NaBH_4$: 0.4 g/g. / 38

Figure 3.6. Five successive loadings of the reactant solution: 10 wt.% $NaBH_4$, 7 wt.% NaOH, 83 wt.% H_2O, with Ni-based/$NaBH_4$: 0.4g/g, performed in the batch reactor LR (646 cm^3), showing the temperature profile inside the reactor at two specific points (bottom and top of reactor). / 39

Figure 3.7. Hydrogen generation in batch reactor LR (646 cm^3) of five successive loadings of the reactant solution: 10 wt.% $NaBH_4$, 7 wt.% NaOH, 83 wt.% H_2O, with Ru-Ni based catalyst/$NaBH_4$: 0.4g/g. / 40

Figure 3.8. Hydrogen generation in batch reactor MR (369 cm^3) of seven successive loadings of the reactant solution: 10 wt.% $NaBH_4$, 7 wt.% NaOH, 83 wt.% H_2O, with Ru-Ni based catalyst/$NaBH_4$: 0.4g/g. / 41

Figure 3.9. Two images of reaction "gaseous" by-product, after seven successive loadings of reactant solution (10 wt.% $NaBH_4$, 7 wt.% NaOH, 83 wt.% H_2O). The H_2 release shows the gas capability to agitate the nickel-based powdered catalyst presented at the reactor liquid phase. / 41

Figure 3.10. Hydrogen generation in batch reactor LR (646 cm^3) of eight successive loadings of the reactant solution: 10 wt.% $NaBH_4$, 7 wt.% NaOH, 83 wt.% H_2O, with Ru-Ni based catalyst/$NaBH_4$: 0.4g/g (the 8^{th} loading was performed with magnetic stirring). / 42

Figure 3.11. Crystals pictures of the by-product *classic* hydrolysis of sodium borohydride, obtained by slow evaporation of a water solution at room temperature (≈ 25 ºC). / 43

Figure 3.12. Views of crystal structure of sodium metaborate dehydrate showing stacking layers formed by BO_3 triangles and by Na and water molecules: (a) view along the *a*-axis and (b) view along the *c*-axis. Na in violet, O in red, B in pink and H in white. / 44

CHAPTER 4

Figure 4.1. Pictures showing the preparation of the reactant blend (catalyst plus $NaBH_4$, both solids) to use in *alkali free* hydrolysis experiments. From left to right: Ru-Ni based catalyst, anhydrous sodium borohydride and the bottom of MR reactor with the mixture (stored in bottom conical shape). / 52

Figure 4.2. Hydrogen generation in the flat bottom batch reactor LR (646 cm^3) for experiments with Ru – Ni based catalyst/$NaBH_4$: 0.4 g/g and H_2O/$NaBH_4$: 2-8 mol/mol. / 53

Figure 4.3. Hydrogen generation in the batch reactor LR (646 cm^3) with Ni-based/$NaBH_4$: 0.4 g/g (27 and 28 times reused) and H_2O/$NaBH_4$: 2 mol/mol, after two successive loadings of pure water (of the same molar quantity). / 55

Figure 4.4. Hydrogen yield as a function of added water, H_2O/$NaBH_4$ (mol/mol), in batch reactor LG (646 cm^3). / 55

Figure 4.5. Influence of the amount of catalyst/$NaBH_4$ (g/g) on hydrogen generation. / 56

Figure 4.6. Hydrogen generation in the studied three batch reactors - LR (646 cm^3), MR (369 cm^3) and SR (229 cm^3), with Ni-Ru based catalyst/$NaBH_4$: 0.4 g/g (111, 150 and 151 times reused, respectively for LR, MR and SR) and H_2O/$NaBH_4$: 4 mol/mol. / 57

Figure 4.7. Influence of pressure on H_2 yield (Experiments done in three batch reactors at the temperature range of 289-295 K, with catalyst reused ≈150 times). / 57

Figure 4.8. Influence of reactor bottom shape on H_2 yield, rate and lag time (experiments performed in batch reactors LR (646 cm^3) and MR (369 cm^3), with flat and conical bottom shapes, respectively; at temperature range of 289-295 K, with catalyst reused ≈150 times). / 58

Figure 4.9. Photographs of MR reactor (with conical bottom shape) after an *alkali free* hydrolysis of $NaBH_4$ experiment. In the right, a view of the solid mixture of the by-product plus the catalyst. / 59

Figure 4.10. Temperature of the hydrolyzed $NaBH_4$ as a function of time by different pressures. / 60

Figure 4.11. Influence of temperature on hydrogen generation rate and yield. / 61

Figure 4.12. View along the *c*-axis of the crystal structure of sodium metaborate hydrate: (a) $4H_2O$, in MR at 0.69 MPa and (b) $2H_2O$, in SR at 1.26 MPa. The element color code, from black to light grey, is B, O, Na and H. / 64

CHAPTER 5

Figure 5.1 Hydrogen generation by a single loading of 20 cm^3 of reactant solution, at 45 ºC, with Ni-Ru based catalyst/$NaBH_4$: 0.4 g/g: (a) MR batch reactor [0.369 L] and (b) SR batch reactor [0.229 L]. / 70

Figure 5.2. View along the *a*-axis of the crystal structure of sodium borate anhydrous, showing the BO_4 tetrahedral arrangement and the Na bound network. Na in violet, O in red and B in pink. / 73

Figure 5.3. View along the *a*-axis of the crystal structure of sodium borate anhydrous, showing the BO_3 triangular and the BO_4 tetrahedral arrangements sharing oxygen atoms and the Na bound network. Na in violet, O in red and B in pink. / 73

Figure 5.4. Gravimetric H_2 storage density (reactants basis) for the three systems studied in this chapter. / 75

CHAPTER 6

Figure 6.1. Nitrogen isotherms of powder Ru-Ni based catalyst 200 times reused. / 80

Figure 6.2. Pore size distributions of powder Ru-Ni based catalyst 200 times reused. / 80

Figure 6.3. SEM micrographs of powder Ru-Ni based catalyst, 200 times reused. Magnifications between 200 and 100 000X, increasing from (a) to (e). / 82

Figure 6.4. SEM image coupled with EDS spectrum of Ru-Ni based catalyst 200 times reused and a magnification of 200X. / 83

Figure 6.5. SEM image coupled with EDS spectrum of Ru-Ni based catalyst 200 times reused and a magnification of 1500X. / 84

Figure 6.6. SEM image coupled with EDS spectrum, at three different selected areas, of Ru-Ni based catalyst 200 times reused and a magnification of 10 000X. / 85

Figure 6.7. Photograph of Ru-Ni based catalyst 200 times reused pellet, with 10 mm in diameter, for use in XPS analysis. / 86

Figure 6.8. A survey XPS spectrum of Ru-Ni based catalyst 200 times reused. / 86

Figure 6.9. XPS spectra for Ru-Ni based powdered catalyst 200 times reused. / 87

Figure 6.10. Hydrogen generation plots with a $NaBH_4$ concentration of 10%, an inhibitor concentration of 7%, for two different stages of catalyst reutilization (28 times reused and 200 times reused). The reactions, for 10 cm^3 of reactant solution, were performed in LR batch reactor (646 cm^3) with a proportion of Ru-Ni based catalyst/$NaBH_4$: 0.4 g/g, at room temperature of ≈ 25 ºC. / 89

LIST OF TABLES

CHAPTER 1

Table 1.1 – Combustion enthalpies for some common fuels [1.2]. / 2

Table 1.2 – FreedomCar requirements stated by the US DOE [1.4]. / 6

CHAPTER 2

Table 2.1 – Textural properties of catalyst powder used in this work before use. / 18

CHAPTER 3

Table 3.1 – Excess hydration factor, *x*, of aqueous solutions of sodium borohydride. / 28

Table 3.2 – Comparison of gravimetric efficiencies of various reactant preparations. / 29

CHAPTER 4

Table 4.1 - The FreedomCAR targets publish by US Department Of Energy (DOE). / 62

Table 4.2 - Influence of Ni-Ru based catalyst/$NaBH_4$ on gravimetric hydrogen density and hydrogen yield for $H_2O/NaBH_4$: 4 mol/mol. Prediction of the volumetric hydrogen density*. / 63

CHAPTER 5

Table 5.1 – Hydrogen yield for the studied reactant solutions in the two batch reactors and prevision of respective H_2 solubility effects, at 45 ºC. / 71

Table 5.2 – Values of conductivity and pH of the studied reactant solutions, before and after reaction completion. / 72

CHAPTER 6

Table 6.1 - Textural properties of powder Ni-Ru based catalyst 200 times reused sample. / 80

Table 6.2 - Specific conditions for XPS analysis of Ni-Ru based catalyst 200 times reused. / 86

Table 6.3 - Results of XPS analysis of Ni-Ru based catalyst 200 times reused. / 88

Table 6.4 - Results for yield, lag time and dP/dt slope in hydrogen generation of 10 mL of 10wt% $NaBH_4$ and 7wt% NaOH solution, at two different stages of Ni-Ru based catalyst reutilization (for 28 and 200 times reused), in batch reactor LR (646 cm^3). / 89

NOMENCLATURE

yield, yield = $n(H_2)_{exp} / n(H_2)_{theoretical}$ (n= number of moles)

x , excess hydration factor

V_{μ} , micropore volume by t-method;

V_p , total pore volume, for P/P_0=0.986.

V , molar volume of the liquid

$t_{1/2}$, the half-life time, min

T , absolute temperature, K

S_{ext} , (mesopore + macropore) surface areas by t-method;

S_{BET} ,BET surface area;

r , the pore radius

P / P_0 , relative pressure

Greek letters

ϕ, contact angle

γ , its surface tension

CHAPTER 1

Introduction

In this introductory chapter the topic and main objectives of this dissertation, entitled "Catalytic generation and storage of hydrogen from hydrolysis of sodium borohydride solutions under pressure – application in a hydrogen/oxygen fuel cell" are presented. A general introduction to hydrogen gas as an energy carrier, to sodium borohydride as hydrogen carrier and to polymer electrolyte membrane fuel cells is carried out.

1.1 GENERAL INTRODUCTION

This dissertation investigates a potential improvement to hydrogen (H_2) generation and simultaneous storage, by catalytic hydrolysis of sodium borohydride ($NaBH_4$) under pressure, for supply fuel cells of the type PEM – Polymer Electrolyte Membrane.

Due to the accelerate decrease of fossil fuels resources and the continuous growing of energy demand, the development of alternative and clean renewable energy carriers is of the utmost importance. In fact, the world may be even closer to running out of oil than usually admitted [1.1].

The transportation sector and other portable applications are areas where an alternative energy source may have a particularly great impact. Thus, employment of a concentrated energy (electricity) carrier is of vital interest and priority. In this context, hydrogen (H_2) is presented as an environmental friendly energy vector, since it may serve as an intermediate through which a primary energy source (for example, solar) can be effectively transmitted and consumed.

1.1.1 Hydrogen as energy carrier

The hydrogen is the simplest and the most abundant atom both on the Universe and in Earth. The supreme important characteristic of hydrogen gas, the lightest and smallest molecule on our planet, is the fact that it has the highest energy to weight ratio, or

gravimetric energy density, of the energy sources known today. Table 1.1, shows the combustion enthalpies for some of the most common used fuels [1.2].

Table 1.1 – Combustion enthalpies for some common fuels [1.2].

fuel	*reaction*	*energy/mole*	*energy/kg*
Ethanol	$C_2H_5OH + 3O_2 \rightarrow 2CO_2 + 3H_2O$	1367 kJ	2.97×10^4 kJ
Coal	$C + O_2 \rightarrow CO_2$	393 kJ	3.27×10^4 kJ
Petroleum	$2C_8H_{18} + 25O_2 \rightarrow 16CO_2 + 18H_2O$	5452 kJ	4.47×10^4 kJ
Natural gas	$CH_4 + 2O_2 \rightarrow CO_2 + 2H_2O$	883 kJ	5.50×10^4 kJ
Hydrogen	$2H_5 + O_2 \rightarrow 2H_2O$	247 kJ	12.24×10^4 kJ

These enthalpic values reflect ideal (100%) combustion at 25 ºC.
* Octane is only one of the many hydrocarbons in petroleum.
º Methane is the primary constituent (>90%) of natural gas.

As can be seen from the previous table, H_2 gravimetric storage density is the highest, 12.24×10^4 kJ, almost three times more than the average value of the others presented fuels. Additionally, hydrogen as a fuel offers a number of attractive advantages, namely [1.2]:

i) minimal pollution characteristics;

ii) mass transportability comparable to that of petroleum;

iii) combustibility in internal combustion engines (Carnot cycle devices);

iv) feasibility of electrochemical combination with an oxidant in fuel cells (free energy type devices).

Unfortunately, large quantities of molecular hydrogen do not exist in a readily usable form, so it must be synthesized from other energy sources, and then used to transfer energy to another use. For this intrinsic fact, clean and efficient hydrogen production and storage methods still remain a great challenge.

Although the viability of hydrogen combustion, as illustrated in Table 1.1, fuel cells utilization of H_2 is potentially even more attractive. In truth, hydrogen can be used directly in a PEMFC to generate electricity, producing water as a by-product. Since a PEMFC operates at lower temperature and offers a higher power density than most fuel cells, it has been widely accepted for use with automobiles and other portable applications. Additionally, fuel cells are noiseless and have no moving parts. However, PEM fuel cell is not free from problems mostly because it requires pure hydrogen. In Section 1.2, below, a more detailed explanation of PEMFC is provided.

A system for production and distribution of H_2 will most certainly be dependent on the type of hydrogen storage used. Indeed, hydrogen has a very low volumetric energy density, so it is very difficult to store a sufficient amount of hydrogen in a small and light enough

vessel. In fact, the challenge of hydrogen storage has proved to be the greatest obstacle preventing hydrogen from replacing fossil fuels. Hence, a safe, efficient and economical method of storing hydrogen must be available to implement a hydrogen economy based on renewable resources.

There are presently four main approaches to store and deliver pure H_2 gas at the point of use: compressed gas, cryogenic liquid, reversible sorption/desorption, and chemical storage. Each one of these technologies has practical challenges associated with its use. Gravimetric and volumetric capacities of the storage system are the two primary screening criteria. The gravimetric capacity or specific energy is a measure of the usable energy per kilogram of system mass. In practical terms, this quantity is usually expressed as a weight percentage of hydrogen. Volumetric capacity or energy density is the useful energy per litre of system volume. Hydrogen poses unique storage challenges, because it is the lightest and least dense gas, with only 8.98×10^{-5} kg/L at STP conditions. The current gravimetric and volumetric efficiencies for the four pure hydrogen storage technologies are compared in Figure 1.1 [1.3]. FreedomCAR targets published by US Department Of Energy (DOE) [1.4] for automotive hydrogen storage systems in 2010 and 2015, are also shown.

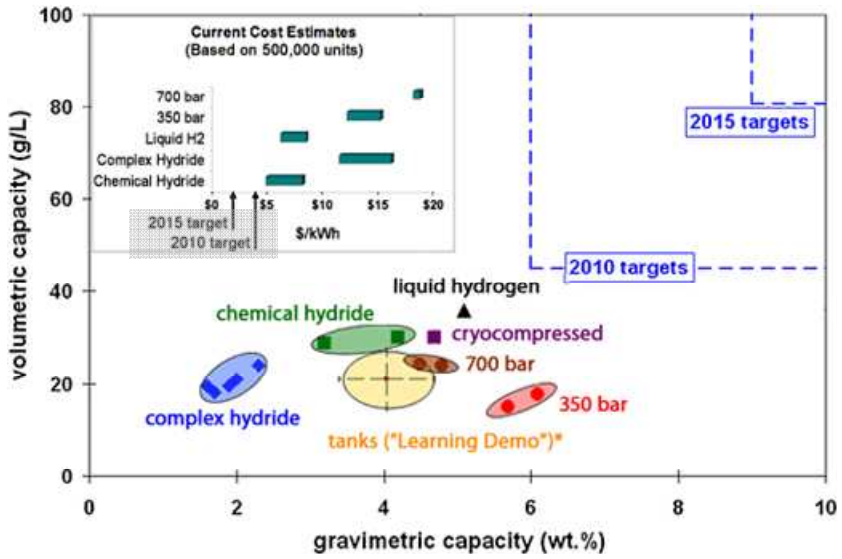

Figure 1.1. Volumetric and gravimetric capacities for several possible H_2 storage technologies. [1.3]

Regarding to the information depicted in Fig.1.1, an alternative to a fossil fuel or metal complex alloy (low H_2 density) based hydrogen delivery system, can be offered by inorganic hydride salts – chemical hydrides, and may be utilized as a primary hydrogen storage medium.

1.1.2 Chemical hydrides as hydrogen carrier: the particular case of $NaBH_4$

Chemical hydrides are materials that produce hydrogen *on demand* through a chemical reaction with water; and generally, they exhibit greater gravimetric energy densities and are stable during long periods of storage without usage. Among the chemical hydrides, sodium borohydride ($NaBH_4$) is an example of a chemical hydride that has the advantage of storing hydrogen in a stable and safe solution. Its hydrogen content is of 10.6 wt%, what makes itself one of the highest hydrogen containing compounds.

Sodium borohydride reacts with water to generate molecular hydrogen according to the hydrolysis reaction shown in equation (1.1):

$$NaBH_4 + (2+x)\ H_2O \rightarrow NaBO_2.xH_2O + 4\ H_2 + \text{heat.} \qquad (1.1)$$

The standard state enthalpy change of the above reaction at 25 ºC is -217 kJ and is therefore exothermic [1.5]. Unluckily, the rate of hydrogen release during the hydrolysis reaction is low due to the increase of the solution pH as the basic metaborate ($NaBO_2$) by-product is formed. Schlesinger *et al.* [1.5] recognized the particular striking catalytic effect of certain transition metals and their salts on sodium borohydride hydrolysis rate. Regarding to equation (1.1), ideal hydrolysis is attained for $x = 0$ [1.5], but in practice excess of water is required accounting for the fact that the solid by-product ($NaBO_2.xH_2O$) can exist with varying degrees of hydration [1.6]. Lyttle *et al.* [1.7] observed that commercial borohydride deteriorates rapidly in aqueous solution, but is fairly stable in basic solutions and furthermore the higher the pH the greater the stability. This finding turned the solution pH as the limiting parameter of reaction (1.1) and forced researchers to find a practical and controlled way of producing hydrogen by using catalysts or small amounts of acid. Hence, heterogeneous catalysis offers a number of advantages: independence of solution pH over a wide range, controllable hydrolysis rate and the reuse of the catalyst.

In fact, hydrogen storage density of sodium borohydride can be calculated in several ways, depending on the compound on which the weight density of hydrogen is based on. For instance, the hydrogen storage capacity of sodium borohydride is 10.92 wt% by weight and can be calculated by dividing the molar mass of hydrogen produced by the total molar mass of $NaBH_4$ plus the molar mass of the stoichiometric amount of water needed for reaction (ideal hydrolysis, $x = 0$). As mentioned before, a PEMFC produces water as a by-product. If this water is recycled to produce hydrogen from $NaBH_4$, the storage capacity

increases to 21.3 wt% [1.8]. However, one important factor to regard is that the by-product of the chemical reaction (1.1) is still carried on-board. Hence, it must be included in the storage density calculations. If so, the H_2 storage density drops from 21.3 wt% to 12.2 wt%. As previously stated, the solid by-product, $NaBO_2$, can exist with varying degrees of hydration ($NaBO_2.xH_2O$), such as the tetrahydrate metaborate, $NaBO_2.4H_2O$. In this case, the hydrogen storage density decreases to a level ≈ 4 wt%.

The US Department Of Energy (DOE) has published FreedomCAR requirements for automotive hydrogen storage systems [1.4], probably the most stringent targets yet articulated for hydrogen storage systems. These specifications are based on system mass and volume, i.e., not only the storage material itself (materials-only basis) but also the reactors, tanks, valves, and all supplementary equipment, which usually are call *hardware*.

In Figure 1.2, below, emphasis is given to chemical hydrides as materials with effective high H_2 storage capacities. The position of the several chemical hydrides shown in that plot is calculated for materials-only basis.

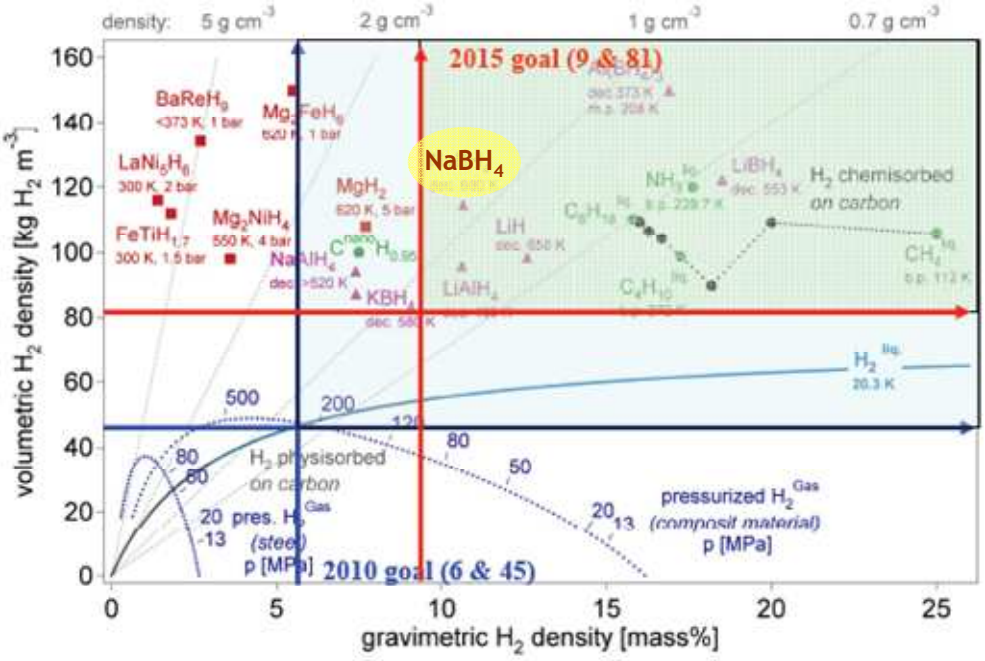

Figure 1.2. Status of hydrogen storage technologies. Capacities for both materials-only basis and total system are shown [1.9].

As illustrate in the previous figure, chemical bonding of hydrogen is the only available storage technique that can produce energy densities approaching to the FreedomCAR targets. The potential of sodium borohydride system to meet these targets on a reactant-

only basis is highlighted and can be evaluated using the stoichiometry of equation (1.1). As stated before, for the case of *ideal* hydrolysis (x = 0), the hydrogen storage capacity is 10.92 wt% or 0.1092 kg H_2/kg reactants. Therefore, the hydrolysis of $NaBH_4$ has the potential to meet FreedomCar 2015 requirements (0.09 kg H_2/kg system) for specific energy if x is close to zero.

The mass that can be allocated for the *hardware* components can be estimate from the FreedomCar targets and the calculated reactant-only specific energy. To compute the mass that can be allocated for hardware, the FreedomCar 2015 target is compared to the maximum theoretical specific energy, as shown below [1.6]:

$$\frac{0.1092\ \text{kg H}_2}{1\ \text{kg reactants} + \text{y kg hardware}} = \frac{0.09\ \text{kg H}_2}{1\ \text{kg system}} \Leftrightarrow \text{y} = \frac{0.2\ \text{kg hardware}}{\text{kg reactants}}. \qquad (1.2)$$

As shown in (1.2), for $NaBH_4$ with x=0, the allowable hardware mass is 0.2 kg of reactor per kg of reactants, or 17% of the total system mass. As x increases, the allowable component mass decreases until, at a value of x= 0.84, it is no longer possible to meet the FreedomCar 2015 requirements. Hence, for an excess hydration of 2 the allowable reactor mass is negative. This means that is not possible to design a reactor that meets the FreedomCAR 2015 target if x=2. Table 1.2 shows the FreedomCar requirements for specific energy density for the years 2010 and 2015, along with the allowable excess hydration factor based on sodium borohydride hydrolysis [1.6]. Similar calculations can be done for the other FreedomCar targets.

Table 1.2 – FreedomCar requirements stated by the US DOE [1.4].

Year	*2010*	*2015*
Usable specific energy from hydrogen		
Target (kWh/kg system)	2.0	3.0
Target (kg H_2/kg system)	**0.06**	**0.09**
Usable energy density from hydrogen		
Target (kWh/L system)	1.5	2.7
Target (kg H_2/m^3 system)	**45**	**81**
Allowable excess hydration factor based on $NaBH_4$ hydrolysis		
x (reactants basis)	3.31	0.84
Allowed reactor mass ratio (reactor mass/mass of reactants)		
x = 0	0.807	0.204
x = 2	0.214	-0.190

We may conclude if *x*= 2 or even 4 the materials-only storage capacity is still promising for some other niche of applications [1.10]. But, in practice to date the best systems require that the $NaBH_4$ be pre-dissolved in a large excess of water; the excess water and the mass of the system equipment, significantly reduce the storage efficiency. However it is of great interest to determine the amount of structural water that remains bound to the metaborate product, for example, by X-Ray Diffractometry.

1.2 HYDROGEN/OXIGEN FUEL CELL

Fuel cells are not a new invention. In fact, the first recorded fuel cell utilized carbon and nitric acid as fuel and was constructed in 1801 by Sir Humphrey Davy. The accreditation for the invention of the fuel cell, however, is awarded to William Grove, who in 1839 used hydrogen and oxygen to produce electricity. Grove discovered that by arranging two platinum electrodes with one end of each immersed in a container of sulphuric acid and the other ends separately sealed in containers of oxygen and hydrogen, a constant current would flow between the electrodes. The sealed containers held water as well as the gases, and he noted that the water level rose in both tubes as the current flowed. Grove realized that combining several sets of these electrodes in a series circuit he might "effect the decomposition of water by means of its composition". Then after, he gave the name of a 'gas battery' – the first fuel cell (see Figure 1.3) [1.11].

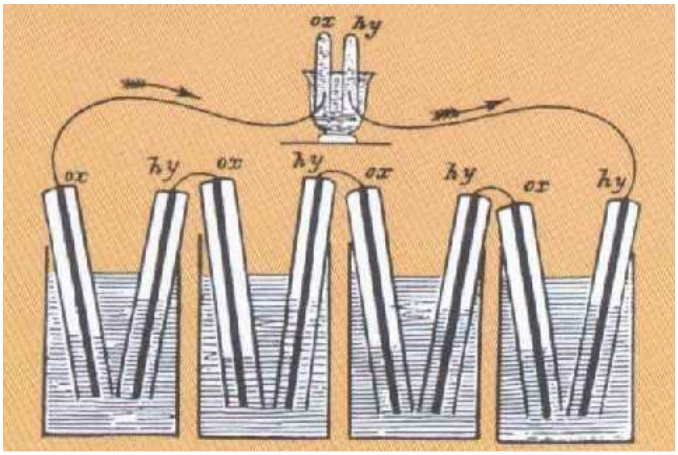

Figure 1.3. The first fuel cell, by William Grove (1839).

The fuel cell invented by Grove stimulated research in nineteen century, but no practical applications was developed. In twentieth century, during World War II, the british scientist

Francis Bacon designed the first alkaline fuel cell. In the 1960s, NASA showed some of the potential applications for fuel cells by using them to provide power on space missions.

Currently, five types of fuel cells are receiving attention for energy production in stationary or transportation applications. These are Alkaline Fuel Cells (AFC), Molten Carbonate Fuel Cells (MCFC), Phosphoric Acid Fuel Cells (PAFC), Solid Oxide Fuel Cells (SOFC), and Polymer Electrolyte Membrane Fuel Cells (PEMFC). All of these fuel cell types have been demonstrated as stationary power plants with the advantage of providing high quality on-site electrical power. The last decade has focused primarily on using PEMFC's for transportation purposes. Fuel cells also have the benefit of producing constant amounts of electrical energy.

Hydrogen is the ideal fuel for fuel cells. In all types of fuel cells mention in the above paragraph, hydrogen exhibits fast reaction kinetics and the only by product of the reaction when oxygen is used as the oxidant is water.

1.2.1 Polymer Electrolyte Membrane Fuel Cell (PEMFC)

Polymer Electrolyte Membrane Fuel Cells (PEMFCs) have been the focus of a great deal of research in the last few years due to the increasing demand for clean power that can be supplied from a lightweight system. PEMFCs fall into this category due to their membrane electrode assemblies (MEA). The MEA is sandwich composed of three different layers. The first layer is the catalyst material, which consists of platinum particles (Pt) loaded into a carbon cloth support. The next layer is the PEM. Although there are a few different types of PEM materials, the industry standard is a copolymer of tetrafluoroethylene and perfluoro[2-(fluorosulfonylethoxy)propylviny] ether. This material has a trade name, Nafion®, and is made by DuPont [1.12]. The third layer is another Pt loaded catalyst layer usually of the same composition as the first catalyst layer, depending on the fuel types. The typical MEA is roughly 0.02'' thick, and has negligible weight. Since the cell operates at temperatures below 100 ºC, the shell of the fuel cell can be made out of lightweight plastics. These characteristics make the PEMFC ideal for transportation power applications. Figure 1.4 shows a typical PEMFC [1.13] and the chemical structure for Nafion® Polymer Electrolyte Membrane Structure from DuPont.

The circled portion within Figure 1.2 shows the MEA.

The Polymer Electrolyte Membrane (PEM) is responsible for transporting the hydrogen ion produced through catalysis at the anode to the cathode, where it recombines with

oxygen ions and electrons to form water. The transport of the hydrogen ion, a proton, is made possible by the structure of Nafion®.

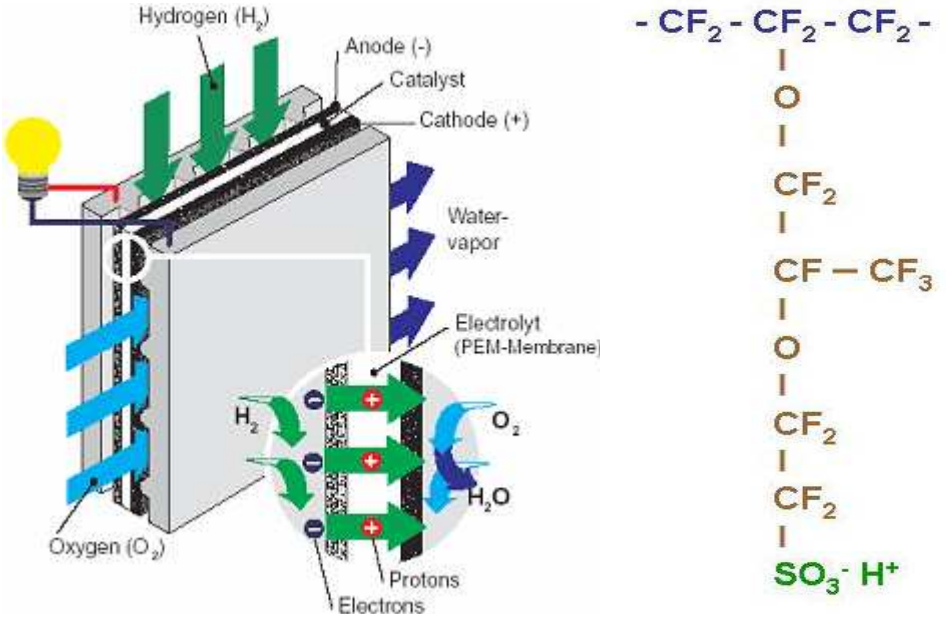

(A) (B)

Figure 1.4. (A) Schematic of a typical H_2/O_2 PEMFC [1.13]. (B) Nafion® Polymer Electrolyte Membrane Structure and Characteristics.

The blue section is a Teflon-like, fluorocarbon backbone that has hundreds of repeating CF_2-CF_2-CF_2- units. The brown section (vertical section of the molecular chain) is a side chain that connects the backbone to the sulfonic acid ions. The SO^{3-} anions are permanently attached, but the H^+ ions become mobile upon hydration of the membrane. Thus, for a fuel cell to be functional, the fuel must be hydrated before entering the cell. For hydrogen, this is done by running the gas through a washing bottle. In the case of methanol or ethanol, the alcohol is in a water solution. The ion exchange capacity of Nafion® is 0.91meq/g (equivalent hydrogen mass per mass of dried Nafion®) [1.12].

In brief, the electrochemical reactions within an electrochemical cell are segregated to two half cells, where an electrochemical reaction occurs at each half cell. Therefore, the half cell reactions of a hydrogen/oxygen fuel cell, in an acidic electrolyte, are

Anode: $H_2 \rightarrow 2H^+ + 2e^-$ (1.3)

Cathode: $\frac{1}{2}O_2 + 2H^+ + 2e^- \rightarrow H_2O^-$ (1.4)

Overall: $H_2 + \frac{1}{2}O_2 \rightarrow H_2O^-$ (1.5)

The future of hydrogen as an energy carrier will be determined by the oil market and the price that society is willing to pay for an energy supply that is poor in carbon dioxide. The costs of hydrogen production are, for the time being, prohibitive of any introduction into the energy market. As soon as the world energy price permits, the hydrogen/electricity combination will be open to an interesting future.

1.2.2 The "MicroBoro Bus" – a didactic demonstration prototype

The hydrogen generated in the experiments performed during this dissertation, was supplied to a PEMFC single cell that was housed in a bus like shaped mobile platform, used for didactic proposes – the "MicroBoro Bus" [1.14]. Figure 1.5 shows two pictures, a side view and a top view, of the Microboro Bus. The single cell was fed with hydrogen generated by the catalytic hydrolysis of $NaBH_4$ experiments.

The developed low power PEM fuel cell uses an air breathing cathode and humidified hydrogen produced by the borohydride reactor. Natural convection to air feed the cathode is used when the platform is located on a stand and the energy conversion required is just the one needed to make the wheels of the platform turn. Forced convection, by means of a fan, supplies air to the cathode when the platform as a whole is programmed to move. The necessary energy to drive the fan is provided by the fuel cell [1.14].

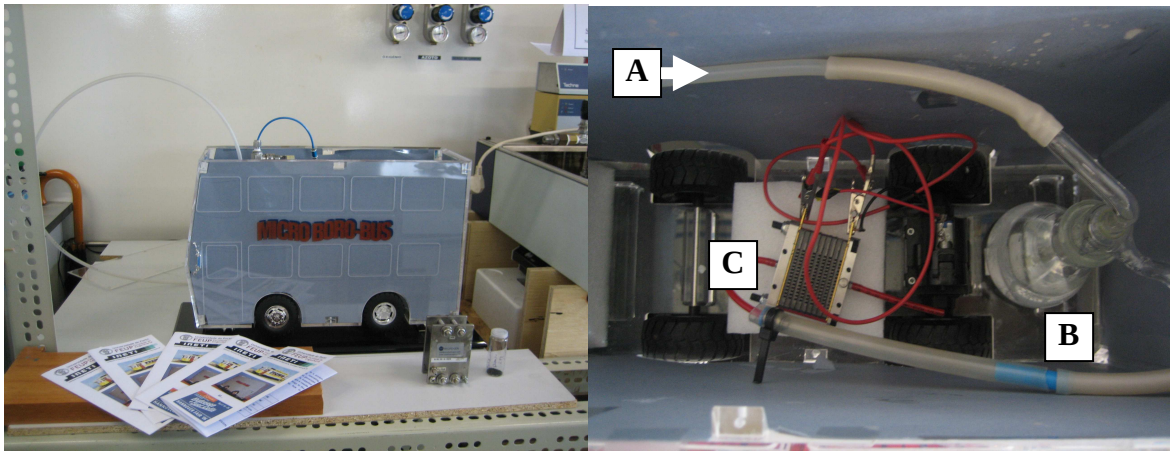

Figure 1.5. Front view and top view of the "MicroBoro Bus" (A – connection to the H_2 generator and storage tank; B- gas-washing bottle; C- PEMFC single cell).

1.3 OBJECTIVES AND ORGANIZATION OF THE DISSERTATION

It is the objective of the present research to better understand the kinetic mechanism of catalysed hydrolysis of sodium borohydride for producing molecular hydrogen at elevated yields and rates, with high gravimetric and volumetric hydrogen densities. Hence, three main different series of kinetic experiments of hydrolysis of sodium borohydride under pressure, in the presence of reused nickel-ruthenium based catalyst, were carried out to achieve this goal.

The present dissertation evaluates the following objectives:

1) Perform catalysed hydrolysis reactions of sodium borohydride in three different ways:

- by joining an alkali to sodium borohydride solutions – *alkali* hydrolysis;
- without joining an inhibitor – *alkali free* hydrolysis;
- by joining an organic polymer or surfactant – *lPOPS* hydrolysis,

to understand deeply the kinetic and chemistry of the hydrolysis and to investigate the influence of pressure, temperature and reactant concentrations on the reactions rates and yields;

2) Verify the influence of reactor bottom shape on hydrogen generation yields and rates;

3) Produce hydrogen by the concept of successive loadings of reactant solution;

4) Analyze the influence of magnetic stirring in refuelling hydrolysis;

5) Study the catalyst reutilization/durability and performance/capacity, after 200 times of being used;

6) Characterise the catalyst, in terms textural properties, morphology and XPS analysis, after a long period of reutilization.

The organization of the dissertation involves eight chapters concerned with:

Chapter 1, Introduction

Introduces the research topic and present the main objectives of this dissertation, entitled "Catalytic generation and storage of hydrogen from hydrolysis of sodium borohydride solutions under pressure – application in a hydrogen/oxygen fuel cell". Short reviews of hydrogen as a energy carrier, sodium borohydride as hydrogen carrier and PEM fuel cells are presented.

Chapter 2, Experimental techniques and apparatus.

In this chapter the materials used in all the experimental studies are described, including the nickel based bimetallic catalyst. For the latter, a textural and morphological characterization is provided. The experimental rig, with special emphasis given to the reactor design, and also a brief mention to reaction products analysis are offered.

Chapter 3, Alkali hydrolysis/Results for sodium borohydride kinetic experiments.

This chapter presents the results of *alkali* hydrolysis of sodium borohydride in the presence of a reused nickel based bimetallic catalyst. The effects of temperature, $NaBH_4$ concentration, NaOH concentration, and system pressure and reactor bottom shape on the hydrogen generation rate are investigated. Particular importance is given to the effect of successive loadings of reactant on catalyst activity, with and with out magnetic stirring. Selected XRD analysis for the reaction by-product is also presented.

Chapter 4, Alkali free hydrolysis/Results for sodium borohydride kinetic experiments.

This chapter shows the results obtained on *alkali free* hydrolysis of sodium borohydride in the presence of a reused nickel based bimetallic catalyst. A discussion on the stoichiometry of hydrolysis, in terms of the number of added water molecules to solid $NaBH_4$, is carried out, based on the results of hydrogen generation rate and yields. Emphasis is given to reactor bottom design effects on the hydrogen production. The reaction by-products are analysed by XRD.

Chapter 5, less Polar Organic Polymeric Solutions for sodium borohydride kinetic experiments.

This chapter illustrates the results obtained on *lPOPS* hydrolysis of sodium borohydride plus small additions of an organic polymer and surfactant, in the presence of a reused nickel based bimetallic catalyst. With the aim of improve the solubility of H_2 in the remaining solution, a discussion of the results of hydrogen generation rate and yields is carried out. The reaction by-products are analysed by XRD.

Chapter 6, Nickel based bimetallic catalyst characterization / results after 200 reutilizations.

This chapter focuses on the characterization of the nickel based bimetallic catalyst after 200 reutilizations. Textural properties based on nitrogen adsorption isotherms; surface morphology by scanning electron microscopy (SEM) coupled with EDS spectroscopy and X-ray photoelectron spectroscopy (XPS) analysis, were used to characterized the powder catalyst.

Chapter 7, Conclusion.

This chapter is devoted to conclusions and suggestions for future work. Conclusions drawn from the results indicate that the reused ruthenium nickel based catalyst is capable of catalyzing the sodium borohydride solutions at sufficient rates, in the three schemes presented in this dissertation for comparison – *alkali* hydrolysis, *alkali free* hydrolysis and *lPOPS* hydrolysis of sodium borohydride for hydrogen generation under pressure.

1.4 CONCLUSIONS

High performance fuel cells rely on a source of hydrogen for operation. Distribution of hydrogen either in the gaseous or liquid state is energy intensive and requires extensive infrastructure development to become a safe and reliable source of energy.

In this introductory chapter a short literature survey identified hydrogen gas as energy carrier and chemical hydrides as high density hydrogen carriers. Special emphasis was given to sodium borohydride which is stable in basic solution and can easily be manipulated. The inherent capacity for on-site hydrogen generation further enhances the projection for $NaBH_4$ as hydrogen vector for supplying hydrogen/oxygen fuel cells. Hence, a briefly outline of PEM fuel cells was also exposed.

Finally, the feasibility of borohydride source hydrogen in an operational PEM fuel cell has been established. In truth, the hydrogen generated in the experiments performed during this dissertation, was supplied to a PEM single fuel cell that was housed in a bus like shaped mobile platform, used for didactic proposes – the "MicroBoro Bus" [1.14]

1.5 REFERENCES

[1.1] 'Crucial data distorted as global oil runs dry', The Guardian weekly, 13-19 Nov. 2009.

[1.2] 'Catalytic generation of hydrogen from the hydrolysis of sodium borohydride. Application in a hydrogen/oxygen fuel cell. C.M. Kaufman, PhD Thesis, 1981.

[1.3] http://www1.eere.energy.gov/hydrogenandfuelcells/storage/tech_status.html.

[1.4] U.S. Department of Energy Hydrogen Program. Available from: http://www.hydrogen.energy.gov/ .

[1.5] H.I. Schlesinger, H.C. Brown, A.E. Finholt, J.R. Gilbreath, H.E. Hoeskstra, K. Hyde, Sodium borohydride, its hydrolysis and its use as a reducing agent and in the generation of hydrogen, J. Am. Chem. Soc. 75 (1953) 215-219.

[1.6] E. Marrero-Alfonso, J.R. Gray, T.A. Davis, M.A. Matthews, Hydrolysis of sodium borohydride with steam, Int. J. Hydrogen Energy 32 (2007) 4717-4722; Minimizing water utilization in hydrolysis of sodium borohydride: the role of sodium metaborate hydrates, Int. J. Hydrogen Energy 32 (2007) 4723-4730.

[1.7] D.A. Lyttle, E.H. Jensen, W.A. Struck, A simple volumetric assay for sodium borohydride, Analytical Chem. 24 (1952) 1843-1844.

[1.8] V.C.Y. Kong, F.R. Foulkes, D.W. Kirk, J.T. Hinatsu, Development of hydrogen storage for fuel cell generators. I – Hydrogen generation using hydrolysis hydrides, Int. J. Hydrogen Energy 124 (1999) 665-675.

[1.9] A. Züttel, P. Wenger, S. Rentsch, P. udan, Ph. Mauron, Ch. Emmenegger, LiBH4 a new hydrogen storage material. J. Power Sources 118 (2003) 1-7.

[1.10] U.B. Demirci, O. Akdim, P. Miele, Ten-year efforts and a no-go recommendation for sodium borohydride for on-board automotive hydrogen storage, Int. J. Hydrogen Energy 34 (2009) 2638-2645.

[1.11] W.R. Grove, Phi. Mag, 14 (1839) 127.

[1.12] DuPont, Nafion® perfluorinated polymer products, Product Information Guide, 2000.

[1.13] European Fuel Cell GMBH, 2005.

[1.14] Rangel C.M., Silva R.A., Pinto A.M.F.R. Fuel cells and on-demand hydrogen production: didactic demonstration prototype. Proceedings of the International Conference in Power Engineering and Electric Drives", Eds. L.S. Martins and P. Santos, Setúbal, Portugal, September 12-14, 2007, paper 237.

CHAPTER 2

Experimental techniques and apparatus

In this chapter the materials used in all the experimental studies are described, including the nickel based bimetallic catalyst, the experimental setup with special emphasis to the reactor design, and also a brief mention of reaction products analysis.

2.1 INTRODUCTION

A detailed description of the materials used in the kinetic studies of the catalytic hydrolysis of sodium borohydride is presented, both for the reactant solutions and for the nickel-based bimetallic catalyst. The methods of preparation of the reactant solutions and/or pre-treatment of the catalyst, the experimental rig design and detailed experimental plan for three different kinds of kinetics studies: *alkali* hydrolysis, *alkali free* hydrolysis and *less Polar Organic Polymeric Solutions (lPOPS)* are presented. The techniques used for reaction products analysis: *pure* molecular hydrogen and sodium borates by-product are also mentioned.

2.2 MATERIALS

2.2.1 Sodium borohydride

Anhydrous sodium borohydride powder (96% purity) was provided by MERCK (No.: 1.06371.0100) and stored in a dessicator until use.

In the experiments with the *fuel* ($NaBH_4$) in the liquid form, used in *alkali* hydrolysis and in *lPOPS* hydrolysis, the reactant solutions were stabilized by the addition of small quantities of sodium hydroxide pellets as a hydrolysis inhibitor. The sodium hydroxide

(98% purity) was supplied by EKA (No.: 1310.73.2). Deionised water was used to prepare all the aqueous reactant solutions and, in all of them, the initial pH was approximately 14.

In the experiments with *alkali free* hydrolysis of $NaBH_4$ for hydrogen generation, the anhydrous sodium borohydride powder was used in the solid state.

2.2.2 Nickel based bimetallic catalyst

The catalyst used in all the experiments reported in this dissertation is a nickel based bimetallic catalyst, synthesized at LNEG – Laboratório Nacional de Energia e Geologia, Fuel Cells and Hydrogen Unit, Lisbon – Portugal.

Catalyst preparation

The catalyst, in the form of a finely divided black powder (see Figure 2.1), unsupported, was prepared from a mixture of precursors in deionised water - impregnating small quantities of ruthenium in the nickel salts (Riedel-de Haën) - by chemical reaction with 10 wt% stabilised borohydride solution (Rohm and Haas), as the reducing environment. When the reduction was complete the catalyst was appropriately decanted, washed, filtered, dried and heat-treated at 110ºC. The catalyst was kept in a dessicator until use.

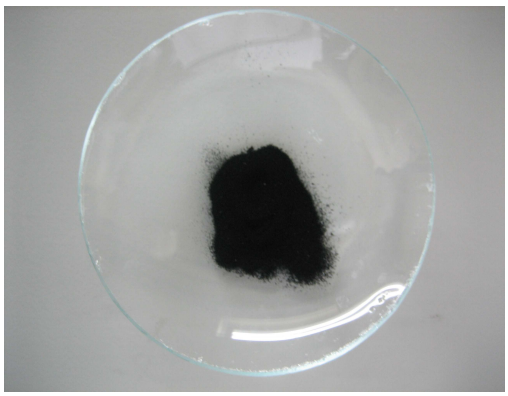

Figure 2.1. Photograph of the nickel based bimetallic catalyst in the form of a finely divided black powder.

Catalyst samples were analyzed for textural properties. The determination of surface areas (S_{BET}), by N_2 physisorption was undertaken at 77K, using a Quantachrome Instruments Nova 4200e apparatus. Prior to the analysis, the samples (0.127 g) were degassed at 160 ºC for 3 h. Pore size distributions were obtained from the desorption branch of the isotherms using the Barrett, Joyner and Halenda (BJH) method. The micropore volumes and mesopore surface areas were determined by the t-method.

Morphology and elemental composition analysis of the catalyst were done on a Scanning Electron Microscopy (SEM) coupled with EDS unit FEI Quanta 400 FEG ESEM/EDAX Genesis X4M operating at 15 kV in low vacuum mode (LVSEM for uncoated non conductive sample). The powder sample was prepared by simple dispersion over a double side adhesive carbon tape. X-Ray Photoelectron spectroscopy (XPS) of the catalyst before use, after the powder sample was made into a pellet of 10 mm diameter, was carried out on a VG Scientific ESCALAB 200 A spectrometer using Mg Kα (1,253.6 eV) as a radiation source. The photoelectrons were analysed at a takeoff angle of 0º.

Catalyst characterization before used

The catalyst used in this work is a powder containing Ni and Ru species with nanometric particle size, as evident in Figure 2.2a). The amount of ruthenium is small and was not detectable by EDAX, see Figure 2.2b). However, by XPS analysis less than 1 At% Ru was indicated.

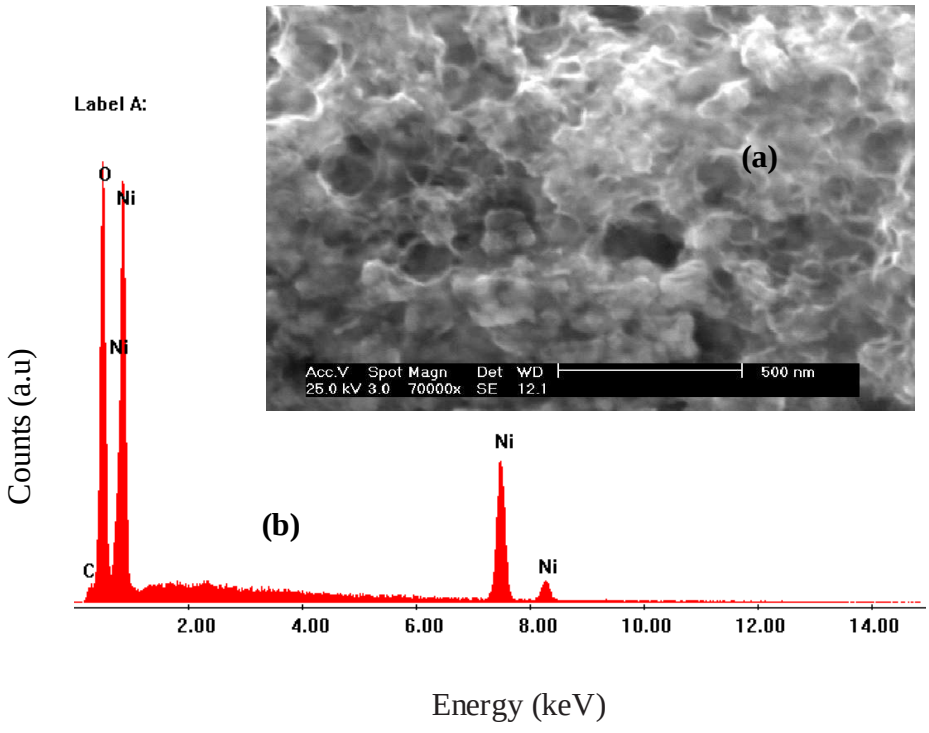

Figure 2.2. Photo Scanning electron microscope view of the synthesized catalyst powder (a) and associated elemental analysis EDAX (b).

The nitrogen (N_2) adsorption and desorption data as a function of pressure (at liquid nitrogen temperature) are displayed in Figure 2.3. The results shows that de N_2 isotherm

shape is of type IV, validating the BJH method used for characterized the textural properties of our powder catalyst. Total specific surface area, as determined by N_2 physisorption, gave a value of 54 m^2g^-1 and negligible micropore volume. In Table 2.1 the textural properties of Ni-Ru based catalyst before used are summarized.

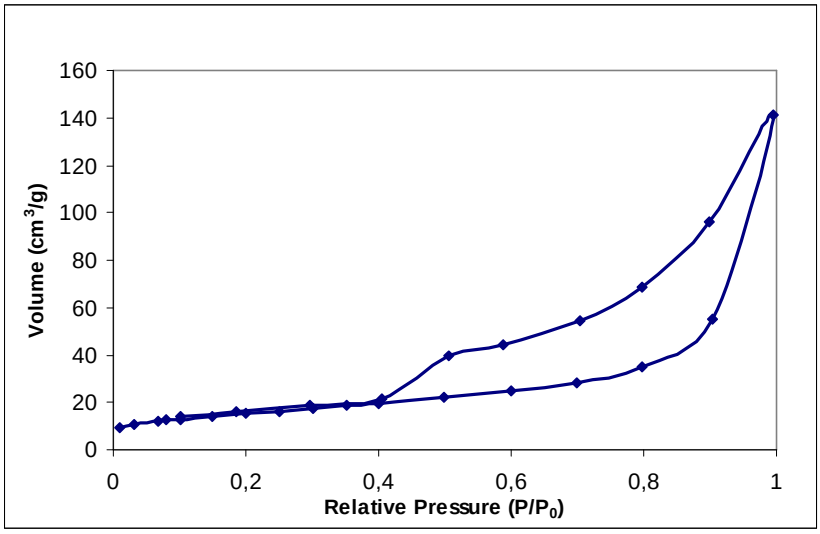

Figure 2.3. Nitrogen adsorption/desorption isotherms.

Table 2.1 – Textural properties of catalyst powder used in this work before use.

Catalyst	S_{BET} / m^2g^{-1}	V_μ / cm^3 g^{-1}	S_{ext} / m^2 g^{-1}	V_p / cm^3 g^{-1}
Before use	54	0	52	0.22

S_{BET} = BET surface area;
V_μ = micropore volume by t-method;
S_{ext} = (mesopore + macropore) surface areas by t-method;
V_p = total pore volume

After some preliminary hydrolysis rate tests with different proportions of Ni-based bimetallic catalyst/$NaBH_4$, it was decided that the appropriate relation to use in most of the experiments reported in this dissertation is Ni-based bimetallic catalyst/$NaBH_4$: 0.4 g/g.

After the first utilizations, the consequent kinetic experiments were done with reused catalyst. The procedure adopted for the reutilization of the catalyst was to recover it from the remaining solution in the reactor, to wash it five times with distilled water, then carry out sedimentation by gravity for complete physical separation from distilled water, and finally, dry the catalyst in an oven at 60 ºC for four hours.

2.3 APPARATUS FOR KINETIC STUDIES

2.3.1 Reactor design

The hydrolysis reactions were carried out in batch reactors, especially designed for the experiments reported in this dissertation, all of them performed at pressures up to 3MPa. The main batch reactor has an internal volume of 646 cm^3 and was made of stainless steel AISI 316, with wall width equal to 10 mm. Special care was taken with the value of the wall width during the reactor design because all the kinetic experiments were to be done at high pressures. As it is well known, hydrogen dissolution and permeation can be significant at high pressure through most of materials, including stainless steels. This may affect the integrity of structural components used for H_2 storage during reaction, since hydrogen can embrittle metals [2.1]. In order to allow for changes in the internal volume of the main reactor, another two separate filled pieces that can be introduced inside the main vessel without gap were designed and constructed as well in stainless steel AISI 316. The three possible final design combinations of interest result in three different batch reactors, named LR, MR and SR, with internal free volumes of 646 cm^3, 369 cm^3 and 229 cm^3, respectively. Figure 2.4 shows a photograph of the main reaction container with the two different separate filled pieces.

Figure 2.4. Photograph of the main batch reactor with the two separate filling pieces used to change the internal free volume for $NaBH_4$ hydrolysis reactions.

In comparison with the reactor used on an earlier work [2.2], two major improvements were made in the reactor design. The upgrading is related with the reactor sealing, i.e., an axial installation of the O-ring for the vessel sealing instead of a radial one; and with the

possibility of following the reaction temperature at two different cottas inside the vessel by using two k thermocouples positioned at two distinct points: one near its bottom (named T.Bottom) and the other one very close to its top (named T.Top). The first one is used to monitor the increase of temperature in the *core* of the exothermic catalytic reaction, and the second one, simply measures the temperature of molecular hydrogen in the free volume of the container opened for the gas.

With the objective of studying the possible effect of the reactor bottom shape on the hydrogen generation rates - this constitutes one of the *originalities* of the present dissertation, an inside flat bottom and a conical bottom geometry were designed, to enable non-dispersible effects during the contact of the fine powder catalyst either with the reactant solutions or with the solid $NaBH_4$ plus the injected pure water, the latter in the *alkali free* hydrolysis experiments. Figure 2.5 show the exposed view of the inside designed reactors.

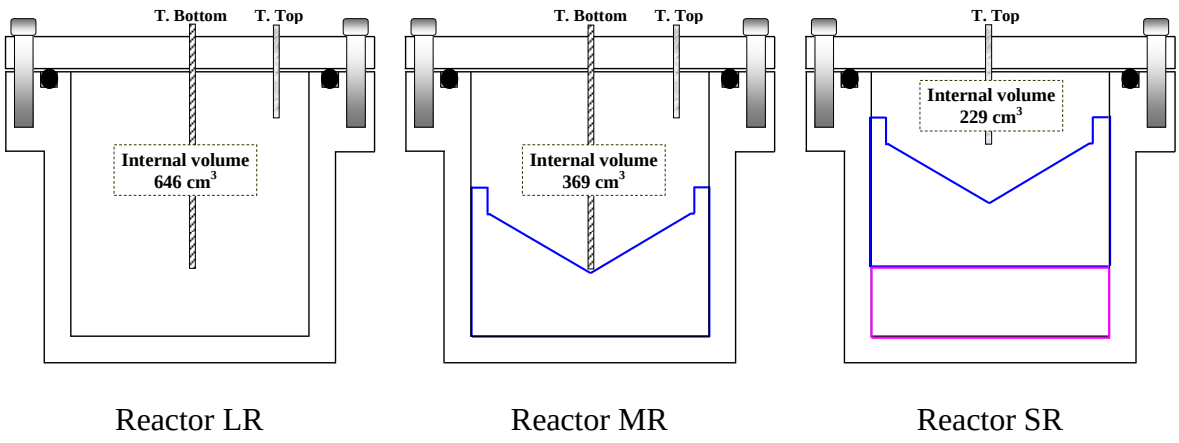

Figure 2.5. Schematic view of the reactors inside: reactor LG – flat bottom, and reactors MR and SR – conical bottom, with mention of the internal available free volume.

2.3.2 Experimental rig

An overview photograph of the experimental rig is offered in Figure 2.6.

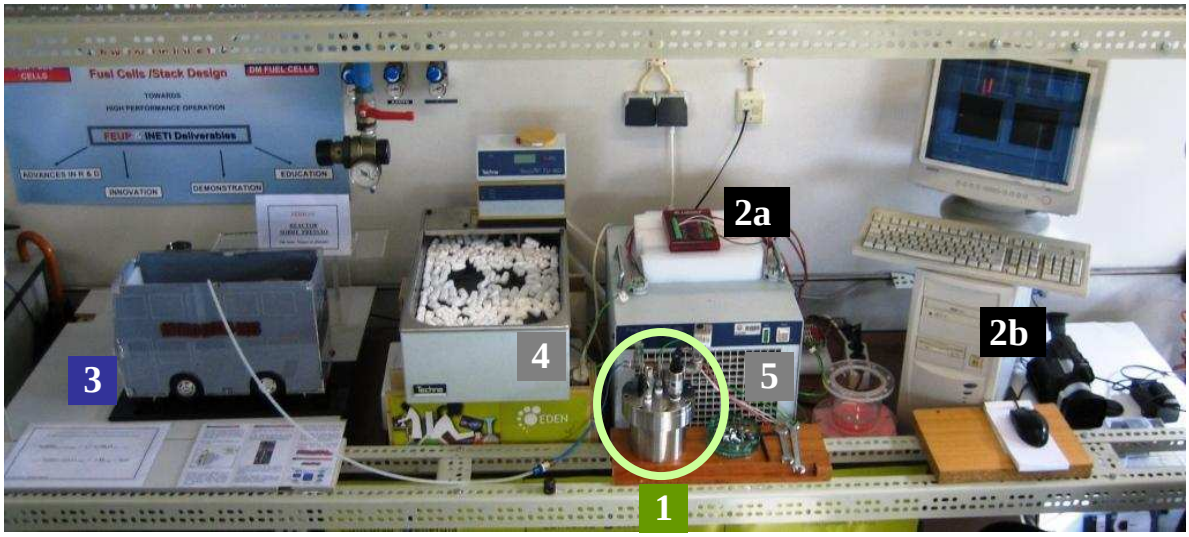

Figure 2.6 Global picture of the experimental setup used for the kinetics studies of hydrogen production via catalytic hydrolysis of sodium borohydride, under pressure. (1) batch reactor; (2a-2b) data acquisition system; (3) "MicroBoro bus" with a PEM fuel cell; (4) thermostatic bath and (5) refrigeration unit.

The typical hydrogen generation experiments involve the preparation of the reacting solution by adding the appropriate amount of $NaBH_4$ to a certain volume of aqueous solution of the inhibitor NaOH (with a chosen hydroxide concentration) in the case of the *alkali* hydrolysis or, a certain molar quantity of pure water, in the case of the *alkali free* hydrolysis. After perfectly sealing the reaction autoclave, an adequate volume of reacting solution (or pure water) is rapidly injected into the reactor by means of a syringe with a large needle length (150 mm), to ensure that the reacting solution (or distilled water) is delivered very close to the nickel-based bimetallic powder catalyst. This catalyst has been previously stored in the bottom of the reactor, in a proper quantity, measured in an analytical balance.

The temperature of the reactor medium was monitored at two different points, as mentioned above, and recorded simultaneously with a data acquisition system (see 2a and 2b in Fig.2.6), using Labview software. To monitor the rate of hydrogen generation, using the same data acquisition system, the gas pressure inside the reactor was followed with an appropriate pressure transducer calibrated from 0-40 bar gauge and also by a Bourdon manometer (from 0-60 bar gauge), until attaining a constant pressure inside the reactor. An overview of the instrumentation fixed on the cover of the reaction chamber is offered in Figure 2.7.

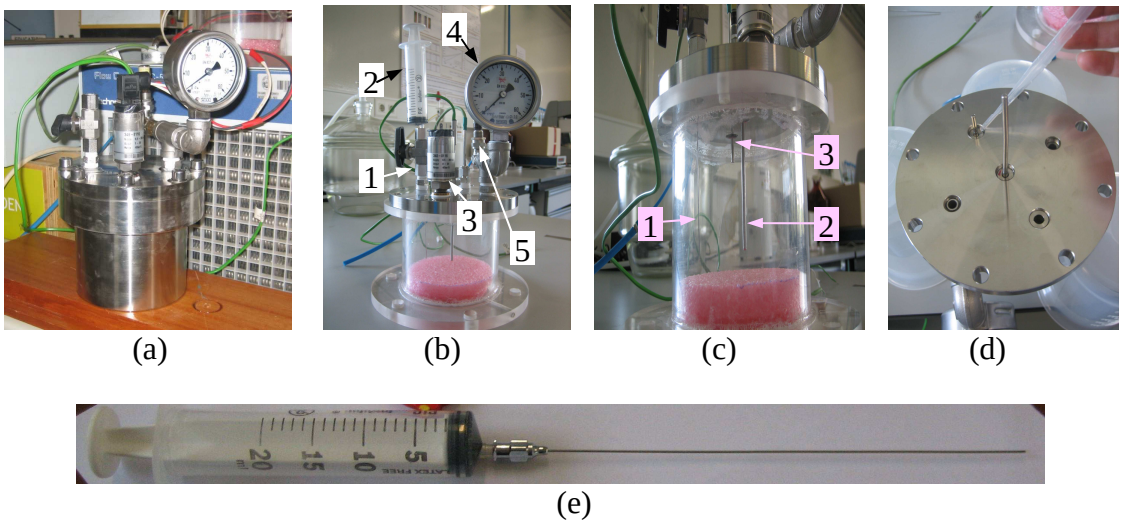

(a) (b) (c) (d)

(e)

Figure 2.7. Survey picture of the: (a) main reaction vessel / LR; (b) accessories fixed on the outside lid of the reactor: 1- reactor inlet bore valve, 2- syringe, 3- pressure probe, 4- Bourdon manometer and 5- reactor exhaustion needle valve; (c) ascendant view of the inside lid of the reactor: 1- needle of the syringe, 2- "T.Bottom" k thermocouple and 3- "T.Top" k thermocouple; (d) top view of the inside lid of the reactor showing the left 'holes' after connecting the some accessories; (e) syringe with needle (150 mm length).

Almost all the experiments reported on this dissertation were done with one single injection of reactant solution and without magnetic stirring.

A thermostatic bath, coupled with a refrigeration unit (see 4 and 5 in Fig.2.6), was efficiently used to control the reaction temperature, at a desired value between 19.5 and 55 ºC, in almost all the kinetic studied hydrolysis. In addition, some experiments were done without temperature control, i.e., in environmental conditions, in order to compare the hydrogen generation rates.

It is important to notice that prior to any of the studied hydrolysis, the atmospheric air inside the reactor was not purged and no vacuum was done. So, the final gas predicted pressure, assuming 100% conversion efficiency and by applying the ideal gas law, was corrected by the addition of the corresponding air pressure (of the initial moles of air inside the free volume of the reactor chamber).

2.4 GENERAL PLAN FOR $NaBH_4$ HYDROLYSIS EXPERIMENTS

2.4.1 *Alkali* hydrolysis

Alkali catalytic hydrolysis of sodium borohydride for hydrogen generation under pressure comprises a series of experiments done in the three batch reactors (LR, MR and SM), in the presence of the powder reused nickel-based bimetallic catalyst, in a proportion of catalyst/$NaBH_4$: 0.4 g/g. The *fuel*, in the liquid form, was prepared with different weight concentrations of the chemical hydride and inhibitor.

Briefly, the study developed under this research topic has the objective of revising the effect of:

i) reaction temperature;

ii) $NaBH_4$ concentration;

iii) NaOH concentration;

iv) pressure;

v) reactor bottom shape,

on hydrogen generation rates and yields.

Experimental tests were performed without magnetic stirring and, most often, at controlled temperature (292-328 K).

2.4.1.1 *Successive loadings* of reactant solution

Also related with the item of *alkali* catalytic hydrolysis of sodium borohydride for hydrogen production under pressure, a study of successive loadings of reactant solutions is presented in this dissertation. The central target is to verify the activity of the Ni-based bimetallic catalyst and put in evidence the capability of re-using a constant amount of catalyst during successive loadings of *fuel*.

The experimental work comprises tests in two different batch reactors chosen, LR and MR, in the presence of powder reused nickel-based bimetallic catalyst, in a proportion of catalyst/$NaBH_4$: 0.4 g/g. The tests were performed under uncontrolled ambient conditions and without stirring.

In addition, and with the purpose of verifying the influence of agitation on hydrogen reaction rate during successive loadings of *fuel*, a Teflon^{TM} magnetic stirrer was placed inside the reactor before one loading injection. Vigorous magnetic stirring was used to promote complete mass transfer (to overcome diffusion limitations).

2.4.2 *Alkali free* hydrolysis

Alkali free catalytic hydrolysis of sodium borohydride for hydrogen generation under pressure comprises also a series of experiments done in the three batch reactors (LR, MR and SM), in the presence of powder reused nickel-based bimetallic catalyst. The reactant blend was produced without adding NaOH aqueous solution to solid $NaBH_4$, so this research topic explores the *alkali free* hydrolysis of sodium borohydride for hydrogen production. In this case, a proper quantity of powder catalyst and solid $NaBH_4$, both measured in an analytical balance, are mixed together in the solid state, and then stored in

the bottom of the reactor. After sealing perfectly the reaction vessel, a stoichiometric amount of pure liquid water is rapidly injected into the reactor by means of a syringe.

The main inspiration behind developing this experimental *item* was to produce pure hydrogen gas with very high gravimetric and volumetric densities.

In a few words, the *alkali free* hydrolysis experimental work aims at studying the influence of:

i) $H_2O/NaBH_4$ (mol/mol) ratios between 2 and 8 mol;

ii) reactor pressure;

iii) reactor bottom shape; and

iv) catalyst/$NaBH_4$ (g/g) ratios of 0.2 and 0.4 g,

on hydrogen generation rates and yields.

These experimental tests were performed without magnetic stirring and without temperature control.

2.4.3 *less Polar Organic Polymeric Solutions (lPOPS)* hydrolysis

less Polar Organic Polymeric Solutions (*lPOPS*) hydrolysis of sodium borohydride for hydrogen generation under pressure embraces a series of experimental work done in the two batch reactors with conical bottom shape (MR and SM), in the presence of powder nickel-based bimetallic catalyst, reused about 160 times. The reactant solutions were produced by small additions of an organic polymer or surfactant to the stabilized aqueous solution of $NaBH_4$.

Also in this case, a proper quantity of powder reused Ni-Ru based catalyst, in the proportion of catalyst/$NaBH_4$: 0.4 g/g, measured in an analytical balance, was stored in the bottom of the reactor. After sealing perfectly the reaction vessel, 20 mL of the reactant solution was rapidly injected into the reactor by means of a syringe. After reaction completion, magnetic stirring inside de reactor was allowed for 30 minutes to promote complete saturation of H_2 with the remaining by-product solution. All the experimental tests were performed with temperature control at 45 ºC.

The motivation behind developing the *lPOPS* was to increase the non-polar hydrogen-electrolyte interactions and hence improve the affinity for H_2 storage in the liquid phase by solubility's effects. Therefore, the *lPOPS* hydrolysis experiments aims at studying the influence of:

i) the addition of 0.25 wt% CMC (Carboxil-Methyl-Cellulose) to the stabilized solution of 10 wt% $NaBH_4$ and 7 wt% NaOH;

ii) the addition of 0.25 wt% SDS (Sodium-Dodecyl-Sulphate) to the stabilized solution of 10 wt% $NaBH_4$ and 7 wt% NaOH; and

iii) the reactor pressure,

on hydrogen generation rates and yields, conducive to H_2 solubility effects.

2.5 REACTION PRODUCTS ANALYSYS

2.5.1 Molecular hydrogen

The main product of the hydrolysis reactions mentioned above is hydrogen gas. A simple verification that the gas feed to the PEMFC, when the reactor exhaustion needle valve is opened, is molecular hydrogen, we forced the gas to go all the way through a gas-washing bottle, filled with ultra pure water (conductivity of 1.48 μS/cm at 25 ºC). After a period of noteworthy H_2 bubbling, the values of pH and conductivity of the remaining water inside the gas-washing bottle were checked. In general, no major variance in the values of pH and conductivity were found (typical final marks of 7.5 and 10 μS/cm were found, respectively, at 25 ºC). Although the proper analytical method to verify the composition of the exhausted gas from the reaction vessel is the gas chromatography, it is reasonable to assume that the great majority of the gas captured during the experimental work, which is used to feed a PEM fuel cell hosted in a "Microboro bus" didactic prototype, is essentially hydrogen.

2.5.2 *Sodium borates* by-products

The different course of hydrolysis reactions studied in this dissertation also produced certain by-products, namely sodium *borates* (or oxygen-containing compounds of boron).

The by-product of the hydrogen generation reactions was dried by slow evaporation of a water solution at the environmental conditions vivid in the laboratory. Suitable crystals were then obtained and subsequently analyzed using one of the most common analytical techniques to identify solid samples: the X-Ray Diffractometry (XRD). In fact, the X-ray diffraction is primarily of value for the study of crystalline material. X rays are reflected off the surfaces of crystals, and by studying the patterns of reflection as the crystalline material is rotated in the path of the X rays, much information about the structure of the material can be obtained.

The diffraction data were colleted at 293 K with a Gemini PX Ultra equipped with MoKα radiation and with CuKα radiation (facility of IBMC - Instituto de Biologia Molecular e Celular, University of Porto, Portugal).

2.6 CONCLUSIONS

In this chapter the materials used in all the experimental work were described, including the nickel based bimetallic catalyst. The experimental setup gives special emphasis to the reactor design, made of stainless steel AISI 316. To study the catalytic hydrolysis of sodium borohydride under pressure, the O-ring used to seal the vessel was installed axially instead of a radially. Moreover, to follow the reaction temperature at two different cottas inside the vessel, two k thermocouples were positioned at distinct points: one near the bottom and the other very close to the top. To study the influence of reactor bottom shape on the hydrogen generation rates - this constitutes one of the *originalities* of the present dissertation, two different bottom geometries were designed – one flat and the other conical. The latter has the purpose of enabling non-dispersible effects during the contact of the catalyst with the reactant solution.

The hydrolysis experiments were performed in the presence and in the absence of an alkali, namely, *alkali* hydrolysis and *alkali free* hydrolysis of sodium borohydride, respectively. Special attention is given to the refuelling experiments in order to validate the catalyst activity. Also, a small addition of an organic polymer or surfactant was added to the stabilized reactant solution with the objective of studying the H_2 solubility effects in the remaining solution inside the reactor after reaction completion.

Finally, suitable crystal of the by-products of the hydrolysis of sodium borohydride, made by slow evaporation of a water content, where analyzed by XRD.

2.7 REFERENCES

[2.1] C. San Marchi, B.P. Somerday, S.L. Robinson, Permeability, solubility and diffusivity of hydrogen isotopes in stainless steels at high gas pressures, Int. J. Hydrogen Energy 32 (2007) 100-116.

[2.2] A.M.F.R. Pinto, D.S. Falcão, R.A. Silva, C.M. Rangel, Hydrogen generation and storage from hydrolysis of sodium borohydride in batch reactors, Int. J. Hydrogen Energy 31 (2006) 1341-1347.

CHAPTER 3

Alkali hydrolysis
Results for sodium borohydride kinetic experiments

This chapter presents the results of alkali hydrolysis of sodium borohydride in the presence of a reused nickel based bimetallic catalyst. The effects of temperature, $NaBH_4$ concentration, NaOH concentration, system pressure and reactor bottom shape on the hydrogen generation rate are investigated. Particular importance is given to the effect of successive loadings of reactant on the catalyst activity. Selected XRD analysis for the reaction by-product is also presented.

3.1 INTRODUCTION

Sodium borohydride has been extensively studied as a hydrogen storage medium because it is readily available, relatively inexpensive, and more stable than other chemical hydrides (for instance, lithium or aluminium borohydrides) [3.1-3.7]. Almost all prior work uses an excess of liquid water, with a catalyst or promoter to achieve high yields and rates of hydrogen.

$NaBH_4$ reacts with water to generate molecular hydrogen according to the hydrolysis reaction shown in Eq.(3.1):

$$NaBH_4 + (2+x)\ H_2O \rightarrow NaBO_2.xH_2O + 4\ H_2 + \text{heat}. \qquad (3.1)$$

Ideal hydrolysis is attained for $x = 0$ [3.1], but in practice excess of water is required to pre-dissolve the hydride for storage or to keep the by-products in solution (accounting for the fact that the solid by-product, hydrated metaborate ($NaBO_2.xH_2O$), can exist with various degrees of hydration [3.8-3.10]).

Table 3.1 show values of *x* (excess hydration factor) corresponding to aqueous solutions of sodium borohydride, ranging from 5 wt% to 35 wt% (approximately the solubility limit of $NaBH_4$), found in most hydrolysis schemes published in literature.

Table 3.1 – Excess hydration factor, *x*, of aqueous solutions of sodium borohydride.

$NaBH_4$ weight, %	5	7.5	10	20	30	35
x	37.9	23.9	16.9	6.4	2.9	1.9

From the values in Table 3.1 it is clear that solubility considerations alone cause chemical hydride systems to lose significant storage efficiency relative to the hydrogen content on a materials only basis. Hydrolysis is typically conducted in the aqueous phase at lower temperatures, and large quantities of excess water are required because of the low solubility of both $NaBH_4$ and the borate by-products in water [3.11]. In pure liquid water the reaction generates basic species that are thermodynamically and kinetically metastable. Metastability causes the reaction to cease at low yields of hydrogen even though the reaction is strongly favoured thermodynamically [3.12-3.14]. The metastable species require addition of mineral acid or use of a heterogeneous catalyst to drive the reaction to completion. Furthermore, the solid products of the reaction are an unknown mixture of hydrated sodium metaborates. Hydrated products capture water that is not reduced to hydrogen, further decreasing the efficiency of the reaction.

Most systems that have been engineered to date utilize a route wherein both the hydride reactant as well as the product is dissolved in excess water. Because the solubility of the chemical hydride (55g $NaBH_4$/100g H_2O at 25 ºC) [3.15] is relatively low, and the solubility of the oxides is even lower (28g $NaBO_2$/100g H_2O at 25 ºC) [3.7], such systems inherently have a greatly reduced gravimetric efficiency (hydrogen storage capacity on a materials-only basis) compared to the ideal.

Table 3.2, shows the effective value of *x* for different amounts of water, and the corresponding hydrogen storage capacity on a materials-only basis. Ideal hydrolysis requires no excess water. Complete dissolution of $NaBH_4$ at 25 ºC requires extra water corresponding to x=1.81. If sufficient water is added to keep the $NaBO_2$ in solution, the effective value of *x* is 11.04.

Table 3.2 – Comparison of gravimetric efficiencies of various reactant preparations.

	Molar ratio, $NaBH_4/H_2O$	x	H_2 storage capacity, wt%
Ideal hydrolysis	1 / 2	0	10.92
Saturated $NaBH_4$ solution, 25 ºC	1 / 3.81	1.81	7.57
$NaBO_2$ solubility limit, 25 ºC	1 / 13.04	11.04	2.96
8.5 wt% $NaBH_4$ plus 5 wt% NaOH	1 / 21.37	19.37	1.81

Furthermore, the addition of NaOH or other base to stabilize the solutions also affects the hydrogen storage density. Shang et al. [3.11] found that the optimum concentration, where the compounds are stable and dissolve in solution, is 8.5wt% $NaBH_4$/5wt% NaOH resulting in a theoretical gravimetric storage efficiency of only 1.81wt% H_2 (x=19.37). Clearly, addition of water to achieve solubility of the reactants and/or products drives the storage efficiency down rapidly.

Almost all research to date is based on conducting the reaction in an aqueous mixture, with large amounts of excess water. Despite favourable thermodynamics, as said before, aqueous phase reactions with pure water give conversions of less than 5%.

It has been reported that the decrease in the initial rate of hydrogen and reaction yield is due to an increase in the pH of the solution, caused by the formation of the strongly basic metaborate ion [3.1]. This stabilization under high pH conditions has also been exploited to prevent premature reaction.

Fundamental investigations on the hydrolysis of chemical hydrides, particularly lithium and sodium borohydrides, were performed by Schlesinger *et al.* [3.1] in the early 1950s. They observed that the rate of the aqueous hydrolysis reaction decreased with the formation of the basic sodium metaborate (BO^{2-}) product, and concluded that the reaction rate is dependent on both temperature and pH. Kreevoy *et al.* [3.16] later described this dependence by the empirical rate law presented by Equation (3.2),

$$\log(t_{1/2}) = pH - (0.034T - 1.92), \tag{3.2}$$

where $t_{1/2}$ is the half-life of self-hydrolysis of $NaBH_4$ in minutes at a particular temperature T in K and pH is the solution pH value (in the absence of catalyst). That is to say, alkaline $NaBH_4$ solution at pH 14 can be kept for 430 days from self-decaying at room temperature.

The reaction yield also depends heavily on the pH and temperature. Kojima *et al.* [3.7] reported that at room temperature (20-23 ºC) the overall reaction conversion stabilizes at

7% as the basic borate by-product is formed. Moon *et al.* [3.17] investigated the pH and temperature effects on the rate of decomposition of more concentrated $NaBH_4$ solutions.

Therefore, previous studies have shown that the uncatalyzed aqueous hydrolysis reaction of $NaBH_4$ proceeds at a very slow rate. In more concentrated solutions, the rate was diminished probably due to solubility and mobility inhibition by the $NaBO_2$ product [3.17]. In all solutions with inhibitor, the kinetics of H_2 generation was initially linear, but non-zero-order behaviour became evident after several hours. It was found that the addition of alkali stabilizers such as $NaBO_2$, KOH and NaOH depressed the hydrogen evolution, a property utilized in many practical chemical hydride systems to promote stable long term storage.

Indeed, to create a basic environment in which $NaBH_4$ hydrolysis is stifled, simple hydroxides such as NaOH and KOH should be added. However, the resulting alkaline solution continues to undergo slow reaction to release H_2. Several studies have looked at the decomposition rate of these solutions at various NaOH and $NaBH_4$ concentrations and temperatures to gauge their shelf life. It is apparent that the rate of hydrolysis for dilute solutions is much different than that of concentrated solutions and that temperature has a dramatic effect on the stability of the solutions.

The concentration of $NaBH_4$ in solution must be maximized to improve energy density but low enough to keep the $NaBO_2$ by-product in solution [3.11]. Minkina *et al.* [3.18] investigated the effects of temperature and NaOH concentration on the degradation of concentrated $NaBH_4$ solutions. They suggest that above 30 ºC, at least 5wt% NaOH must be added to slow the hydrolysis, which is consistent with Shang work who suggested working on systems of 8.5 wt% $NaBH_4$ and 5wt% NaOH solution at room temperature [3.11].

In order to release the hydrogen from these basic stabilized solutions, metal or acid catalysts are required [3.1]. Various studies have been performed on the catalyzed hydrolysis reaction of sodium borohydride [3.5-3.7,3.19]. It is documented in the literature [3.12, 3.14] that sodium borohydride undergoes hydrolysis in aqueous solution to give boric acid in more acidic solutions (pH<9) and borate in more basic solutions (pH>9), as shown in the following equations:

$$BH^{4-} + H^{+} + 3H_2O \rightarrow B(OH)^{3-} + 4H_2 , \quad pH<9 \tag{3.3}$$

$$BH^{4-} + 4H_2O \rightarrow B(OH)^{4-} + 4H_2 , \quad pH>9 \tag{3.4}$$

If sodium metaborate, a water soluble and environmentally benign solid, is assumed to be the sole product, the reaction can be written simply as in Equation (3.1).

In fact, catalysts play such a vital role in hydrogen evolution from hydrolysis of $NaBH_4$, that a huge number of substances have been attempted to be efficacious in increasing the rate of hydrogen evolution but never to yield in lowering the controllability of hydrogen generation.

Several metal catalysts are effective reaction catalysts to enhance hydrolysis of the alkaline sodium borohydride solution. Among them, the catalysts with precious metals most used are: rhodium, platinum, ruthenium [3.5, 3.6, 3.20], platinum supported on $LiCoO_2$, CoO and TiO_2 [3.7, 3.21, 3.22] or carbon [3.23], ruthenium supported on IRA-400 anion resin [3.24] or alumina pellets [3.25], ruthenium nanoclusters [3.26], and Pt/Pd on carbon nanotubes (CNT) paper [3.27].

The most used high-performance catalysts containing non-noble metals are: nickel [3.1, 3.28], nickel and/or cobalt borides [3.12, 3.29, 3.30-3.37], cobalt boride supported on nickel foam [3.38, 3.39] or carbon [3.40], cobalt boride amorphous alloy powder and Pd/C [3.42], cobalt on γ-alumina [3.43], hydrogenphosphate stabilized nickel(0) nanoclusters [3.44], Co-Mn-B supported on nickel foam [3.45], and Co-P catalyst [3.46,3.47]. A metal alloy catalyst containing a less precious metal: $Ru_{60}Co_{20}Fe_{20}$ supported on activated carbon fibber, has been reported by Park *et al.* [3.48], who found high hydrogen release in the reaction given by Eq.(3.1).

In the present work particularly interested is focused in the work published on Ru catalysts, preferably unsupported, for results comparison. Elsewhere, a comparative study of the catalysts mentioned in the previous paragraphs with the Ni-Ru based powdered catalyst will be published (but that study is not included in this dissertation).

After this short review, in the following sections, the results obtained with the ruthenium nickel based powdered catalyst, unsupported, in the study of the hydrogen release from *alkali* hydrolysis of sodium borohydride ($NaBH_4$) will be presented. Reports on hydrogen rates and yields are given where a proportion of 0.4 g/g in catalyst/chemical hydride was found suitable, after preliminary kinetic tests. The effects of $NaBH_4$ and an inhibitor (sodium hydroxide, NaOH) concentration, as well as the process temperature, on the rate of hydrogen production were also analysed.

3.2 EXPERIMENTAL PROCEDURE

The *alkali* catalytic hydrolysis of sodium borohydride for hydrogen generation under pressure comprises a series of experiments done in the three batch reactors LR, MR and SR, with internal free volumes of 646 cm^3, 369 cm^3 and 229 cm^3, respectively described in the previous chapter.

The experimental conditions of the investigations done on the effects of reaction temperature, $NaBH_4$ concentration, NaOH concentration, pressure of system and reactor bottom shape on hydrogen generation rates and yields, are given below, separately.

The experimental method used for the particular case study of successive loadings of reactant solutions, to verify the activity of the Ni-based bimetallic catalyst in active refuelling, is also specified.

The hydrogen yield in reaction (3.1) was calculated by the following equation

$$\text{Hydrogen yield} = n(H_2)_{exp} / n(H_2)_{theoretical} \ , \qquad (3.5)$$

where $n(H_2)_{exp}$ is the number of moles (mol) of generated H_2 and $n(H_2)_{theoretical}$ is the theoretical amount of generated H_2 assuming 100% conversion of $NaBH_4$ by applying the ideal gas law to the final volume of gas inside the reactor.

3.2.1 Effect of reaction temperature on hydrogen generation rate

To investigate the effect of reaction temperature on hydrogen generation rate of the catalytic hydrolysis of sodium borohydride, a series of kinetic experiments were carried out in a extensive range of temperatures of: 19.5, 23, 30, 45 and 55 ºC, to satisfy *part* of real environmental conditions throughout the year (very low temperatures were not considered in this dissertation).

The hydrolysis reactions were carried out in the batch reactor MR (internal volume equal to 369 cm^3), using 20 cm^3 of 10 wt% $NaBH_4$ and 3 wt% NaOH solution ($\rho = 1.045\ g/cm^3$).

After a proper quantity of reused Ni-Ru based powdered catalyst (≈ 0.85 g) was stored in the bottom of the reactor and the reaction vessel was perfectly sealed, the batch reactor RM was placed in a thermostatic bath to reach and maintain constant the system temperature at each of the values of the set given above. Then, 20 cm^3 of the reactant

solution was rapidly injected and the inlet valve closed (see legend of Fig.2.5b), with the reactor submersed in the water bath. The generation of hydrogen was followed using the data acquisition system until a constant pressure inside the reactor is reached. No magnetic stirring was used.

In the experiments reported in this section, the Ni-Ru based powdered catalyst was reused between 157 and 161 times.

3.2.2 Effect of $NaBH_4$ concentration on hydrogen generation rate

To explore the effect of sodium borohydride concentration on hydrogen generation rate of the catalytic hydrolysis of sodium borohydride, a series of kinetic experiments was conceived at seven different weight amounts of $NaBH_4$: 5, 10, 15, 20, 25, 30 and 40 wt%, for a constant concentration of an inhibitor (NaOH) of 3 wt%. All the hydrolysis reactions were executed in the batch reactor LR (internal volume of 646 cm^3), using 20 cm^3 of reactant solution, at constant temperature of 27 ºC. The experimental procedure on this research item is similar to that described on the above section. No magnetic stirring was used.

In the experiments run in this part of the analysis, the Ni-Ru based powdered catalyst was reused between 35 and 41 times.

3.2.3 Effect of NaOH concentration on hydrogen generation rate

To examine the effect of the inhibitor sodium hydroxide concentration on the hydrogen generation rate of the catalytic hydrolysis of sodium borohydride, a sequence of kinetic experiments were conceived at six different weight amounts of NaOH: 1, 3, 7, 10, 20 and 30 wt%, for a constant concentration of $NaBH_4$ of 10 wt%. All the hydrolysis reactions were conducted in the batch reactor LR (internal free volume of 646 cm^3), using 10 cm^3 of reactant solution, at constant temperature of 25 ºC. The experimental procedure of this research topic is analogous to that described on 3.2.1. No magnetic stirring was used.

In the experiments reported in this part of the analysis, the Ni-Ru based powdered catalyst was reused between 57 and 62 times.

3.2.4 Effect of pressure on hydrogen generation rate

To study the influence of pressure on the hydrogen generation rate of the catalytic hydrolysis of sodium borohydride, three individual experiments were carried out in each

one of the designed reactors: LR (646 cm^3), MR (369 cm^3) and SR (229 cm^3). A volume of 20 cm^3 of 10 wt% $NaBH_4$ and 7 wt% NaOH solution ($\rho = 1.085\,g/cm^3$) was injected; and the reaction evolved at controllable temperature of 45 ºC, by immersing the reaction vessel in the thermostatic bath. No agitation was present in the solution inside the reactors.

In this section, the Ni-Ru based powdered catalyst was reused 141 times, 154 times and 170 times, respectively, for the experiments performed in reactors LR, MR and SM.

3.2.5 Effect of reactor bottom shape on hydrogen generation rate

To understand the influence of the reactor bottom shape on the hydrogen production rate - this topic constitutes one of the *originalities* of the present dissertation, two different batch reactors were used in the kinetic studies, both with approximately the same internal volume (≈ 369 cm^3) but with different bottom shapes: one has a flat bottom and the other a conical bottom geometry. A volume of 10 cm^3 of 10 wt% $NaBH_4$ and 7 wt% NaOH solution ($\rho = 1.085\,g/cm^3$) was chosen; and the reaction advanced more or less at a constant room temperature of ≈ 26 ºC. A proportion of Ni-Ru based catalyst/$NaBH_4$: 0.4 g/g (≈ 0.43 g) was found suitable for the experiments. No agitation was present in the solution inside the reactors.

The Ru-Ni based catalyst at this section was virgin, i.e., 0 times reused!

3.2.6 Effect of *successive loadings* of reactant solution on catalyst activity

With the objective of studying the influence of successive loadings of reactant solution on the catalyst activity, an experimental work was performed with several successive loadings of reactant alkaline $NaBH_4$ solution, with a concentration of 10 wt% $NaBH_4$ and 7 wt% NaOH by weight ($\rho = 1.085\,g/cm^3$), in two different batch reactors. *Fuel* loadings of 10 cm^3 were established and a proportion of Ni-Ru based/$NaBH_4$: 0.4g/g (≈ 0.43 g) was found appropriate and used in all experiments.

The hydrogen yield in reaction (3.1) was calculated assuming 100 % conversion of $NaBH_4$ by applying the ideal gas law to the final volume of gas inside the reactor, with x=2. Special care was taken to correct the free varying volume of gas inside the reactor between each successive reactant loading.

Reactors LR (646 cm^3) and MR (369 cm^3) were preferred in this research topic to perform the entire experimental work, at uncontrolled room temperature and without magnetic stirring.

The Ni-Ru based powdered catalyst was reused between 2 and 6 times in the experiments conducted in the MR batch reactor, and reused between 28 and 34 times in the experiments performed in the LR reactor.

3.2.6.1 Effect of agitation on hydrogen reaction rate

With the intention of verifying the influence of agitation on hydrogen reaction rate during successive loadings of *fuel*, a Teflon™ magnetic stirrer was placed inside the reactor LR after the 7th successive loading and prior to the 8th *fuel* injection, in a run of experiments with eight successive loadings. Vigorous magnetic stirring, set at a high level (level 8 of 10 of the stirrer), was allowed immediately after the 8th injection and the inlet reactor valve closed. The generation of H_2 was followed using the data acquisition system until reaching a constant pressure inside the LR reactor. Inspection on the variation of system pressure with time, during the 8th H_2 generation, put forward the importance of considering diffusion limitations in this particular subject of successive *fuel* loadings.

The Ni-Ru based powdered catalyst was reused between 226 and 233 times in these experiments!

3.3 RESULTS AND DISCUSSION

3.3.1 Effect of reaction temperature on hydrogen generation rate

The influence of temperature on the velocity of hydrogen generation is put in evidence in Figure 3.1.

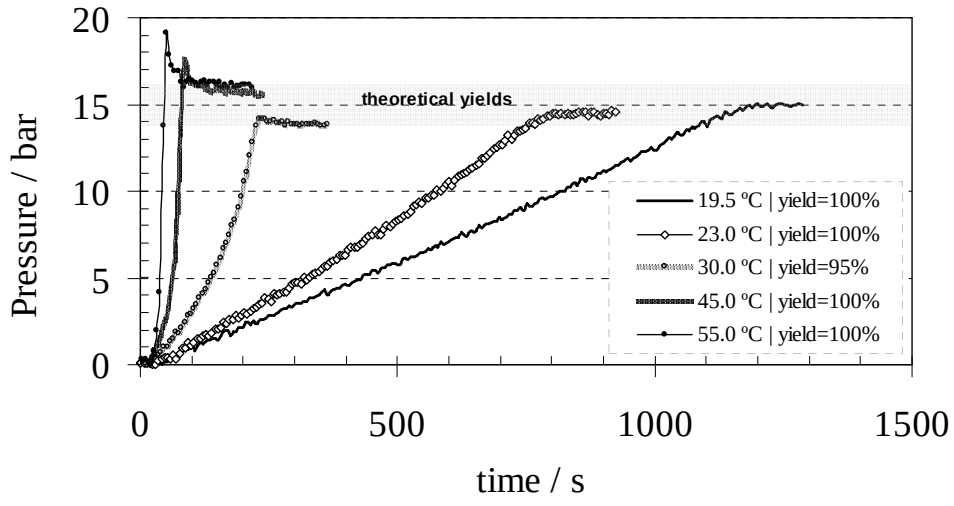

Figure 3.1. Hydrogen generation plot with a $NaBH_4$ concentration of 10%, an inhibitor concentration of 3%, at different temperatures. The reactions, for 20 cm^3 of reactant solution, were performed in the MR batch reactor (369 cm^3) with a proportion of Ni-Ru based catalyst/$NaBH_4$: 0.4 g/g.

As can be seen in the figure, the reaction rate is very sensitive to this variable. As expected, the rate rises with the increase in temperature and the hydrogen pressure demonstrates a near linear variation with reaction time. The influence of temperature is clearly shown by the increasing slope values on the linear region of the plots, for increasing values of the reaction temperature. The reaction rate remains practically constant when, during the hydrolysis process, the $NaBH_4$ concentration decreases due to hydride and water consumption, demonstrating, under the experimental conditions studied zero-order reaction as was also found by Kaufman and Sen [3.12] and Hua *et al.* [3.30]. The time needed for the reaction to begin is almost the same for al the reactions depicted in Fig.3.1.

3.3.2 Effect of $NaBH_4$ concentration on hydrogen generation rate

Figure 3.2, shows the hydrogen generation rate curves obtained with seven different concentrations of $NaBH_4$.

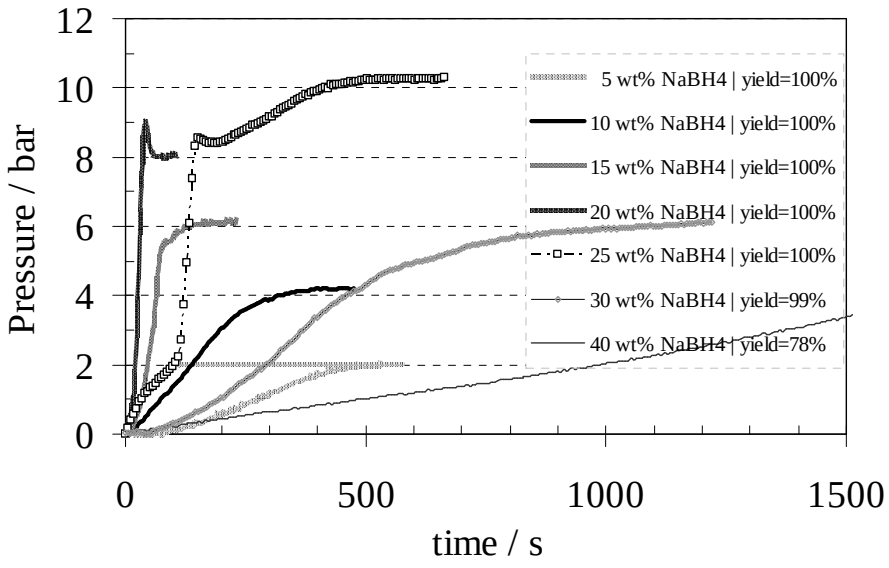

Figure 3.2. Hydrogen generation plot with an inhibitor concentration of 3%, at 27 ºC, and with different $NaBH_4$ concentrations. The reactions where performed in LR batch reactor (646 cm^3) with a proportion of Ni-Ru based catalyst/$NaBH_4$: 0.4 g/g.

Hydrogen generation rate increases with increasing the alkali concentrations up to 20 wt% in the alkali. Then, the reaction rate and hydrogen yield are both slightly lower for the higher concentration of borohydride, above 20 wt%. This is due to the fact that, for these levels of $NaBH_4$ concentrations, as the hydrolysis reaction proceeds, the concentration of the reaction product $NaBO_2$ exceeds its solubility limit and precipitates out of solution, as

has been mentioned in Section 3.1. This fact may block catalysts sites, thereby affecting the generation rate. This explanation was already proposed by Amendola *et al.* [3.5,3.6].

3.3.3 Effect of NaOH concentration on hydrogen generation rate

Figure 3.3 shows the dependence of the *classic* hydrolysis reaction rate on the NaOH concentration.

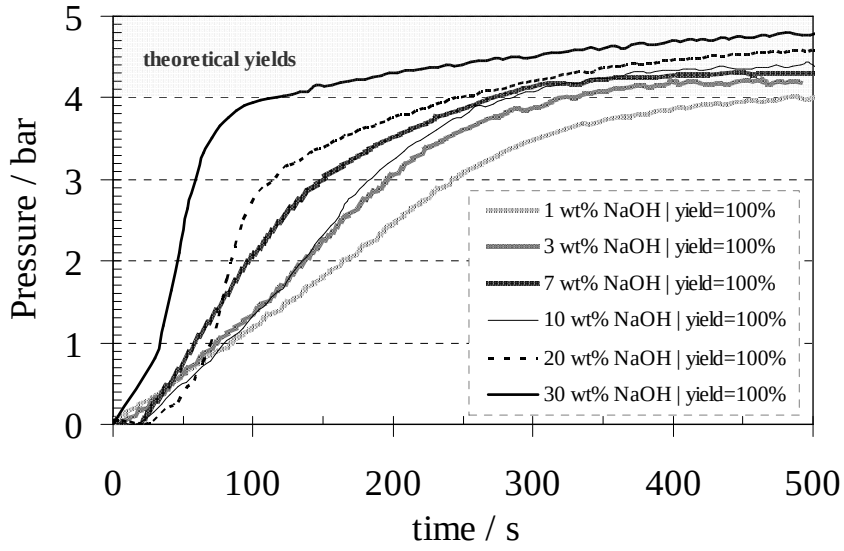

Figure 3.3. Hydrogen generation with a $NaBH_4$ concentration of 10%, at 25 ºC, with different NaOH concentrations. The reactions, for 10 cm^3 of reactant solution, were performed in LR batch reactor (646 cm^3) with a proportion of Ni-Ru based catalyst/$NaBH_4$: 0.4 g/g.

The reaction rate is greatly enhanced by the increase of the NaOH concentration, as can be see if Fig.3.3, with the highest value found for inhibitor concentration of 30 wt%. This result was already reported by Hua *et al.* [3.30] who used a nickel boride catalyst.

3.3.4 Effect of pressure on hydrogen generation rate

The influence of the pressure in the hydrogen generation efficiency is put in evidence in the plot of Figure 3.4.

In fact, for two of the experiments performed in this section, in reactors MR and SR, an average yield of 92% was reached, i.e., the maximum hydrogen pressures reached were substantially lower than the maximum predicted hydrogen pressure, assuming 100% conversion, by applying the ideal gas law. Pinto *et al.* [3.33], who worked in a similar experimental work, found the same behaviour in the H_2 yield, and related this finding with solubility effects in the liquid phase that remains inside the reactor. Thus, it seems possible

that increasing the gas pressure enhances strongly the H_2 dissolution, forcing part of the molecular H_2 to be in the liquid. Consequently, H_2 yields diminished.

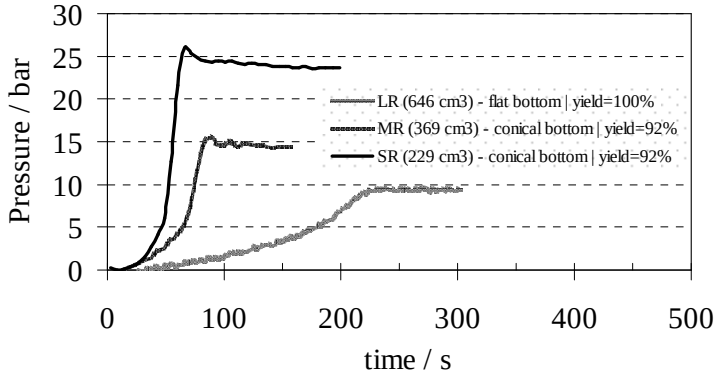

Figure 3.4. Hydrogen generation with a $NaBH_4$ concentration of 10 wt%, an inhibitor concentration of 7wt%, at 45 ºC, for the three design reactors: LR (646 cm^3), MR (369 cm^3) and SR (229 cm^3). The reactions, for 20 cm^3 of reactant solution, were performed with a proportion of Ni-Ru based catalyst/$NaBH_4$: 0.4 g/g.

3.3.5 Effect of reactor bottom shape on hydrogen generation rate

Finally, the effect of reactor bottom shape on hydrogen generation is outlined in Figure 3.5. Definitely, as can be seen in the plot of Fig.3.5, the reactor bottom shape affects the course of hydrogen generation.

Looking at the results illustrated in Fig.3.5, the conical bottom geometry adopted in MR batch reactor increases the reaction rate and yield, in the absence of H_2 lag time (defined as the time required observing formation of H_2).

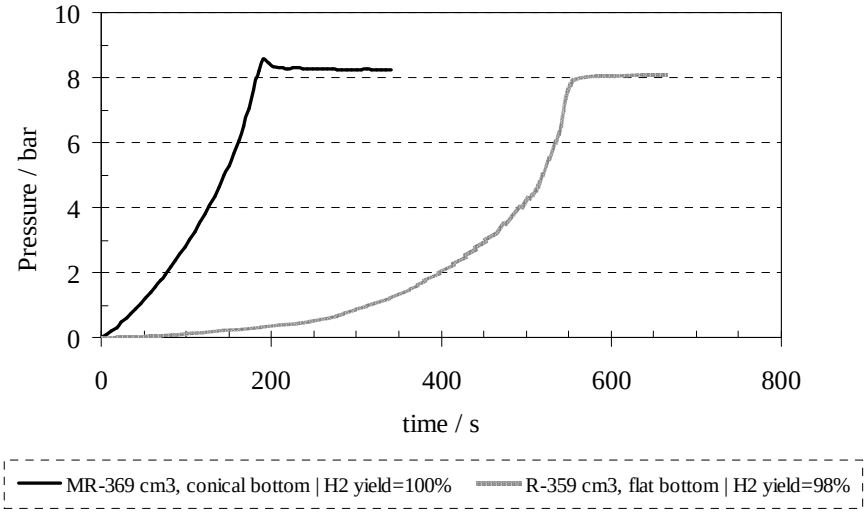

Figure 3.5. Hydrogen generation plots with a $NaBH_4$ concentration of 10%, an inhibitor concentration of 7%, at ≈ 26 ºC, for two batch reactors with different bottom shape. The reactions, for 10 cm^3 of reactant solution, were performed with a proportion of Ni-Ru based catalyst/$NaBH_4$: 0.4 g/g.

3.3.6 Effect of *successive loadings* of reactant solution on catalyst activity

Figure 3.6, shows the '*dP/dt*' behaviour of five 10 cm^3 single successive loadings of reactant solution, with concentration of 10 wt% $NaBH_4$, 7 wt.% NaOH, 83 wt.% H_2O, in the batch reactor LR (646 cm^3). It was found appropriate to show, in the same figure, the variation of temperature inside the reactor that occurs during a single *fuel* loading. Similar trends were detected in the experiments performed in the batch reactor MR.

As can be seen in the plot of Fig. 3.6, the rise of temperature at the bottom of the reactor (T.Bottom) occurs during each individual *fuel* loading until the "plateau" is reached, and this effect is more pronounced in the last loadings. When the temperature of the system is not controlled, as is this case, the exothermic characteristics of reaction (3.1) give rise to the medium gas temperature near the top of the reactor (positioned vertically). This is favourable, due to the hydrolysis kinetic rates, because it leads to an increase of H_2 pressure with smaller amount of the needed activation energy required by the (same quantity of) catalyst, which is housed in the bottom of the reactor.

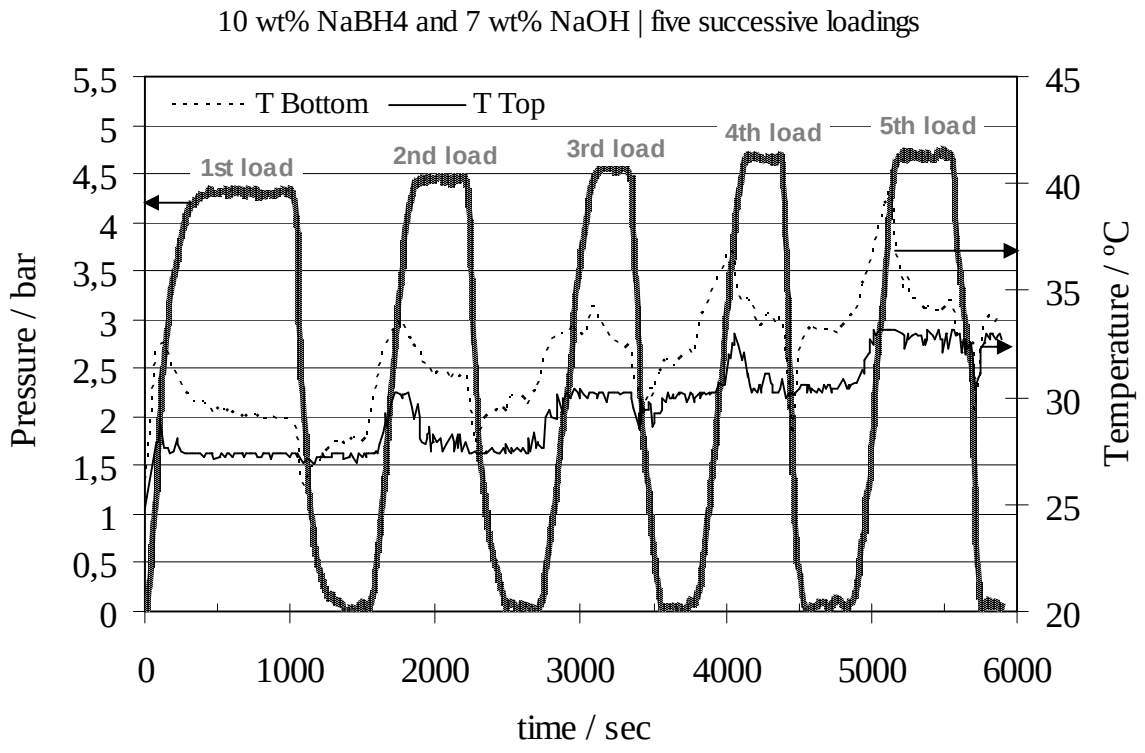

Figure 3.6. Five successive loadings of the reactant solution: 10 wt.% $NaBH_4$, 7 wt.% NaOH, 83 wt.% H_2O, with Ni-Ru based/$NaBH_4$: 0.4g/g, performed in the batch reactor LR (646 cm^3), showing the temperature profile inside the reactor at two specific points (bottom and top of reactor).

The fluctuations detected in the reactor temperature along reaction (see Fig. 3.6), also indicate at which rates the hydrogen is being generated, i.e., a smooth pattern of the internal reactor temperature profile, both at the bottom and at its top, indicates a slowly hydrolysis kinetics; but, an asymptotically and random patterns in reactor temperature profiles, put in evidence the dynamic behaviour of reactants and products inside the reactor due to increased internal pressure. The plot in Figure 3.7 corroborates this assumption, showing slight higher hydrogen rates for the last loadings, in which the variation of temperature were more pronounced.

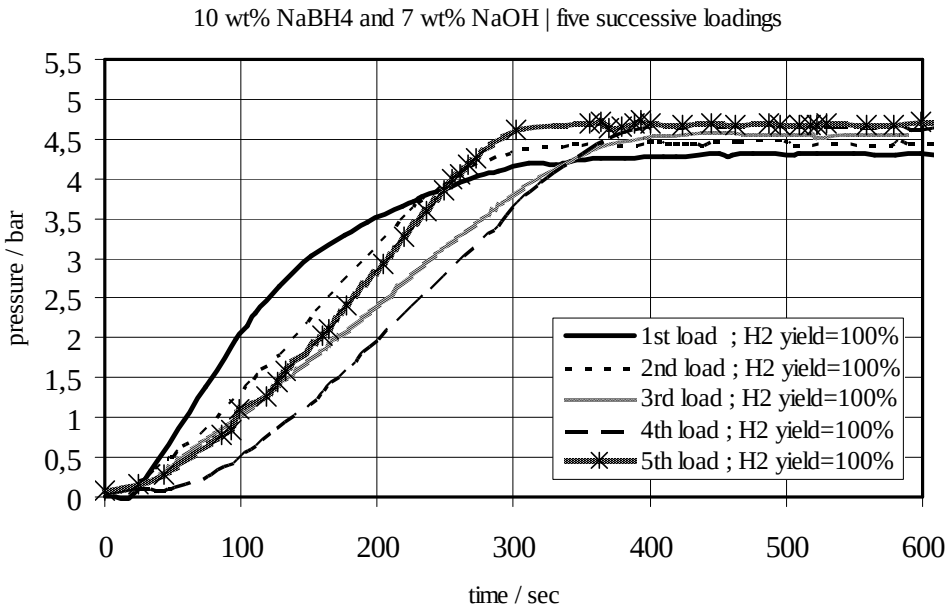

Figure 3.7. Hydrogen generation in batch reactor LR (646 cm^3) of five successive loadings of 10 mL each of the reactant solution: 10 wt.% $NaBH_4$, 7 wt.% NaOH, 83 wt.% H_2O, with Ni-Ru based catalyst/$NaBH_4$: 0.4g/g.

Figure 3.8 show a typical course of hydrogen generation, presented also in terms of the operating pressure as a function of time, for seven successive loadings of *fuel* solution, in batch reactor MR (369 cm^3). These results show an improvement in the performance of the used nickel based catalyst, comparing with similar trend published by Pinto *et al.* [3.33], the latter without ruthenium. In fact, the nano powdered Ni-Ru based catalyst used in the experiments reported on this dissertation, gives higher H_2 yield in a relatively short reaction time until the 'plateau' is achieved.

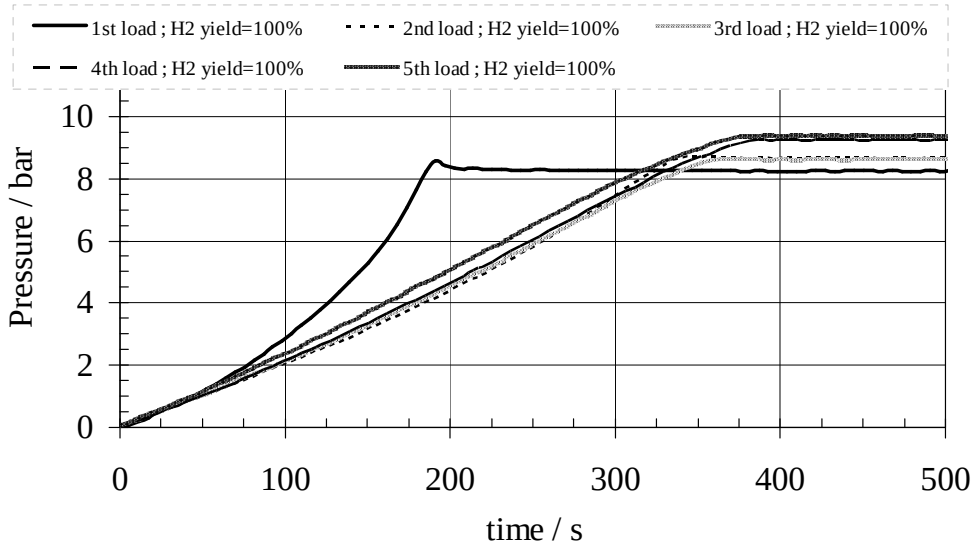

Figure 3.8. Hydrogen generation in batch reactor MR (369 cm^3) of seven successive loadings of the reactant solution: 10 wt.% $NaBH_4$, 7 wt.% NaOH, 83 wt.% H_2O, with Ni-Ru based catalyst/$NaBH_4$: 0.4g/g.

As mentioned by Pinto *et al.* [3.33], the increasing pressure of the gas phase inside the reactor, due to hydrogen generation, forces at the same time, the hydrogen dissolution. This is an interesting finding since molecular hydrogen was generated but also stored in the liquid phase.

Figure 3.9 shows the gaseous reaction products upshot after a quick exit from the reactor, at the end of the reaction of the seven successive loading (the H_2 generated in the previous successive loadings, was released to the atmosphere).

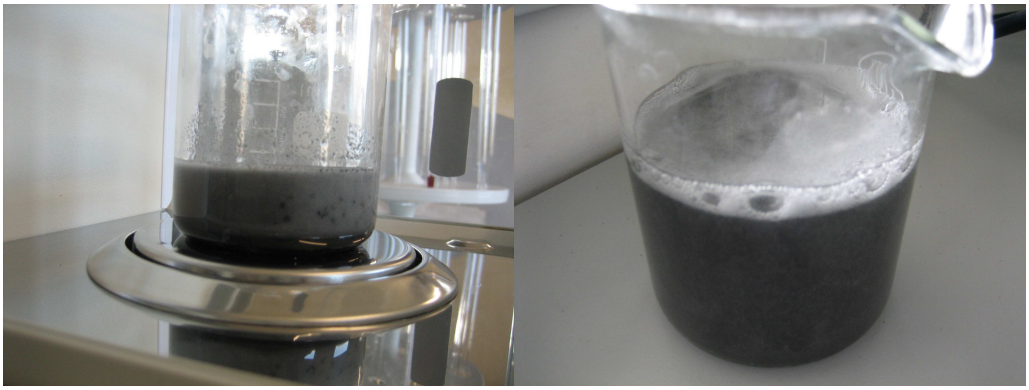

Figure 3.9. Two images of reaction "gaseous" by-product, after seven successive loadings of reactant solution (10 wt.% $NaBH_4$, 7 wt.% NaOH, 83 wt.% H_2O). The H_2 release shows the gas capability to agitate the nickel-based powdered catalyst presented at the reactor liquid phase.

As we can see, the "sparkling" by-product quickly dissipates the H_2 bubbles along the glass goblet, showing the gas capability to agitate the nickel-based bimetallic powdered

catalyst presented at the reactor liquid phase. This attests that a significant amount of the H_2 generated inside the reactor was trapped in the liquid reactor phase, keeping it dissolved. Just after a slight aperture of the reactor exhaustion needle valve, due to pressure differences, the *dissolved* gas (H_2 plus air) is released.

3.3.6.1 Effect of agitation on hydrogen reaction rate

In addition, and with the purpose of verifying the influence of agitation on hydrogen reaction rate during successive loadings of *fuel*, a Teflon™ magnetic stirrer was placed inside the reactor prior to the first loading injection. The series of experiments performed on this section, the Ni-Ru based powdered catalyst was reused between 226 and 233 times.

Vigorous magnetic stirring was allowed during the formation of hydrogen by injection of the 8th loading of reactant in a series of experiments by successive refuelling, to promote complete mass transfer (to overcome diffusion limitation). Figure 3.10, shows an eligible increase in yield and rate of H_2, lowered by a minor reaction induction time (by comparing the results with the previous 6th an 7th loadings). This leads us to infer that mass transfer limitations exist between the reacting solution and the reused (233 times!) catalyst.

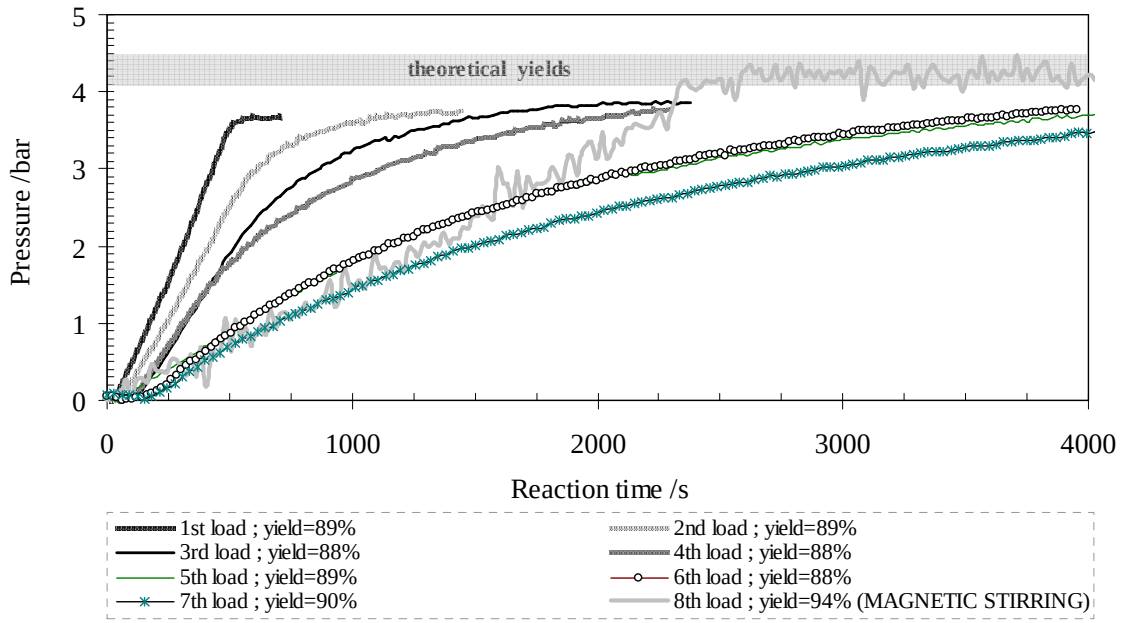

Figure 3.10. Hydrogen generation in batch reactor LR (646 cm^3) of eight successive loadings of 10 mL of the reactant solution: 10 wt.% $NaBH_4$, 7 wt.% NaOH, 83 wt.% H_2O, with Ni-Ru based catalyst/$NaBH_4$: 0.4g/g (the 8th loading was performed with magnetic stirring), at 25 ºC.

3.4 REACTION BY-PRODUCT CHARACTERIZATION

The by-products of the hydrogen generation reactions of all types of experiments reported on this chapter were analyzed by X-Ray Diffractometry. Suitable crystals – see Figure 3.11, were obtained by slow evaporation of a water solution at uncontrolled environmental conditions.

Accordingly to publish literature, boric oxides come in white rhombic crystals or colourless, semi-transparent vitreous granules or flates, or hygroscopic lumps or powder (the crystals, usually forms a glass, have specific gravity's of 1.84-2.46 and melt at 450 ºC) [3.49].

Figure 3.11. Crystals pictures of the by-product *classic* hydrolysis of sodium borohydride, obtained by slow evaporation of a water solution at room temperature (≈ 25 ºC).

3.4.1 Materials and methods

The obtained crystals were found to be orthorhombic, space group $Pca2_1$, cell volume V=364.62(4) Å^3, a = 10.7252(7) Å, b = 5.2525(3) Å, c = 6.4724(4) Å (uncertainties in parentheses). There are four molecules per unit cell, calculated density 2.237 g/cm^3. Diffraction data were collected at 293 K with a Gemini PX Ultra equipped with MoKα radiation (λ=0.71073 Å). A total of 562 independent reflections were measured, of which 501 were observed ($I>2\sigma(I)$). The structure was solved by direct methods using SHELXS-97 [3.50] with atomic positions and displacement parameters refined with SHELXL-97 [3.51]. The non-hydrogen atoms were refined anisotropically and the hydrogen atoms were refined freely with isotropic displacement parameters. The refinement converged to R (all data) = 3.93% and wR^2(all data) = 9.92%.

3.4.2 Results and discussion

The crystal structure of the reaction (3.1) by-product reveals that the boron atoms are in a triangular configuration with three oxygen atoms, with B-O bond lengths between 1.27 and

1.29 Å. The BO_3 triangular arrangement was already found in the crystal structure of orthorhombic [3.52] and monoclinic [3.53] metaboric acid although in the title crystal structure the oxygen atoms are bound to just one B atom. The BO_3 triangles form layers 3.238 Å apart that sandwich a layer of sodium and water molecules. For each boron atom there are three bounded oxygen atoms and one water oxygen.

Half of the sodium atoms have their valence strength distributed between six Na-O bonds and the other half between seven Na-O bonds (as already determined in other sodium metaborate structures [3.54]). The water molecules are involved in a net of interactions with the sodium atoms. Figure 3.12, below, shows two different views of the crystal structure.

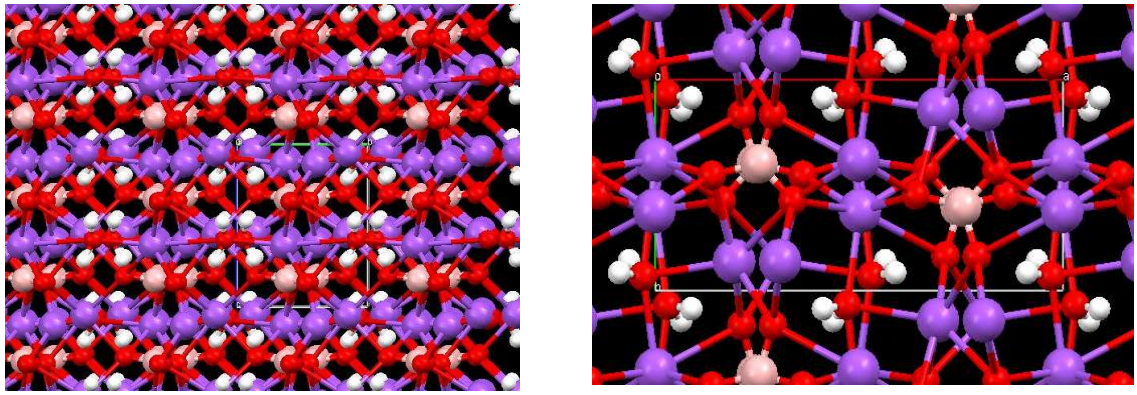

(a) (b)

Figure 3.12. Views of crystal structure of sodium metaborate dehydrate showing stacking layers formed by BO_3 triangles and by Na and water molecules: (a) view along the *a*-axis and (b) view along the *c*-axis. Na in violet, O in red, B in pink and H in white.

We may conclude that the reaction (3.1) by-product, in all the types of experiments performed by *alkali* hydrolysis of $NaBH_4$ under pressure, is a sodium metaborate dehydrated, $NaBO_2.2H_2O$, as expected. Therefore, equation (3.1) can be re-written as follows:

$$NaBH_4 + \mathbf{4}\, H_2O \rightarrow NaBO_2.\mathbf{2}H_2O + 4\, H_2 + \text{heat}\,. \qquad (3.6)$$

3.5 CONCLUSIONS

In this chapter the results of an extensive experimental work done with the objective of studying various effects in hydrogen generation rate, yield and lag time, by catalytic *alkali* hydrolysis of sodium borohydride, are reported. Briefly, the main conclusions are:

- increasing the temperature of the reaction medium, increases the rate of H_2 generation;
- the reaction rate increases with increasing the hydride concentration up to 20 wt% of $NaBH_4$. Above this value, a slight decrease on both H_2 and yield was found;
- the reaction rate is greatly enhanced by the increase of the NaOH concentration, ensuring good efficiency of hydrogen generation;
- an average yield of ≈ 90% was found in H_2 generation; this is substantially lower than the maximum predicted hydrogen pressure, assuming 100% conversion and applying the ideal gas law. Pinto *et al.* [3.33] suggests that this fact is related with solubility effects in the liquid phase that remains inside the reactor;
- the reactor bottom shape affects the course of hydrogen generation. It was found that the conical bottom geometry leads to an increase on reaction rate and yield, and slightest in H_2 time lag;
- the Ni-Ru based catalyst has a good performance in refueling experiments. In fact, it was found that the catalyst tends to perform better, after the first loading of reactant (the amount of catalyst remains the same from the first to the last loading);
- a vigorous stirring of the solution inside the batch reactor, during the experiments with successive fuel loadings, reveals minor reaction induction time and a slight higher yield in hydrogen generation. This indicates possible mass transfer limitations during the course of reaction between the fuel and the active sites of the catalyst.

The x-ray diffractions analysis revealed a sodium metaborate dehydrated, $NaBO_2.2H_2O$, as the by-product of all experiments performed in the several subsections of this chapter.

3.6 REFERENCES

[3.1] H. I. Schlesinger, H. C. Brown, A. E. Finholt, J. R. Gilbreath, H. R. Hoekstra, E. K. Hyde, Sodium Borohydride, Its Hydrolysis and Its Use as a Reducing Agent and in the Generation of Hydrogen, J. Am. Chem. Soc. 75(1953) 215-219.

[3.2] V. C. Y. Kong, F. R. Foulkes, D. W. Kirk, J. T. Hinatsu, Development of Hydrogen Storage for Fuel Cell Generators. I: Hydrogen Generation Using Hydrolysis of Hydrides, Int. J. Hydrogen Energy 24, 7 (1999) 665-675.

[3.3] W. H. Stockmayer, R. R. Miller, R. J. Zeto, Kinetics of Borohydride Hydrolysis. J. Phys. Chem. 65 (1961) 1076-1077.

[3.4] R. Aiello, J. H. Sharp, M. A. Matthews, Production of Hydrogen from Chemical Hydrides via Hydrolysis with Steam, Int. J. Hydrogen Energy 24, 12 (1999) 1123-1130.

[3.5] S. C. Amendola, S. L Sharp-Goldman, M. S. Janjua, M. T. Kelly, P. J. Petillo, M. Binder, An Ultrasafe Hydrogen Generator: Aqueous, Alkaline Borohydride Solutions and Ru Catalyst, J. Power Sources 85, 2 (2000) 186-189.

[3.6] Amendola S. C., S. L. Sharp-Goldman, M. S. Janjua, N. C. Spencer, M. T. Kelly, P. J. Petillo, M. Binder, A Safe, Portable, Hydrogen Gas Generator Using Aqueous Borohydride Solution and Ru Catalyst, Int. J. Hydrogen Energy 25, 10 (2000) 969-975.

[3.7] Y. Kojima, K.-I. Suzuki, K. Fukumoto, M. Sasaki, T. Yamamoto, Y. Kawai, H. Hayashi, Hydrogen Generation Using Sodium Borohydride Solution and Metal Catalyst Coated on Metal Oxide, Int. J. Hydrogen Energy 27,10 (2002) 1029-1034.

[3.8] W.C. Blasdale, C.M. Slansky, The solubility curves of boric acid and the borates of sodium, J. Am. Chem. Soc. 61 (1939) 917-920.

[3.9] E. Marrero-Alfonso, J.R. Gray, T.A. Davis, M.A. Matthews, Hydrolysis of sodium borohydride with steam, Int. J. Hydrogen Energy 32 (2007) 4717-4722.

[3.10] E. Marrero-Alfonso, J.R. Gray, T.A. Davis, M.A. Matthews, Minimizing water utilization in hydrolysis of sodium borohydride: the role of sodium metaborate hydrates, Int. J. Hydrogen Energy 32 (2007) 4723-4730.

[3.11] Y. Shang, R. Chen, Hydrogen storage via the hydrolysis of $NaBH_4$ basic solution: optimization of $NaBH_4$ concentration, Energy & Fuels 20 (2006) 2142-2148.

[3.12] C. M. Kaufman, B. Sen, Hydrogen generation by hydrolysis of sodium tetrahydroborate: effects of acids and transition metals and their salts, J. Chem. Soc. Dalton 2 (1985) 307-313.

[3.13] M. Kreevoy, J. Hutchins, H_2BH_3 as an intermediate in tetrahydridoborate hydrolysis, J. Am. Chem. Soc. 94, 18 (1972) 6371-6376.

[3.14] F. T. Wang, W. L. Jolly, Kinetic study of the intermediates in the hydrolysis of the hydroborate ion, Inorg. Chem. 11, 8 (1972) 1933-1941.

[3.15] B. D. James, M. G. H. Wallbridge, Metal tetrahydroborates, Prog. Inorg. Chem. 11 (1970) 199-231.

[3.16] M. M. Kreevoy, R. W. Jacobson, The rate of decomposition of sodium borohydride in basic aqueous solutions, Ventron Alembic 15 (1979) 2-3.

[3.17]. G. Y. Moon, S. S. Lee, K. Y. Lee, S. H. Kim, K. H. Song, Behavior of hydrogen evolution of aqueous sodium borohydride solutions, J. Ind. Eng. Chem. 14, 1 (2008) 94-99.

[3.18] V. G. Minkina, S. I. Shabunya, V. I. Kalinin, V. V. Martynenko, Stability of aqueous-alkaline sodium borohydride formulations. Russ. J. Appl. Chem. 81, 3 (2008) 380-385.

[3.19] Y. Kojima, Y. Kawai, M. Kimbara, H. Nakanishi, S. Matsumoto, Hydrogen Generation by Hydrolysis Reaction of Lithium Borohydride, Int. J. Hydrogen Energy 29, 12 (2004) 1213-1217.

[3.20] H.C. Brown, C.A. Brown, New highly active metal catalysts for the hydrolysis of borohydride, J. Am. Chem. Soc. 84 (1962) 1493-1494.

[3.21] Y. Kojima, K.-I. Suzuki, K. Fukumoto, Y. Kawai, M. Kimbara, H. Nakanishi, S. Matsumoto, Development of 10 kW-scale hydrogen generation using chemical hydride, J. Power Sources 125 (2004) 22-26.

[3.22] Y. Kojima, Y. Kawai, H. Nakanishi, S. Matsumoto, Compressed hydrogen generation using chemical hydride, J. Power Sources 135 (2004) 36-41.

[3.23] C. Wu, H. Zhang, B. Yi, Hydrogen generation from catalytic hydrolysis of sodium borohydride for proton exchange membrane fuel cells, Cat. Today 93-95 (2004) 477-483.

[3.24] P. Krishnan, T.H. Yang, W.Y. Lee, C.S. Kim, PtRu-$LiCoO_2$ an efficient catalyst for hydrogen generation from sodium borohydride solutions, J. Power Sources 143 (2005) 17-23.

[3.25] J.S. Zhang, W.N. Delgass, T.S. Fisher, J.P. Gore, Kinetics of Ru-catalyzed sodium borohydride hydrolysis, J. Power Sources 164 (2007) 772-781.

[3.26] S. Özkar, M. Zahmakiran, Hydrogen generation from hydrolysis of sodium borohydride usisng Ru(0) nanoclusters as catalyst, J. Alloys Comp 404-406 (2005) 728-731.

[3.27] R. Peña-Alonso, A. Sicurelli, E. Callone, G. Carturan, R. Raj, A picoscale catalyst for hydrogen generation from $NaBH_4$ for fuel cells, J. Power Sources 165 (2007) 315-323.

[3.28] J.H. Kim, K.T. Kim, Y.M. Kang, H.S. Kim, M.S. Song, Y.J. Lee, P.S. Lee, J.Y. Lee, Study on degradation of filamentary Ni catalyst on hydrolysis of sodium boroydride, J. Alloys and Compounds 379 (2004) 222-227.

[3.29] A. Levy, J.B. Brown, C.J. Lyons, Catalyzed hydrolysis of sodium borohydride, Ind. Engng Chem. 52 (1960) 211-214.

[3.30] D. Hua, Y. Hanxi, A. Xinping, C. Chuansin, Hydrogen production from catalytic hydrolysis of sodium borohydride solution using nickel borid catalyst, Int. J. Hydrogen Energy 28 (2003) 1095-2000.

[3.31] S.U. Jeong, R.K. Kim, E.A. Cho, H.J. Kim, S.W. Nam, I.H. Oh, S.A. Hong, S.H. Kim, A study on hydrogen generation from $NaBH_4$ solution using the high-performance Co-B catalyst, J. Power Sources 144 (2005) 129-134.

[3.32] B.H. Liu, Z.P. Li, S. Suda, Nickel and cobalt-based catalyst for hydrogen generation by hydrolysis of borohydride, J. Alloys and Compounds 415 (2006) 288-293.

[3.33] A.M.F.R. Pinto, D.S. Falcão, R.A. Silva, C.M. Rangel, Hydrogen generation and storage from hydrolysis of sodium borohydride in batch reactors, Int. J. Hydrogen Energy 31 (2006) 1341-1347.

[3.34] C.M. Rangel, R.A. Silva, A.M.F.R. Pinto, Fuel cells and on-demand hydrogen production: didactic demonstration prototype, Proceedings of the International Conference in Power Engineering and Electric Drives, Eds. L.S. Martins and P. Santos, Setúbal, Portugal, September 12-14, 2007, paper 237.

[3.35] J.C. Ingersoll, N. Mani, J.C. Thenmozhiyal, A. Muthaiah, Catalytic hydrolysis of sodium borohydride by a novel nickel-cobalt-boride catalyst, J. Power Sources 173 (2007) 450-457.

[3.36] S.U. Jeong, E.A. Cho, S.W. Nam, I.H. Oh, U.H. Jung, S.H. Kim, Effect of preparation method on Co-B catalytic activity for hydrogen generation from alkali $NaBH_4$ solution, Int. J. Hydrogen Energy 32 (2007) 1749-1754.

[3.37] J.C. Walter, A. Zurawski, D. Mongomery, M. Thornburg, S. Revankar, Sodium borohydride hydrolysis kinetics comparison for nickel, cobalt and ruthenium boride catalyst, J. Power Sources 179 (2008) 335-339.

[3.38] S.J. Kim, J. Lee, K.Y. Kong, C.R. Jung, I.G. Min, S.Y. Lee, H.J. Kim, S.W. Nam, T.H. Lim, Hydrogen generation system using borohydride for operation of a 400 W-sacle polymer electrolyte fuel cell stack, J. Power Sources 170 (2007) 412-418.

[3.39] J. Lee, K.Y. Kong, C.R. Jung, E. Cho, S.P. Yoon, J. Han, T.G. Lee, S.W. Nam, A structured Co-B catalyst for hydrogen extraction from $NaBH_4$ solution, Cat. Today 120 (2007) 305-310.

[3.40] J. Zhao, H. Ma, J. Chen, Improved hydrogen generation from alkaline $NaBH_4$ solution using carbon-supported Co-B a catalyst, Int. J. Hydrogen Energy 32 (2007) 4711-4716.

[3.42] C. Zanchetta, B. Patton, G. Guella, A. Miotello, An integrated apparatus for production and measurement of molecular hydrogen, Meas. Sci. Tech. 18 (2007) N21-N26.

[3.43] W. Ye, H. Zhang, D. Xu, L. Ma, B. Yi, Hydrogen generation utilizing alkaline sodium borohydride solution and supported cobalt catalyst, J. Power Sources 164 (2007) 544-548.

[3.44] Ö. Metin, S. Özkar, Hydrogen generation from the hydrolysis of sodium borohydride by using water dispersible, hydrogenphosphate-stabilized nickel(0) nanoclusters as catalyst, Int. J. Hydrogen Energy 32 (2007) 1707-1715.

[3.45] M. Mitov, R. Rashkov, N. Atanassov, A. Zielonka, Effects of nickel foam dimensions on catalytic activity of supported Co-Mn-B nanocomposites for hydrogen generation from stabilized borohydride solutions, J. Mater. Sci. (42) 2007 3367-3372.

[3.46] K.W. Cho, H.S. Kwon, Effects of electrodeposited Co and Co-P catalysts on the hydrogen generation properties from hydrolysis of alkaline sodium borohydride solution, Cat. Today 120 (2007) 298-304.

[3.47] K. Eom, K.W. Cho, H.S. Kwon, Effects of electroless deposition conditions on microstructures of cobalt-phosphorous catalysts and their hydrogen generation properties in alkaline sdium borohydride solution, J. Power Sources 180 (2008) 484-490.

[3.48] J.H. Park, P. Shakkthivel, H.J. Kim, M.K. Han, J.H. Jang, Y.R. Kim, H.S. Kim, Y.G. Shul, Investigation of metal alloy catalyst for hydrogen release from sodium borohydride for polymer electrolyte membrane fuel cell application, Int. J. Hydrogen Energy 33 (2008) 1845-1852.

[3.49] F. A. Cotton, G. Wilkinson, *in* "Advanced Inorganic Chemistry", John Wiley & Sons, 5th Edition, Chapter Six, p.162.

[3.50] G.M. Sheldrick, SHELXS-97, Program for the solution of crystal structures; University of Göttingen: Germany 1997.

[3.51] G.M. Sheldrick, SHELXL-97, Program for the refinement of crystal structures; University of Göttingen: Germany 1997.

[3.52] H. Tazaki, The structure of orthorhombic metaboric acid, HBO_2 (α), J. Sci. Hiroshima Univ. A10, 37 (1940) 55-61.

[3.53] W.H. Zachariasen, The crystal structure of monoclinic metaboric acid, Acta Cryst. 16 (1963) 385-389.

[3.54] M. Marezio, H.A. Plettinger, W.H. Zachariasen, The bond lengths in the sodium metaborate structure, Acta Cryst. 16 (1963) 594-595.

CHAPTER 4

Alkali free hydrolysis
Results for sodium borohydride kinetic experiments

This chapter shows the results obtained on alkali free hydrolysis of sodium borohydride in the presence of a reused nickel based bimetallic catalyst. A discussion on the stoichiometry of hydrolysis, in terms of the number of added water molecules to solid $NaBH_4$, is carried out, based on the results of hydrogen generation rate and yields. Emphasis is given to reactor bottom design effects on the hydrogen production. The reaction by-products are analysed by XRD.

4.1 INTRODUCTION

The main inspiration behind developing this experimental *item* was to be capable of producing pure molecular hydrogen with very high gravimetric and volumetric densities.

The gravimetric and volumetric energy densities attainable from hydrolysis of chemical hydrides depend in large measure on the amount of water required for the process. It is well known that hydrolysis of sodium borohydride produces hydrated metaborate by-products in which the degree of hydration of the metaborate is closely joined to the amount of water present in the reaction [4.1].

In the previous chapter, attention was focused on studying the catalytic stabilized hydrolysis of sodium borohydride in the presence of water excess, namely *alkali* hydrolysis of sodium borohydride, for hydrogen generation (this reaction generates basic species that are thermodynamically and kinetically metastable, causing the reaction to cease at low yields of hydrogen even though the reaction is strongly favoured thermodynamically [4.2]). The results revealed that when working at high pressures, and in the presence of a Ni-Ru based catalyst, even with water in excess, it is possible to produce

compressed H_2 at ≈ 99% yields. The *alkali* hydrolysis by-products were $NaBO_2.2H_2O$ under a variety of reaction conditions.

The objective of the study presented in this chapter, is practically the same - produce hydrogen at high pressures, but with very high gravimetric hydrogen density. Then, instead of dealing with an excess of water, a solid *fuel* plus a stoichiometric amount of pure water was used, in the absence of an alkali inhibitor. In this way, it is suitable to call this research topic *alkali free* hydrolysis of sodium borohydride for hydrogen generation. The latter will occur only when the measured amount of Ni-Ru based catalyst and the solid hydride closely tie to a fixed stoichiometric amount of pure water. Since this research topic does not deal with NaOH, our study does not involve a strongly caustic solution which is excellent from an environmental point of view.

As stated in Chapter 3, $NaBH_4$ reacts with water to generate molecular hydrogen according to the hydrolysis reaction shown in Eq.(4.1):

$$NaBH_4 + (2+x)\ H_2O \rightarrow NaBO_2.xH_2O + 4\ H_2 + \text{heat}. \qquad (4.1)$$

Ideal hydrolysis is attained for the excess hydration factor (x), $x = 0$ [4.3], but in practice an excess of water is required to account for the fact that the solid by-product ($NaBO_2.xH_2O$) can exist in varying degrees of hydration [4.1].

Experimental studies showed that if the excess hydration factor (x) is less that 2 ($x<2$), unreacted hydride remains; but if x>2 there is enough water for complete reaction and hydration of the borate.

Marreo-Alfonso *et al.* [4.1] argued that a hydration factor less than x=0.84 is necessary to meet the FreedomCar DOE specifications related to weight and volume hydrogen efficiency [4.4]. Also, sodium metaborate dehydrate, $NaBO_2.2H_2O$, appears to be the favoured product at temperature up to 110 ºC; and transforms to anhydrous metaborate after being dried at 350 ºC, while $NaBO_2.4H_2O$ becomes anhydrous above 400 ºC.

Based on these results, an excess of water seems to be always necessary to react most of the $NaBH_4$ used in this kind of reaction systems.

As already mentioned, this chapter focuses on the reduction of the factor x, which may be called a “solid phase pathway”. This approach presumably minimizes the water/hydride ratio in the reactor at any instant. This suggests that it may be possible to minimize the excess hydration factor through a pathway that leads toward by-products with lower hydration state. In fact, one of the major challenges for the implementation of hydride-

based storage technologies is to minimize the amount of water for 100% liberation of hydrogen.

Kojima *et al*. [4.5] declare that with a Pt-$LiCoO_2$ catalyst and high H_2 pressure above 0.6 MPa, a nearly theoretically H_2 yield using $x = 0$ in (4.1) was produced. There is no doubt that if reaction (4.1) occurs in the presence of steam instead of liquid water, the solid reaction products should contain less water of hydration, which in the long term will facilitate product recycling and regeneration of the hydride.

It results from the statement in the last paragraph that it is valuable to study the reaction depicted in equation (4.1) at high pressures and with $2<x<4$. Even if impossible to perform the hydrolysis reaction by feeding water in vapour phase, it is always important to work with values of x as low as possible. Maybe working at high pressures and optimizing the reactor design, it may be possible to achieve high H_2 yields at fast rates. Nevertheless to achieve these goals, it is absolutely necessary to fully understand the thermodynamics, kinetics and chemistry of the hydrolysis reaction.

4.2 EXPERIMENTAL PROCEDURE

The *alkali free* catalytic hydrolysis of sodium borohydride for hydrogen generation under pressure comprises a series of experiments done in the three batch reactors LR, MR and SM, with internal free volumes of 646 cm^3, 369 cm^3 and 229 cm^3, respectively.

Sodium borohydride powder ($\geq$ 96% purity) was used in all the experiments in the solid state, and in a constant amount of ≈1.2 g. This value was carefully chosen for comparing the results with those obtained in the *alkali* catalytic hydrolysis of 10 mL of a reactant aqueous solution 10 wt% $NaBH_4$ plus 7 wt% NaOH, by weight (the amount of $NaBH_4$ in this solution is approximately 1.2 g).

As already referred, the reactant blend was produced without adding NaOH aqueous solution to solid $NaBH_4$. Hence, a proper quantity of powder catalyst and solid $NaBH_4$, both measured in an analytical balance, are mixed together in the solid state, forming a solid powder mixture. Next, this mixture is stored at the bottom of the reactor and the reaction vessel is closed. Figure 4.1 shows three photographs that illustrate the described experimental procedure.

As stated in Chapter 2, after sealing perfectly the reactor, an adequate amount of H_2O was rapidly injected into the reactor by means of a syringe with a very high needle length (150 mm) to ensure that the water is delivered very close to the powder moisture ($NaBH_4$ plus catalyst).

Figure 4.1. Pictures showing the preparation of the reactant blend (catalyst plus $NaBH_4$, both solids) to use in *alkali free* hydrolysis experiments. From left to right: Ni-Ru based catalyst, anhydrous sodium borohydride and the bottom of MR reactor with the mixture (stored in bottom conical shape).

Four different studies were performed in this topic of *alkali free* hydrolysis of sodium borohydride with the objective of studying the effects on hydrogen generation rates and yields, by changing:

i) the stoichiometric amount of added water, $H_2O/NaBH_4$ (mol/mol), from ratios 2 to 8 mol;

ii) the quantity of catalyst, catalyst/$NaBH_4$ (g/g), for ratios of 0.2 and 0.4 g;

iii) the system pressure, performing experiments in the three designed reactors (LR, MR and SM), which have different internal free volumes;

iv) reactor bottom shape. Here, the $NaBH_4$ hydrolysis performance is compared in LR reactor (flat bottom) and in MR reactor (conical bottom), and

v) the system temperature.

All the experimental work reported on this chapter was done without magnetic stirring.

The hydrogen yield in reaction (4.1) was calculated by the following equation

$$\text{Hydrogen yield} = n(H_2)_{exp} / n(H_2)_{theoretical} , \quad (4.2)$$

where $n(H_2)_{exp}$ is the number of moles (mol) of generated H_2 and $n(H_2)_{theoretical}$ is the theoretical amount of generated H_2 assuming 100% conversion of $NaBH_4$ by applying the ideal gas law to the final volume of gas inside the reactor.

4.3 RESULTS AND DISCUSSION

As already referred, hydrogen was generated from catalysed hydrolysis of powder $NaBH_4$ with specific stoichiometric amounts of deionised water. The effects of ratios $H_2O/NaBH_4$ (mol/mol) and Ni-Ru based catalyst/$NaBH_4$ (g/g), system pressure, reactor bottom

geometry and reaction temperature on the hydrogen generation yield, rate and induction time were studied, and the results found are next presented and discussed separately.

Kojima *et al.* [4.5] published experimental work on compressed H_2 generation using $NaBH_4$ at pressures up to 5.6 MPa. For this reason, the present results, also on compressed H_2 generation, will be closely compared with those of Kojima *et al.* [4.5]. Excluding their work and those of Pinto *et al.* [4.6], the majority of the papers published on H_2 generation from hydrolysis of $NaBH_4$ are at ambient pressure; therefore, they will be hardly ever mentioned on this section of the dissertation.

4.3.1 Effect of $H_2O/NaBH_4$ (mol/mol) on hydrogen generation yield

Figure 4.2 shows the course of hydrogen generation in terms of H_2 pressure as a function of time, for the batch reactor LR (646 cm^3), with a flat bottom shape, by changing the amount of $H_2O/NaBH_4$ (mol/mol) ratio from 2 to 8 mol. A proportion of Ni-Ru based catalyst/$NaBH_4$: 0.4 g/g was used in all the experiments depicted in that figure and the catalyst for the experiment $H_2O/NaBH_4$: 2 mol/mol was 27 times reused, and for the others, between 109 and 111 times reused.

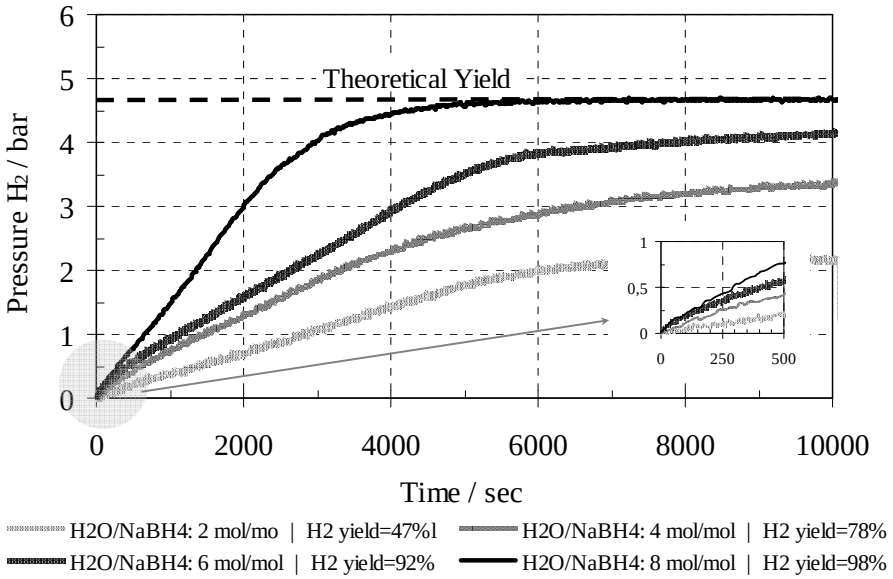

Figure 4.2. Hydrogen generation in the flat bottom batch reactor LR (646 cm^3) for experiments with Ni-Ru based catalyst/$NaBH_4$: 0.4 g/g and $H_2O/NaBH_4$: 2-8 mol/mol.

The results in the Fig.4.2 show the effect of changing the molar ratio $H_2O/NaBH_4$ on H_2 yield and rates. In fact, increasing the number of water molecules, the H_2 generation is achieved not only at higher yields but also a faster rate (for example, for $H_2O/NaBH_4$: 8

mol/mol, the reaction attained completion (time ≈ 83 min) with the highest dP/dt slope in the linear zone, 1.47E-3 bar/s or 0.11 $L(H_2)min^{-1}gcat^{-1}$).

For the experiment with $H_2O/NaBH_4$: 2 mol/mol illustrated in Fig.4.2, a hydrogen yield of about 47 % was reached in 125 min, at 0.22 MPa (dP/dt slope in the linear zone, 3.49E-4 bar/s or 0.026 $L(H_2)min^{-1}gcat^{-1}$). Kojima *et al.* [4.4], reported an H_2 yield of about 80% for the same molar relation and Pt-$LiCoO_2/NaBH_4$: 0.5 g/g, after 400 s, at 0.68 MPa and 296 K. They also reported, for the same experiment, but at atmospheric pressure (0.10 MPa), only 37%, with the plateau reached on 330 s. In fact, the substantial lower yield of 47 %, obtained in this work, can be explained by both the catalyst nature – Kojima *et al.* [4.5] used a Pt-$LiCoO_2$ catalyst, and a higher operating pressure (0.68 MPa).

In Figure 4.2 an enlargement of the left bottom corner of the plot is also represented. The aim is to check the reaction lag time of the experiments. As can be seen, the H_2 generation starts immediately after the injection of water, even at slow rate.

To solve the incompleteness of reaction (1) when $H_2O/NaBH_4$: 2 mol/mol (note that a theoretical final pressure of 0.46 MPa was expected), the reaction vessel was open and a second loading of pure water was injected with the same $H_2O/NaBH_4$ (mol/mol) ratio amount. This new addition of fresh water reacted with the left unreacted $NaBH_4$ present inside the batch reactor. Figure 4.3 shows the result obtained after injecting a second $H_2O/NaBH_4$: 2 mol/mol of distilled water.

As expected, the amount of hydrogen generated by the second injection of pure water was approximately the same registered in the first loading of water, and was produced at similar rates (in the linear zone, dP/dt slopes are quite similar, showed by the parallel straight lines for both water injections).

In Figure 4.4, the influence of added water, $H_2O/NaBH_4$ (mol/mol), on the hydrogen yield is studied and the results presented on this dissertation (at 293-295 K with a Ni-Ru based/$NaBH_4$: 0.4 g/g) are compared with those of Kojima et *al.* [4.5] (at 296 K with Pt-$LiCoO_2/NaBH_4$: 0.5 g/g). It can be observed that the H_2 yield increases with increasing $H_2O/NaBH_4$ ratio. For example, for the results presented on this dissertation, increasing the molar ratio $H_2O/NaBH_4$ from 2 to 6 mol/mol, the corresponding H_2 yield goes from 47 to 92% (these results arise at low pressure range, between 0.22 and 0.45 MPa). Therefore, for $H_2O/NaBH_4$ equal to 8 mol/mol, completion is achieved.

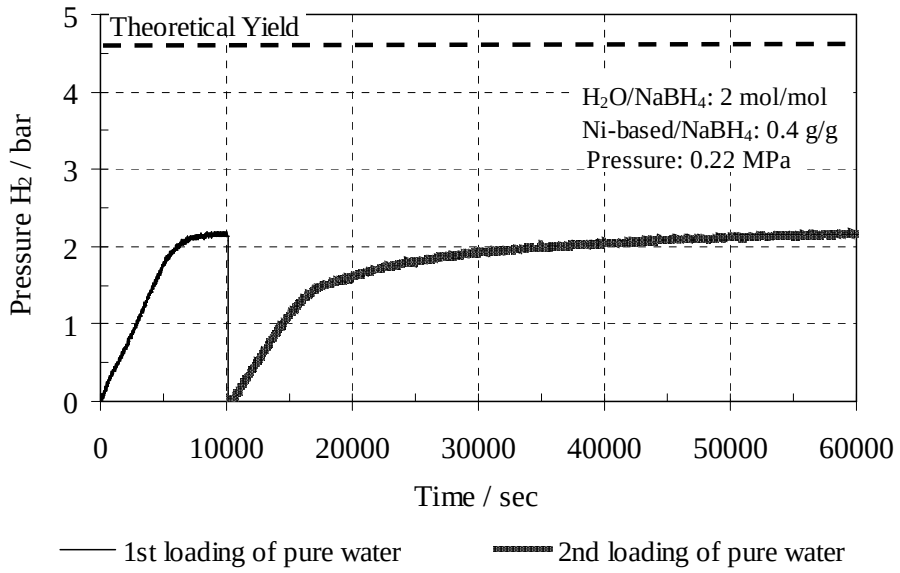

Figure 4.3. Hydrogen generation in the batch reactor LR (646 cm^3) with Ni-Ru based/$NaBH_4$: 0.4 g/g (27 and 28 times reused) and $H_2O/NaBH_4$: 2 mol/mol, after two successive loadings of pure water (of the same molar quantity).

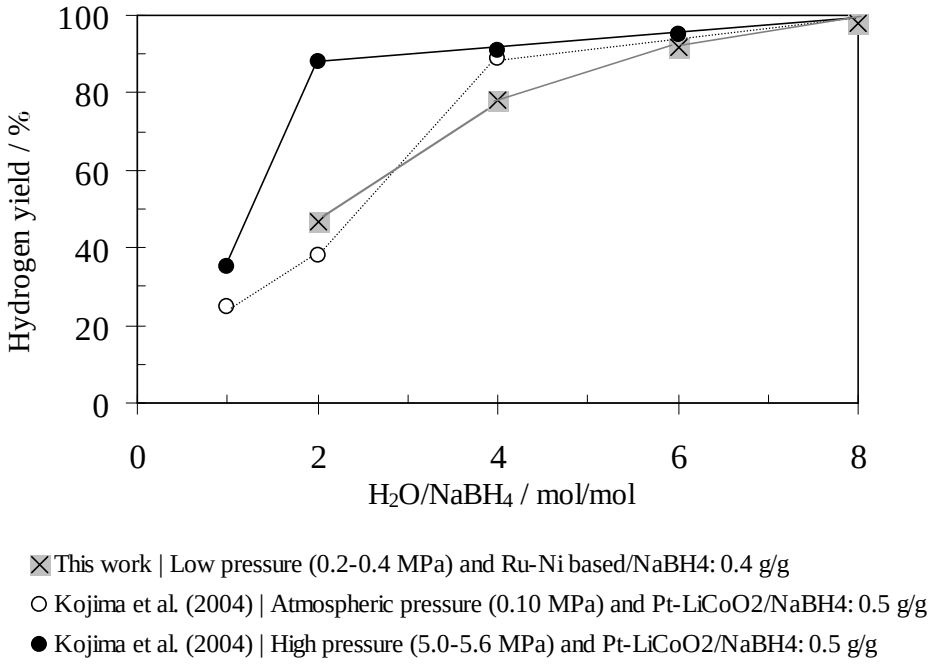

Figure 4.4. Hydrogen yield as a function of added water, $H_2O/NaBH_4$, in batch reactor LG (646 cm^3).

Regarding again the previous figure, Kojima *et al.* [4.5] reported a strikingly sharp increase in H_2 yield as $H_2O/NaBH_4$ departs from 1 to 2, with values of 35% up to 87%. For the case of $H_2O/NaBH_4$ equal to 6 mol/mol, a H_2 yield of 95% was obtained. Note that all those values were obtained at *very* high pressure (5.0-5.6 MPa). For atmospheric, and for

results of the present work - obtained at moderate pressures, high values of H_2 yield are achieved ($\geq$ 80%) if $H_2O/NaBH_4 \geq 4$ mol/mol.

4.3.2 Effect of catalyst/$NaBH_4$ (g/g) on hydrogen generation rate

Figure 4.5 shows the influence of the amount of catalyst used in hydrogen rate and lag time of an alkali free hydrolysis of sodium borohydride experiment, performed in batch reactor LR (646 cm^3).

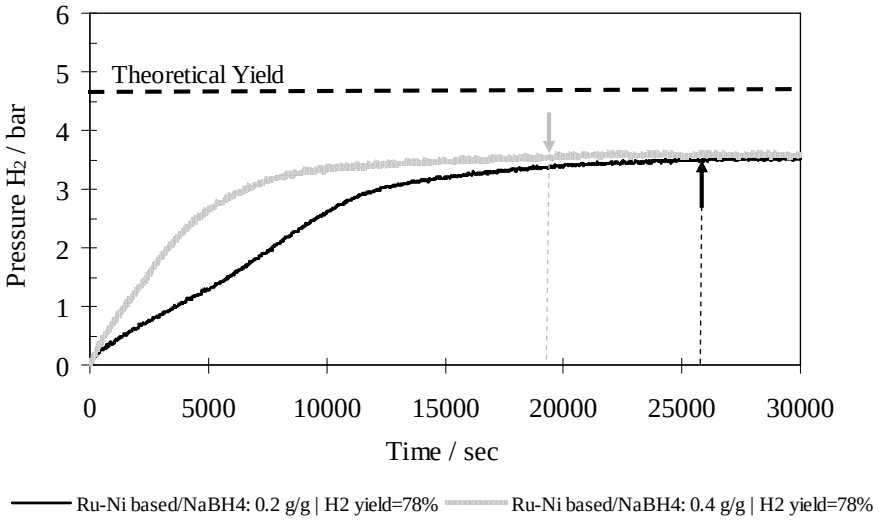

Figure 4.5. Influence of the amount of catalyst/$NaBH_4$ (g/g) on hydrogen generation.

Actually the amount of catalyst is another variable that influences the rate and the lag time. As can be seen in the plot of Fig.4.5, increasing the amount of the catalyst (catalyst/$NaBH_4$: 0.2 g/g $\rightarrow$ 0.4 g/g) increases the dP/dt slope in the linear zone (2.5E-4 bar/s or 0.037 $L(H_2)min^{-1}gcat^{-1}$ $\rightarrow$ 5.5E-4 bar/s or 0.041 $L(H_2)min^{-1}gcat^{-1}$) and decreases the time to reach the 'plateau', but, as expected, the pressure of produced hydrogen was similar ($\approx$ 0.36 MPa and H_2 yield of 78 %) and independent of the temperature.

4.3.3 Effect of pressure on hydrogen generation yield and rate

Figure 4.6 shows the rate of hydrogen generation in terms of H_2 pressure as a function of time, for the three batch reactor LR, MR and SR, at the stoichiometric amount of 4 moles of distilled water, using a proportion Ni-Ru based/$NaBH_4$: 0.4 g/g. The values of H_2 yields achieved are also reported.

The plot in Figure 4.7 shows the H_2 generation yield versus pressure, for the three studied stoichiometric amounts of water, using Ni-Ru based catalyst (Ni-Ru based/$NaBH_4$: 0.4 g/g), and also the results obtained by Kojima *et al.* [4.5], for comparison.

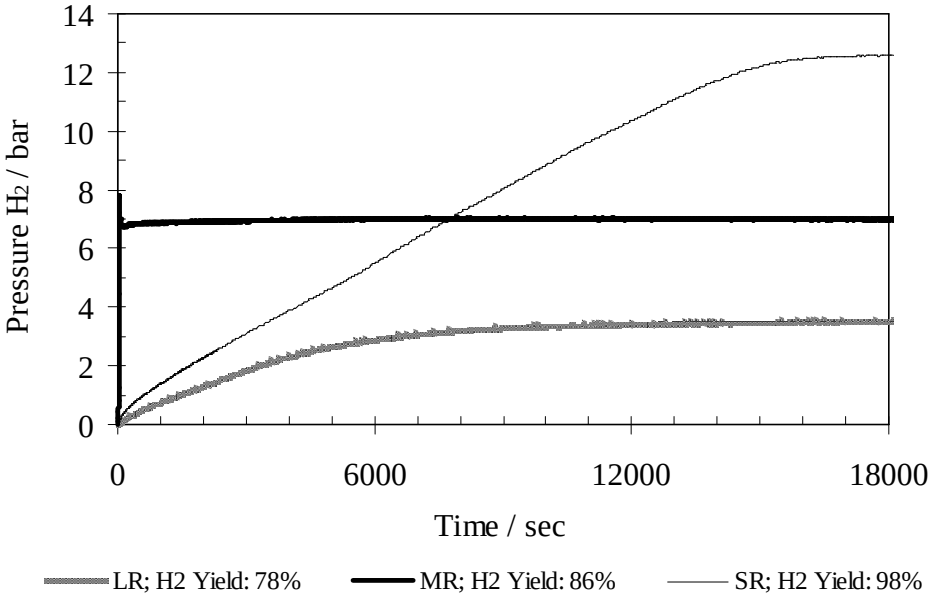

Figure 4.6. Hydrogen generation in the studied three batch reactors - LR (646 cm^3), MR (369 cm^3) and SR (229 cm^3), with Ni-Ru based catalyst/$NaBH_4$: 0.4 g/g (111, 150 and 151 times reused, respectively for LR, MR and SR) and $H_2O/NaBH_4$: 4 mol/mol.

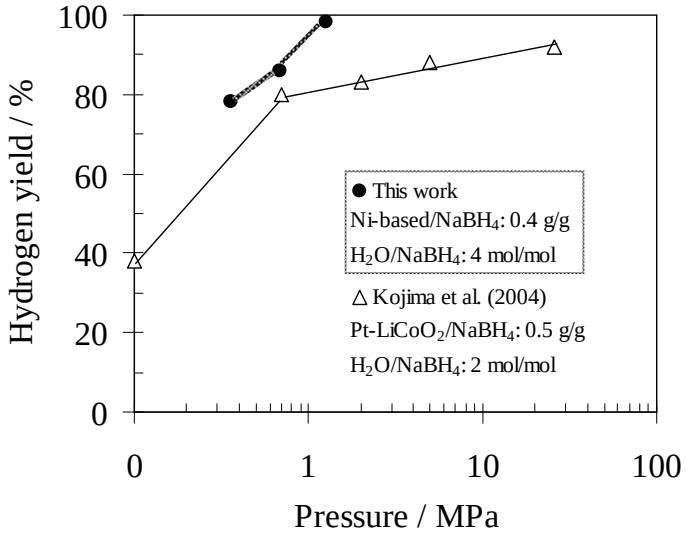

Figure 4.7. Influence of pressure on H_2 yield (Experiments done in three batch reactors at the temperature range of 289-295 K, with catalyst reused ≈150 times).

As can be seen from the plots of Fig.4.6-4.7, the effects of pressure on H_2 yields and rates are remarkable. In truth, we may conclude that increasing the pressure, significantly increases H_2 rates and H_2 yields.

For the operating conditions presented on this dissertation, and for the special case of $H_2O/NaBH_4$: 4 mol/mol, performed at the moderate pressures between 0.36-1.26 MPa, values for H_2 yields up to 78-98% were obtained (see Fig.4.7).

Kojima *et al.* [4.5] reported values of 80-93% for H_2 yields under much higher pressure levels (0.7-25 MPa), with $H_2O/NaBH_4$: 2 mol/mol (see Fig.4.7).

It is worth to notice that the results presented in Fig.4.6 were performed using Ni-Ru based powdered catalyst reused ≈150 times, in batch reactors with flat and conical bottoms. As can be easily checked, the catalyst shows high activity under moderate pressure resulting in a significant increase in the amount of hydrogen generated. Kojima *et al*. [4.5] conclude the same trend (at $H_2O/NaBH_4$: 2 mol/mol) with a noble catalyst Pt-$LiCoO_2/NaBH_4$: 0.5 g/g at higher H_2 pressure, up to 25 MPa.

4.3.4 Effect of reactor bottom shape on hydrogen generation

Looking back to the results plotted in Fig.4.6, presented in the previous section, it seems very important to study the effect of reactor bottom shape on H_2 generation rate and yield.

The plot in Figure 4.8 show the H_2 generation trend for $H_2O/NaBH_4$: 2 mol/mol and Ru-Ni based/$NaBH_4$: 0.4 g/g., in batch reactors LR (646 cm^3) and MR (369 cm^3), with flat and conical bottom shapes, respectively.

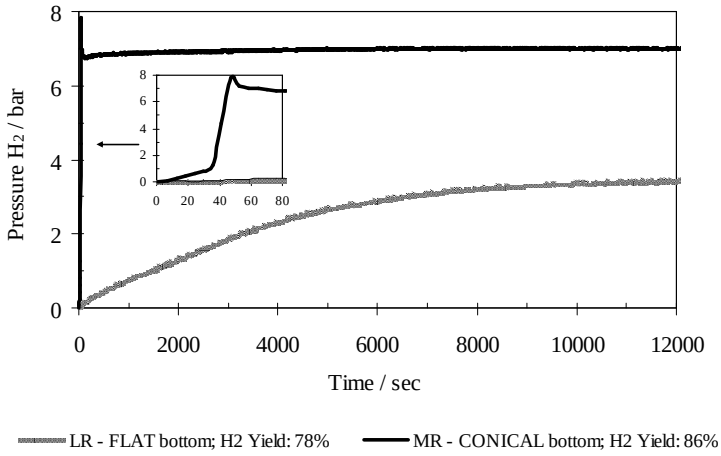

Figure 4.8. Influence of reactor bottom shape on H_2 yield, rate and lag time (experiments performed in batch reactors LR (646 cm^3) and MR (369 cm^3), with flat and conical bottom shapes, respectively; at temperature range of 289-295 K, with catalyst reused ≈150 times).

As can be observed from the plot of Fig.4.8, the influence of reactor bottom shape on H_2 generation is notorious: the conical geometry greatly enhances the rate and yield of H_2

generation. For the batch reactor MR, with conical bottom, a value of dP/dt slope in the linear zone of 5.7E-1 bar/s (24.2 $L(H_2)min^{-1}gcat^{-1}$) was found. In fact, a difference of 10^3 separates this value from that obtained in the reactor with a flat bottom shape (5.8E-4 bar/s or 0.043 $L(H_2)min^{-1}gcat^{-1}$), for the same H_2 reaction.

An enlarged plot on the left side of Fig.4.8 put in evidence the sharply increase of H_2 pressure by time (confirmed by the high value in dP/dt slope mentioned in the previous paragraph), after a period of ≈36 seconds in lag time (the lag time is defined as the length of time required to observe an increase in the H_2 pressure). In reality, the reactor bottom shape influences also the H_2 lag time! Observing Fig.4.8 we may conclude that the conical reactor bottom geometry significantly decreases the lag time. A plausible explanation is that the reactor conical bottom shape enhances the contact between the catalyst and $NaBH_4$ powders, and the injected distilled water. The photographs in Figure 4.9, below, outline this aspect: the MR reactor (left side) when opened after the experiment which results are plotted in Fig.4.8, shows absence of liquid and looks empty. The photograph on the right side of Fig.4.9 shows the reaction by-product plus catalyst, in a form of a swelled aggregated porous solid, shaped by MR reactor conical bottom, which adhered to the T.Bottom k thermocouple, the latter fixed on the top of the reactor lid.

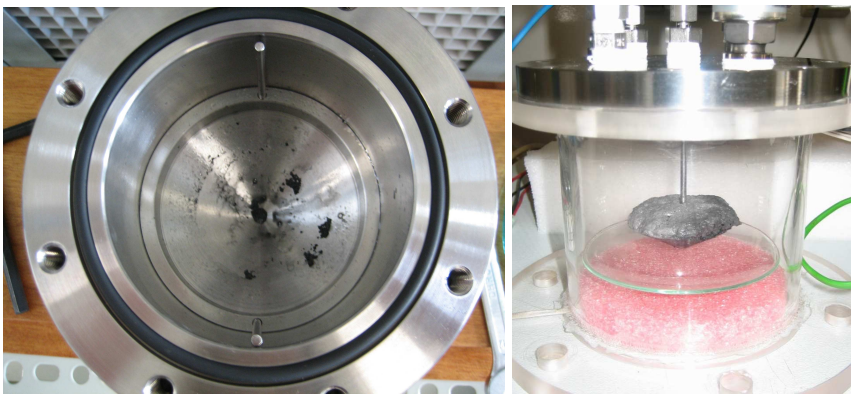

Figure 4.9. Photographs of MR reactor (with conical bottom shape) after an *alkali free* hydrolysis of $NaBH_4$ experiment. In the right, a view of the solid mixture of the by-product plus the catalyst.

The sharp increase of H_2 pressure with time shown in Fig. 4.8, which occurred in the MR batch reactor with a conical bottom, is in some way a consequence of also a sharp increase in the value of temperature of the hydrolyzed $NaBH_4$. Figure 4.10 illustrates the variation of reaction temperature occurred during the hydrogen generation for the two experiments plotted in Fig 4.8.

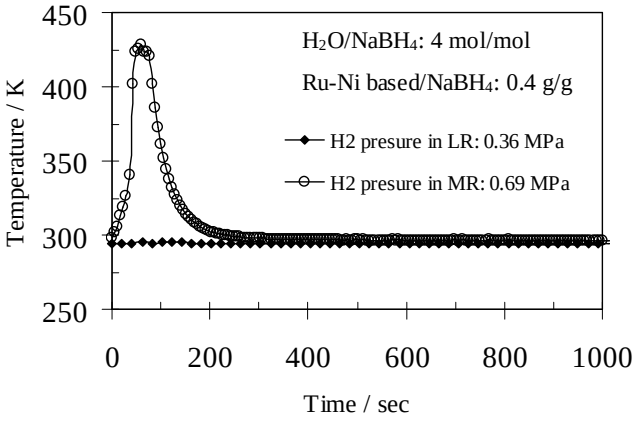

Figure 4.10. Temperature of the hydrolyzed $NaBH_4$ as a function of time by different pressures.

Indeed, in the MR batch reactor, the occurrence of a 'thermal runaway' which was responsible for the increase of about 150 ºC in the reaction temperature, happened in a short time interval, less than one minute, and consequently, accelerated harshly the hydrolysis reaction.

The temperature in the batch reactor (with a conical bottom), at 0.69 MPa, shows the maximum value of 428 K after the induction period, and decreases quickly with time. It may be conclude that when the temperature of hydrolyzed hydride increases the induction period decreased. A similar trend was found by Kojima *et al.* [4.5].

4.3.5 Effect of temperature on hydrogen generation rate

The influence of temperature on the velocity of hydrogen generation is put in evidence in Figure 4.11.

As can be seen in the plot of Fig.4.11, the reaction rate is very sensitive to temperature. As expected, the rate rises with the increase in temperature and the hydrogen pressure demonstrates a near linear variation with reaction time. The influence of temperature is clearly shown by the increasing slope values on the linear region of the plots, for increasing values of the reaction temperature (from 15 to 55 ºC, the rate increases from 5.4E-4 to 4.4E-1 bar/s, or 0.021 $L(H_2)min^{-1}gcat^{-1}$ to 14.4 $L(H_2)min^{-1}gcat^{-1}$). Therefore, it seems that the reaction rate remains practically constant when, during the hydrolysis process, the $NaBH_4$ concentration decreases due to hydride and water consumption, demonstrating a zero-order reaction. A more detailed study of the effects of reactants concentration, operating pressure and temperature is necessary; in order to develop a

kinetic model that accurately reflects the reaction rate as a function of temperature and pressure.

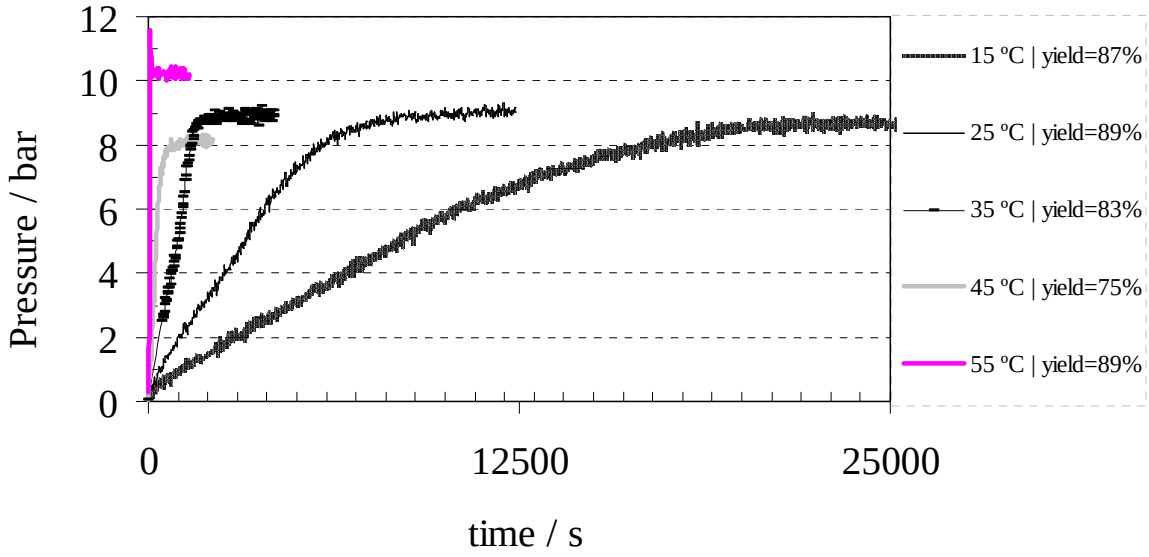

Figure 4.11. Influence of temperature on hydrogen generation rate and yield.

4.3.6 Gravimetric and volumetric densities

It is here worth to remember that the main purpose of the *alkali free* hydrolysis of $NaBH_4$ experiments reported in this dissertation is to produce pure hydrogen gas with very high gravimetric and volumetric densities. And the ability to produce anhydrous sodium borate is the key to increase the overall storage density of systems based on sodium borohydride as the storage media [4.1, 4.5].

Kojima *et al.* [4.5] reported that the structure of the by-product produced from the reaction of $NaBH_4$ and water using Pt-$LiCoO_2$, is $NaBO_2.2H_2O$ at atmospheric pressure, and anhydrous $NaBO_2$ at high pressure. They also mentioned that the temperature of the hydrolyzed $NaBH_4$ is higher in the catalyzed reaction at 0.10 MPa than at 0.68 MPa. A possible explanation can be related with the energy required for the addition of two water molecules in the heat of formation of $NaBO_2.2H_2O$. In some way, similar behaviour was found in the present work (see Figs. 4.8 and 4.10, above). In fact, if we look through the plot of Fig.4.6, the H_2 yield increases from 86% to 98% in the MR (369 cm^3) and SR (229 cm^3) batch reactors, both with conical bottom shape. Why? An inspection of the temperature profile inside of SR reactor shows a lower reaction temperature; maybe because the H_2 is not consumed to hydrate sodium borate by-product. It is therefore

important to investigate the type of by-products formed; and that will be done in Section 4.4.

The US Department Of Energy (DOE) has published FreedomCAR requirements for automotive hydrogen storage systems (probably the most stringent targets yet articulated for hydrogen storage systems). Two of the principal technical targets, based on system mass and volume, are the gravimetric hydrogen density and the volumetric hydrogen density. Table 4.1 shows these FreedomCAR two specifications [4.4].

Table 4.1 - The FreedomCAR targets publish by US Department Of Energy (DOE).

Year	2007	2010	2015
Gravimetric H_2 density / wt.%	4.5	6.0	9.0
Volumetric H_2 density/ kgH_2/m^3	36	45	81

(Note that these specifications are based on system mass and volume, i.e., not only the storage material itself but also the reactors, tanks, valves, and all auxiliary equipment, which usually are call *hardware*.)

Table 4.2 below, presents the predicted values for gravimetric hydrogen density and volumetric hydrogen density, based only on the storage *material* itself, for the systems studied in this chapter: $H_2O/NaBH_4$: 4 mol/mol and Ru-Ni based catalyst/$NaBH_4$: 0.2-0.4 g/g. Hence, the influence of Ni-Ru based catalyst/$NaBH_4$ on gravimetric hydrogen density and on hydrogen yield is also checked.

The density of the *material* ($H_2O/NaBH_4$: 4 mol/mol; Ni-Ru based/$NaBH_4$: 0.2-0.4 g/g) was calculated by adding the densities of $NaBH_4$ (1.07 g/cm^3), water (1.00 g/cm^3) and Ni-Ru based catalyst (3.17 g/cm^3).

It was found that our system of compressed hydrogen generation at moderate pressure of up to 1.26 MPa is currently capable of meeting 6.3 wt% and 70 kg H_2/m^3, respectively, for gravimetric hydrogen density and volumetric hydrogen density, based only on the storage *material* itself (and not on the storage system as a hole or including *hardware*). Hence, it is not correct to compare the values obtained with those in Table 4.1, the 2010 FreedomCAR targets published by the US DOE. Can we ask: Is $NaBH_4$ a suitable hydrogen storage material for portable and/or niche application? It is difficult, indeed, to answer this question. To the best of the authors' knowledge there is no paper or document clearly specifying the targets for portable applications.

Table 4.2 - Influence of Ni-Ru based catalyst/$NaBH_4$ on gravimetric hydrogen density and hydrogen yield for $H_2O/NaBH_4$: 4 mol/mol. Prediction of the volumetric hydrogen density*.

Ni-based/$NaBH_4$ / g/g	Gravimetric H_2 density / wt.%	H_2 yield / %	Volumetric H_2 density* / kgH_2/m^3	Pressure / MPa
0.2	5.3	78	57	0.36
0.4	5.0	78	56	0.36
0.4	5.3	86	59	0.69
0.4	6.3	98	70	1.26

* It was assumed that the average value of the density of our materials, by addition relationship of densities of $NaBH_4$ (1.07 g/cm3), H2O (1.00 g/cm3) and Ni-based catalyst (3.17 g/cm3) is:
1.07 g/cm3, for $H_2O/NaBH_4$: 4 mol/mol, Ni-based catalyst/$NaBH_4$: 0.2 g/g; and
1.11 g/cm3, for $H_2O/NaBH_4$: 4 mol/mol, Ni-based catalyst/$NaBH_4$: 0.4 g/g

Even for the purpose of a didactic demonstration, the MicroBoro Bus plus the H_2 generation system, presented here, delivers pure H_2 in high rates, during a good fraction of time/autonomy. Hence, it seems that $NaBH_4$ has potential for portable applications, or at least niche applications. In a recent paper, the values 3-7 wt% for gravimetric hydrogen storage capacities for $NaBH_4$ systems are mentioned [4.7].

It is important referring that sustainable method to recycle the borate by-products back to $NaBH_4$ would be a very important obstacle to overcome for the adoption of $NaBH_4$ as a hydrogen carrier of choice for portable H_2 fuel cell applications.

4.4 REACTION BY-PRODUCT CHARACTERIZATION

The by-products of the *alkali free* hydrolysis experiments for hydrogen generation, reported on this chapter, were analyzed by X-Ray Diffractometry. As already referred suitable crystals, from the reactions performed under and above 1 MPa pressure, were obtained by slow evaporation of a water solution at uncontrolled room temperatures. The crystal structures were alike with respect to water content.

4.4.1 Materials and methods

For the crystals coming through MR reactor experiments (at 0.69 MPa), XRD analysis revealed that they were monoclinic, space group $C_{2/c}$, cell volume V=1478.8(2) $Å^3$. Unit cell parameters a = 11.8899(9) Å, b = 10.6394(8) Å, c = 12.1989(9) Å, β = 106.609(8)º. Diffraction data were collected at 293 K with a Gemini PX Ultra equipped with MoK_α radiation (λ=0.71073 Å). The structure was solved by direct methods using SHELXS-97 [4.8] with atomic positions and displacement parameters refined with SHELXL-97 [4.9]. The non-hydrogen atoms were refined anisotropically and the hydrogen atoms were

refined freely with isotropic displacement parameters. The refinement converged to *R* (all data) = 5.30% and wR^2 (all data) = 11.87%.

4.4.2 Results and discussion

The crystal structure reveals the B atoms in triangular and tetragonal configuration with O atoms. The Na atoms are coordinated by six water molecules. The molecular formula is $Na_2B_2O_5.4H_20$. Less two water molecules were similarly find in the crystal structure in the SR batch reactor experiments (at 1.26 MPa).

Figure 4.12, below, shows the two crystal structures discovered for the sodium metaborate hydrates.

It may be concluded that the use of Ru-Ni based catalyst, that shows high activity in *alkali free* hydrolysis under high pressure, revelled not only high yields of hydrogen generation, as reported in the above sections, but also, for pressure > 1 MPa, a change in the structure of the by-product from $Na_2B_2O_5.4H_20$ to two less water content. This is an important finding due to gravimetric hydrogen density and borates recycle.

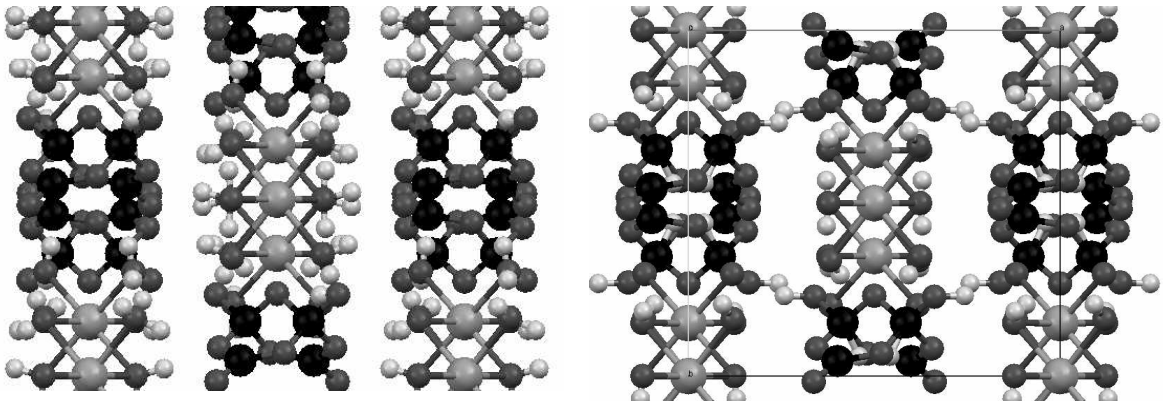

(a) (b)

Figure 4.12. View along the *c*-axis of the crystal structure of sodium metaborate hydrate: (a) $4H_2O$, in MR at 0.69 MPa and (b) $2H_2O$, in SR at 1.26 MPa. The element color code, from black to light grey, is B, O, Na and H.

4.5 CONCLUSIONS

The fundamental understanding of the alkali free hydrolysis of sodium borohydride obtained in this chapter suggests that it is possible to develop a hydrogen reactor/delivery

system that produces pure hydrogen in ≈100% yield, requires a suitable catalyst, does not involve strongly caustic solutions, and uses a minimum/stoichiometric amount of water.

Chemical hydrides have the potential to meet certain H_2 storage targets only if the water consumption is minimized. A key thermophysical requirement is to minimize the "excess hydration factor", as mentioned in this chapter. An *alkali free* hydrolysis under pressure may help to achieve this. Experimentally, we have shown for a system with $H_2O/NaBH_4$: 4 mol/mol and Ru-Ni based/$NaBH_4$: 0.4 g/g, performed in a batch reactor with conical bottom shape (229 cm^3), that the H_2 produced reaches almost 100% conversion of $NaBH_4$, delivered in fast rate and without significant lag time, when the operating pressure is > 1 MPa.

4.6 REFERENCES

[4.1] Marrero-Alfonso E, Gray JR, Davis TA, Matthews MA. Minimizing water utilization in hydrolysis of sodium borohydride: the role of sodium metaborate hydrates. Int. J. Hydrogen Energy 32 (2007) 4723-4730.

[4.2] C.M. Kaufman, S. Buddhadev, Hydrogen generation by hydrolysis of sodium tetrahydroborate: effects of acids and transition metals and their salts, J. Chem. Soc. Dalton Trans. (1985) 307-313.

[4.3] H.I. Schlesinger, H.C. Brown, A.E. Finholt, J.R. Gilbreath, H.E. Hoeskstra, K. Hyde, Sodium borohydride, its hydrolysis and its use as a reducing agent and in the generation of hydrogen, J. Am. Chem. Soc. 75 (1953) 215-219.

[4.4] U.S. Department of Energy Hydrogen Program. Available from: http://www.hydrogen.energy.gov/.

[4.5] Y. Kojima, Y. Kawai, H. Nakanishi, S. Matsumoto, Compressed hydrogen generation using chemical hydride, J. Power Sources 135 (2004) 36-41.

[4.6] A.M.F.R. Pinto, D.S. Falcão, R.A. Silva, C.M. Rangel, Hydrogen generation and storage from hydrolysis of sodium borohydride in batch reactors, Int. J. Hydrogen Energy 31 (2006) 1341-1347.

[4.7] U.B. Demirci, O. Akdim, P. Miele, Ten-year efforts and a no-go recommendation for sodium borohydride for on-board automotive hydrogen storage, Int. J. Hydrogen Energy 34 (2009) 2638-2645.

[4.8] G.M. Sheldrick, SHELXS-97, Program for the solution of crystal structures; University of Göttingen: Germany 1997.

[4.9] G.M. Sheldrick, SHELXL-97, Program for the refinement of crystal structures; University of Göttingen: Germany 1997.

CHAPTER 5

less Polar Organic Polymeric Solutions hydrolysis
Results for sodium borohydride kinetic experiments

This chapter focuses on the results of small additions of an organic polymer or surfactant to the stabilized catalytic hydrolysis of sodium borohydride for simultaneous hydrogen generation and storage in the liquid phase. The effects of pressure and reactor bottom shape on the hydrogen generation rate are investigated. Particular importance is given to H_2 solubility's effect in the liquid phase by increasing the operating pressure. XRD analysis for the reactions by-product is also presented.

5.1 INTRODUCTION

Hydrogen is being focused as the energy source that will replace the current fossil fuel in the 21st century. Pure hydrogen is especially interesting for fuel cell technologies. In fact, fuel cells are alternative power sources for providing clean energy for transportation and personal electronic applications where low system weight and portability are important. But produced hydrogen needs to be stored effectively and safely, with high gravimetric/volumetric storage capacities. This represents the biggest scientific challenge to overcome before the implementation of an economy based on this energy carrier becomes possible.

Currently, there is a great interest in the use of solid state materials for the storage of hydrogen. Hydrides of light elements may represent the only viable method of achieving a high weight percent and high volume density of stored hydrogen; in particular, sodium borohydride ($NaBH_4$) has such features [5.1].

In November 2007 the U.S. Department of Energy (DOE) recommended a no-go for $NaBH_4$ for on-board automotive hydrogen storage [5.2] and, we have to admit, that decision is completely justified. In fact, the 2015 targets for gravimetric (9.0 wt%) and

volumetric (81 kg/m^3) hydrogen storage densities (calculated on 1 kg system-basis), established by the FreedomCAR US DOE [5.3] program (which probably is the most stringent yet articulate for hydrogen storage systems) revealed some penalties. The latter result from the fact that it is obligatory to take into account, on specific H_2 energy calculations, the weight and volume not only of the materials but also of the *hardware* (i.e., the reactors, tanks, valves and all auxiliary equipment) to achieve those targets. Although the intentions of FreedomCAR specifications were to stimulate breakthroughs, both in material storage capacities and in efficient system design, the fact is that system requirements [5.3] lower the gravimetric and volumetric H_2 storage capacities significantly.

However, the intensive literature published after 1999 – a year of a new beginning in the $NaBH_4$ history –about sodium borohydride as an energy/hydrogen carrier, in particular the work of Amendola *et al.* with the title "A safe, portable, hydrogen gas generator using aqueous borohydride solution and Ru catalyst" [5.4], irrefutably showed that $NaBH_4$ has potential for portable applications, at least niche applications.

Sodium borohydride reacts with water to generate molecular hydrogen according to the hydrolysis reaction shown in Eq.(5.1):

$$NaBH_4 + (2+x)\, H_2O \rightarrow NaBO_2.xH_2O + 4\, H_2 + \text{heat}. \qquad (5.1)$$

Ideal hydrolysis is attained for $x = 0$ [5.5], but in practice excess of water is required to account for the fact that the by-product ($NaBO_2.xH_2O$) can exist with various degrees of hydration [5.6].

In this Chapter new and original data are reported on both generated and simultaneously storage molecular hydrogen (in the liquid phase) in a batch reactor, under high pressures, by the addition of small quantities of an organic polymer or surfactant to the reactant solution before the hydrolysis reaction occur inside the reactor, the latter within an appropriate amount of powder catalyst.

The key purpose of the polymer addition or the surfactant addition was to change the polarity of the remaining solution, in order to increase the non-polar hydrogen-electrolyte interactions; and hence, improving the affinity for storage H_2 in the liquid phase by solubility's effects.

The interplay between the H_2 solubility and the gravimetric H_2 density is also an objective point to report in this part of the work.

5.2 EXPERIMENTAL PROCEDURE

The *lPOPS* catalytic hydrolysis of sodium borohydride for hydrogen generation under pressure comprises a series of experiments done in the two batch reactors MR and SR, with internal free volumes of 369 cm^3 and 229 cm^3, respectively.

20 cm^3 of reactant solution, prepared with 10 wt% $NaBH_4$ and stabilized with 7 wt% NaOH, was injected into one of the reactors (0.369 L and 0.229 L) using a syringe. Another two solutions were as well prepared by addition of 0.25 wt% CMC and 0.25 wt% SDS. Weighed amounts of catalyst, reused 160 times, were in the proportion of Ni-Ru based catalyst/$NaBH_4$: 0.4 g/g and had been previously stored in the conical bottom of the two reactors tested. The adopted reactor bottom configuration – conical – enables non-dispersible effects between the contacting powdered catalyst and the injected reactant solution.

All the experimental tests were performed at 318 K, and after reaction completion, magnetic stirring inside de reactor was allowed for 30 minutes to promote complete saturation of H_2 with the remaining by-product solution.

The hydrogen yield in reaction (5.1) was calculated by the following equation

$$\text{yield}\,(H_2) = \frac{n(H_2)_{exp}}{n(H_2)_{theoretical}} \times 100\% \ , \tag{5.2}$$

where $n(H_2)_{exp}$ is the number of moles (mol) of generated H_2 and $n(H_2)_{theoretical}$ is the theoretical amount of generated H_2 assuming 100 % conversion of $NaBH_4$ by applying the ideal gas law to the final volume of gas inside the reactor. Special care was taken to correct the varying free volume of gas inside the reactor due to the consumption of $NaBH_4$ and water.

The by-products of the hydrogen generation reactions were analyzed using X-Ray Diffractometry (XRD). Suitable crystals were obtained by slow evaporation of water solution at uncontrolled room temperature.

5.3 RESULTS AND DISCUSSION

Plots in Figure 5.1 show a typical course of a hydrogen generation reaction, presented in terms of the operating pressure as a function of time, for one single loading *fuel* solution, respectively, in MR and SR batch reactors, both with conical bottom shapes.

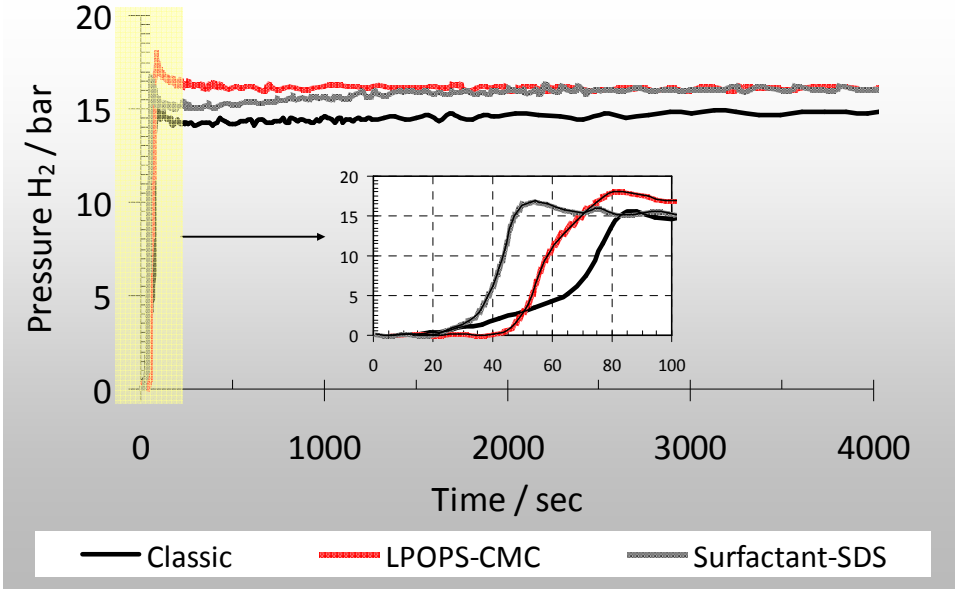

(a)

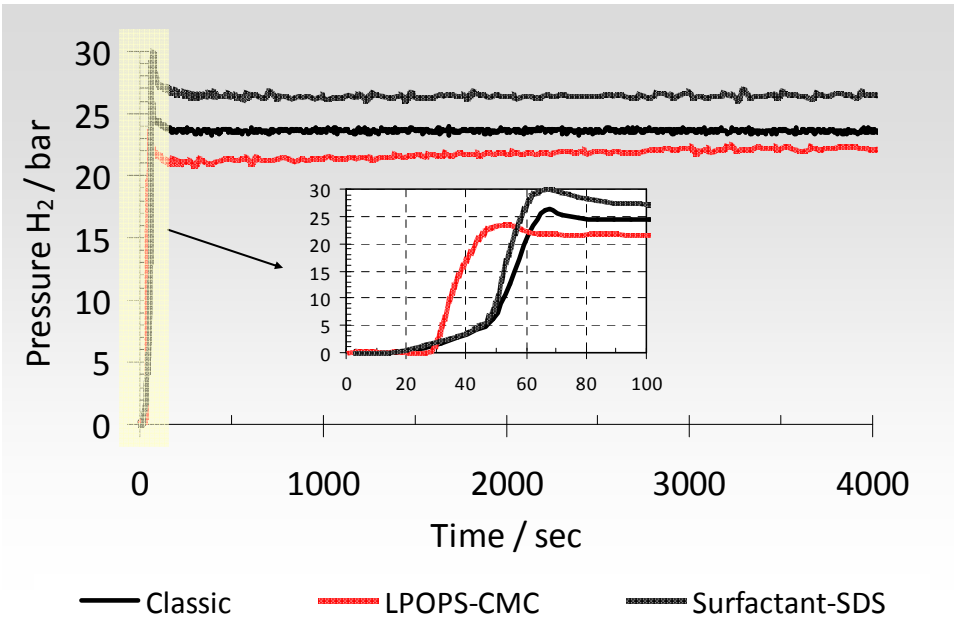

(b)

Figure 5.1. Hydrogen generation by a single loading of 20 cm^3 of reactant solution, at 45 ºC, with Ni-Ru based catalyst/$NaBH_4$: 0.4 g/g: (a) MR batch reactor [0.369 L] and (b) SR batch reactor [0.229 L].

Table 5.1 reports the hydrogen yields for the three studied solutions, in the two batch reactors. Completion was practically achieved in the *classic* hydrolysis and in the reactant solution with the surfactant SDS. For the experiments with the polymer CMC, the maximum hydrogen generated (evaluated by the maximum reached pressure inside the

batch reactor) was found to be lower than that predicted by the ideal gas law, and this effect was more pronounced in the small reactor SR.

Table 5.1 – Hydrogen yield for the studied reactant solutions in the two batch reactors and prevision of respective H_2 solubility effects, at 45 ºC.

		10 wt% $NaBH_4$ and 7 wt% NaOH		
		without polymer	CMC, 0.25 wt%	SDS, 0.25 wt%
REACTOR 1	H2 yield, %	100	98	100
0.369 *l*	Solubility effects, %	0	2	0
REACTOR 2	H2 yield, %	98	95	100
0.229 *l*	Solubility effects, %	2	5	0

A reasonable explanation for this behaviour can be related with solubility effects. In fact, increasing pressure of the gas phase forces the H_2 dissolution in the liquid phase that remains inside the reactor [5.7].

Curiously, the by-product solution of the *lPOPS* catalytic hydrolysis of $NaBH_4$ with the CMC polymer, showed the highest capacities to *store* hydrogen gas in the liquid phase: 2 and 5%, respectively, in reactors MR and SR. Given that H_2 is a non-polar gas, the result found for the *lPOPS*-CMC hydrolysis was in some way expected. In fact, the addition of the polymer CMC (0.25 wt %) probably changes the polarity of the final solution due to the increase of non-polar C-H groups. Thus, we may state that the presence of CMC enhances the affinity to store H_2 in the liquid phase that remains inside the batch reactor, under pressure, owing to the increase of the non polar hydrogen-electrolyte interactions. Therefore, as it is well known, the effect of increasing the gas pressure enhances strongly the gas dissolution in the liquid phase. Observing the values in Table 1 for the reactant solution with CMC, we note an increase in solubility effects from 2 to 5% when the H_2 pressure increased from 16.2 to 22.2 bars in the reactors MR and SR, respectively. Hence, it can be concluded that increasing pressure of the gas phase forces the hydrogen dissolution. As mention by Pinto *et al.* [5.7], this is an interesting result since gaseous hydrogen was generated but also stored in the liquid phase.

The addition of polymer CMC and surfactant SDS results in a *less Polar Organic Polymeric Solution* (*lPOPS*) and this was marked in the change of the overall conductivity of the remaining solution inside the batch reactors. Table 5.2 shows the conductivity and pH of the tested solutions before and after the reaction completion.

Table 5.2 – Values of conductivity and pH of the studied reactant solutions, before and after reaction completion.

	before the reaction		after the reaction	
20 mL reactant solution 10 wt% NaBH4, 7 wt% NaOH	Conductivity (mS/cm)	pH (-)	Conductivity (mS/cm)	pH (-)
Classic - no polymer addition	80,3	13,4	64,5	13,4
plus 0.25 wt% CMC	80,5	13,6	67,5	13,4
plus 0.25 wt% SDS	87,1	13,4	23,0	13,5
temperature	298 K			

As can be seen in the previous table, a decrease of approximately 15 mS/cm in the value of conductivity was registered for both the reactant solutions: [10 wt% $NaBH_4$ + 7wt% NaOH + 83wt% H_2O] and [10wt% $NaBH_4$ + 7wt% NaOH + 0.25wt% CMC + 82.75wt% H_2O], before and after the reaction completion. A decrease of nearly more than four times was observed for the reactant solution with 0.25wt% SDS (23 mS/cm). This result was in some way expected due to the capability of SDS to form micelles. We believe that this aggregate, usually with its hydrophilic *head* oriented to the solvent (water) direction and hydrophobic tail leaning to its centre, had the capability to sequester H_2 to the micelle centre. Definitely that doesn't seem to occur: the value of 0% of H_2 due to solubility effects (see Table 5.1) 'speaks for itself'.

5.4 REACTION BY-PRODUCT CHARACTERIZATION

By-products suitable crystals of the hydrogen generation reactions of all types of experiments reported on this chapter were analyzed by X-Ray Diffractometry. Very interesting results were obtained for the chemical structures of sodium borohydride hydrolysis by-product crystals:

i) For the *classic* reaction (5.1), the crystal structure of the by-product is a metaborate dehydrate, $NaBO_2.2H_2O$, schematically presented in Figure 3.12 (see Chapter 3).

ii) For the reagents presented in reaction (5.1) plus addition of 0.25wt% CMC, the crystal structure of the by-product is a borate anhydrous, $NaBO_4$, schematically presented in Figure 5.2. The crystal structure reveals that the boron atoms are in a tetrahedral configuration with four oxygen atoms, with B-O bond lengths within the interval 1.466 and 1.492 Å. The B-O interatomic distances are around the expected value for a tetrahedral configuration 1.475 Å, which is appreciable higher than observed for triangular

configurations (1.365 Å) [5.8]. The sodium atoms have their valence distributed between five Na-O bonds (bond lengths within 2.329 and 2400 Å). The mean length of the Na-O bonds is 2.512 Å when the Na coordination number is seven and it is 2.450 Å when the coordination number is six [5.9]. It is reasonable to assume that the bond length and the Na coordination number decrease as the bond strength increases.

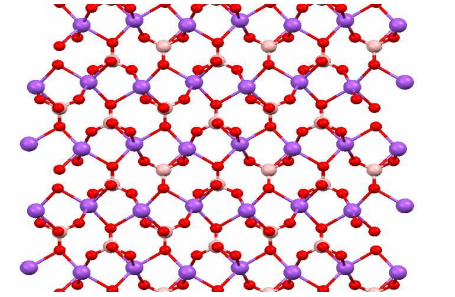

Figure 5.2. View along the *a*-axis of the crystal structure of sodium borate anhydrous, showing the BO_4 tetrahedral arrangement and the Na bound network. Na in violet, O in red and B in pink.

iii) Finally, for the reagents presented in reaction (5.1) plus addition of 0.25wt% SDS, the crystal structure of the by-product reveals that the oxygen atoms adopt a tetrahedral conformation around half of the boron atoms and a triangular conformation around the other half. Tetrahedral B-O bond lengths range from 1.450 and 1.500 Å and triangular B-O bond lengths from 1.355 and 1.387 Å, and are in agreement with the interatomic distances observed in other structures [5.8]. The BO_3 triangles and the BO_4 tetrahedra share oxygen atoms so as to produce endless zigzag chains. The sodium atoms form bonds with six oxygen atoms. The Na-O bond lengths are within 2.386 and 2448 Å, which is slightly lower than it is expected for a Na coordination number of six [5.9]. Therefore, we speculate that a borate anhydrous, formed by $NaBO_3$ and $NaBO_4$ shared molecules, schematically presented in Figure 5.3.

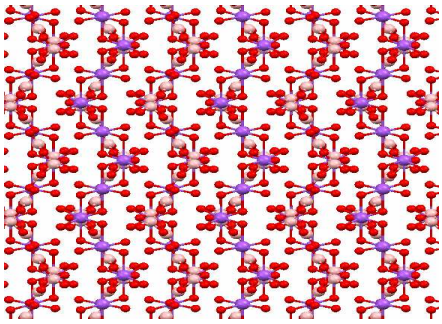

Figure 5.3. View along the *a*-axis of the crystal structure of sodium borate anhydrous, showing the BO_3 triangular and the BO_4 tetrahedral arrangements sharing oxygen atoms and the Na bound network. Na in violet, O in red and B in pink.

At this point, we highlight that adding just 0.25 wt% of CMC or 0.25wt% of SDS to the reactants described in equation 1, leads to the formation of an anhydrous crystalline borate. A pertinent question can now be asked: *what happens to water molecules usually associate to the classic catalytic hydrolysis of $NaBH_4$ by-product?* Unexpectedly, it seems that both CMC polymer and SDS surfactant behave like desiccators of the $NaBH_4$ by-product hydrolysis! Particularly in the latter one, the absence for H_2 solubility effects observed in the remaining solution with 0.25 wt% SDS (see Table 5.1) can now be explained by the capability of SDS to form micelles, enclosing water instead of hydrogen gas, in a way similar to a clathrate.

Based on the above described achievements, it is thought that the results presented are significant findings in terms of:

- *$NaBH_4$ by-product hydrolysis recyclability*. In fact, the inexistence of H_2O in the crystalline borates mention in (*ii*) and (*iii*), marks effectively a cost reduction in the process of recycling these by-products back to $NaBH_4$, comparing the same stage of the process but with the traditional $NaBO_2.2H_2O$. Actually, finding sustainable methods to recycle hydrolysis $NaBH_4$ by-product back to $NaBH_4$, is a very important obstacle to overcome for the adoption of $NaBH_4$ as an hydrogen carrier of choice. Every step is important and our finding is, perhaps, a significant contribution;

- *Gravimetric H_2 storage density*. Beyond doubt, the ability to produce anhydrous sodium borate (or metaborate) may be the key to increase the overall storage density of systems based on sodium borohydride as the storage media [5.1,5.2,5.6]. The gravimetric hydrogen storage density for the experiments reported in this work can be estimated considering the number of water molecules ($2+x$) attached to the by-products found in the crystals structures mentioned above. According to our experimental conditions, we may consider the quantity of water in the ratios $H_2O/NaBH_4$: 4, 2 and 2 mol/mol, respectively, for the crystals structures establish in (*i*), (*ii*) and (*iii*), as the minimum required amount (of water) necessary for reaction (5.1) completion. In this way, the usable specific energy from hydrogen, for the three sets of experiments reported in this work, can be evaluated on a reactant-only basis. The plots in Figure 5.4 show the results for the gravimetric H_2 storage density, for the three reactant systems studied. It can be seen that the gravimetric H_2 density is around 5.7 wt% for the *classic* reactant system and equal to 8.4 wt% and 8.7 wt%, respectively, for reactant systems with 0.25 wt% CMC and 0.25 wt% SDS.

We believe that it is possible to augment the solubility of hydrogen gas in the liquid phase by-product (that remains inside the reactor under pressure) by small additions of

chemical materials, and this may be the key to increase the overall specific H_2 energy of systems based on $NaBH_4$ as hydrogen storage media. As far as the authors are aware, this issue has not been reported in the history of $NaBH_4$ as energy/hydrogen carrier [5.10].

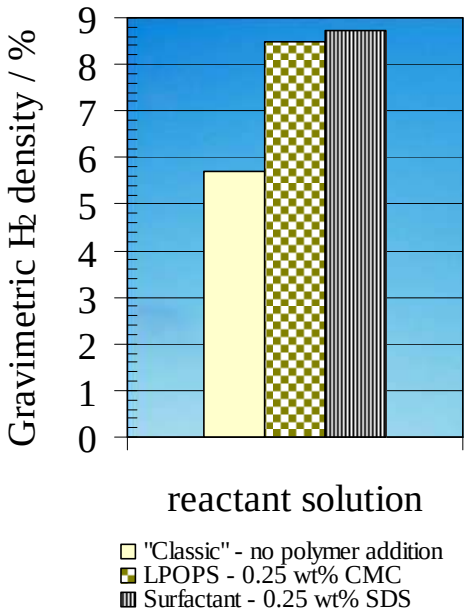

Figure 5.4. Gravimetric H_2 storage density (reactants basis) for the three systems studied in this chapter.

The present results also indicate a remarkable improvement from a previous work by the authors [5.7], in which, using the conventional excess of water method, performed also at moderate pressures (up to 2.6 MPa), a gravimetric hydrogen density of 4.3 % was achieved.

5.5 CONCLUSIONS

The capability of the liquid by-product ($NaBO_2.2H_2O$, metaborate dehydrate) to store hydrogen gas by its dissolution was tested in this dissertation section. With that goal, small amounts of an organic polymer, Carboxyl Methyl Cellulose (CMC), and a surfactant, Sodium Dodecyl Sulphate (SDS), both in the form of fine powder, were added to the reactant solution before its injection in the reactor. The results obtained show that the gas dissolution in the liquid phase and the gravimetric hydrogen density increase with high H_2 pressures, and are additionally enhanced by the polarity change (measured by conductivimetry) of the remaining solution inside the reactor. As a consequence, anhydrous borates were produced in the presence of these additives (CMC or SDS). We

believe that this finding may be the key to increase the overall storage density of systems based on $NaBH_4$ as hydrogen carrier.

To conclude, the results presented in this chapter showed that gravimetric H_2 density of the hydrolysis of sodium tetrahydroborate can be augmented to reach ≈ 9 wt%, by adding small amounts of an organic polymer or surfactant to the stabilized reactant solution. However, the eventual success of this *new* approach will depend upon the development of a simple method of converting borates (BO_2, BO_3, BO_4 groups) into tetrahydroborate.

5.6 REFERENCES

[5.1] L. Schlapbach, A. Züttel, Hydrogen-storage materials for mobile applications, Nature 414 (2001) 353-358.

[5.2] U.B. Demirci, O. Akdim, P. Miele, Ten-year efforts and a no-go recommendation for sodium borohydride for on-board automotive hydrogen storage, Int. J. Hydrogen Energy 34 (2009) 2638-2645.

[5.3] U.S. Department of Energy Hydrogen Program. Available from: http://www.hydrogen.energy.gov/.

[5.4] S.C. Amendola, S.L. Sharp-Goldman, M.S. Janjua, N.C. Spencer, M.T. Kelly, P.J. Petillo, M. Binder, A safe, portable, hydrogen gas generator using aqueous borohydride solution and Ru catalyst, J. Power Sources 85 (2000) 186-189.

[5.5] H.I. Schlesinger, H.C. Brown, A.E. Finholt, J.R. Gilbreath, H.E. Hoeskstra, K. Hyde, Sodium borohydride, its hydrolysis and its use as a reducing agent and in the generation of hydrogen, J. Am. Chem. Soc. 75 (1953) 215-219.

[5.6] E. Marrero-Alfonso, J.R. Gray, T.A. Davis, M.A. Matthews, Minimizing water utilization in hydrolysis of sodium borohydride: the role of sodium metaborate hydrates, Int. J. Hydrogen Energy 32 (2007) 4723-4730.

[5.7] A.M.F.R. Pinto, D.S. Falcão, R.A. Silva, C.M. Rangel, Hydrogen generation and storage from hydrolysis of sodium borohydride in batch reactors, Int. J. Hydrogen Energy 31 (2006) 1341-1347.

[5.8] W.H. Zachariasen, The crystal structure of monoclinic metaboric acid, Acta Cryst. 16 (1963) 385-389.

[5.9] M. Marezio, H.A. Plettinger, W.H. Zachariasen, The bond lengths in the sodium metaborate structure, Acta Cryst. 16 (1963) 594-595.

[5.10] U.B. Demirci, P. Miele, Sodium tetrahydroborate as energy/hydrogen carrier, its history, C. R. Chimie 12 (2009) 943-945.

CHAPTER 6

Nickel based bimetallic catalyst characterization
Results after 200 reutilizations

This chapter focuses in the characterization of the nickel based bimetallic catalyst after 200 reutilizations. Textural properties based on nitrogen adsorption isotherms; surface morphology by scanning electron microscopy (SEM) coupled with EDS spectroscopy and X-ray photoelectron spectroscopy (XPS) analysis, were used to characterized the powder catalyst.

6.1 INTRODUCTION

Most published research papers in the area of this dissertation deal with catalytic material used for hydrolyzing sodium borohydride. It is well known that catalysts suffer from deactivation [6.1]. Nonetheless, very few papers studied the catalyst durability; among these, a good example is the work reported by Kim *et al.* [6.2].

The deterioration of the catalyst activity is a very important issue, since the catalyst is the *key* material for varying the amount of generated molecular hydrogen from $NaBH_4$ hydrolysis reactions. The US DOE set technical targets for durability and operability of catalysts, but the reasoning behind the targets set was not explained in their review [6.3].

It is the aim of this work to analyze the state of '*health*' of the powder nickel based bimetallic catalyst after it was used two hundred times. In fact, the catalyst was used in several different types of kinetic experiments, as described in the previous chapters of this dissertation, and always revealed good activity (by the low values in lag time and high dP/dt slopes in the linear zone).

The fact that the catalyst was used more than 200 times motivated us to carry out a detailed study of the catalyst activity. In truth, the catalyst showed good working efficiency both under higher concentrations of hydride and inhibitor in the *alkali* $NaBH_4$ hydrolysis

with excess of water (even in the experiments with refuelling fresh $NaBH_4$ solution), and with *alkali free* hydrolysis with $2 < H_2O/NaBH_4$, mol/mol < 4. It was also verified that the influence of reactor design (bottom shape) affects the catalyst activity; in particular, the reaction vessel with conical bottom shape promoted an intensification of the catalyst activity, by reducing the lag time of the reaction, in comparison with the flat bottom shape.

6.2 CATALYST CHARACTERIZATION

The Ni-Ru based powdered catalyst after 200 times of reuse was characterized by textural properties based on nitrogen adsorption isotherms; by surface morphology using scanning electron microscopy (SEM) coupled with EDS spectroscopy and by X-ray photoelectron spectroscopy (XPS). A brief description of these instrumental analysis techniques and the results obtained are given in the following sections.

6.2.1 Textural properties

Our concern here is with the internal surface area of the porous Ni-Ru based solid catalyst, and with the nature of the pores giving rise to this area. In most porous solids the external surface is a negligible fraction of the total surface, but if relevant it may readily be estimated by measuring the permeability of gas through a bed of the solid, or by sedimentation. The parameters of interest are then the internal surface area and the pore volume, from which an average pore radius may be obtained, and the pore size distribution. Knowledge of the pore size distribution is obtainable by mercury porosimetry. In this technique, mercury is forced under pressure into the pores, and the greater the pressure, the smaller the pores to which the mercury obtains access. By sensitively measuring the change in volume of the solid plus the mercury with increasing pressure, a picture of the pore size distribution is obtained.

Useful information is also gained by measuring the physical adsorption of gases on porous solids. It is known that the monolayer capacity of a non-porous solid, measured by chemisorption, or by physical adsorption well above the boiling point of the adsorbing gas (usually N_2), can be easily translated into a surface area. However with porous solids, and using temperatures close to the boiling point of the gas, so that multilayer adsorption occurs, several forms of isotherms besides the Langmuir type can be observed. The Type IV is of great interest. This isotherm usually shows a *hysteresis loop*, that is, the isotherm does not follow the same path in the desorption as it does in adsorption. The reason for this

is that evaporation of condensed gas in fine pores does not occur as easily as its condensation; this is because a molecule evaporating from a highly curved meniscus has a higher probability of recondensing than one evaporating from a plane surface. This effect was discussed many years ago by Lord Kelvin who devised the following equation to describe the effect:

$$\ln(P/P_0) = -\frac{2V\gamma}{rRT}\cos\phi\,, \tag{6.1}$$

where V is molar volume of the liquid, γ its surface tension, r the pore radius and ϕ the contact angle (usually taken to be zero); the other symbols have their usual significance. The relative pressure at which condensation will occur in a pore of a given size can thus be determined, and the isotherm then used to obtain a pore size distribution. Hysteresis loops vary greatly in shape, and these too have also been classified in literature [6.4].

The textural characterization of the Ru-Ni based powdered catalyst (after 200 reutilizations), including the determination of surface areas (S_{BET}), was based on the N_2 adsorption isotherms, using a Quantachrome Instruments Nova 4200e apparatus. Prior to the analysis, the sample (0.127 g) was degassed at 160 ºC for 3 h. Nitrogen was used as adsorbate at liquid nitrogen temperature (77 K). Pore size distribution was obtained from the desorption branch of the isotherms using the Barrett, Joyner and Halenda (BJH) method. The micropore volumes and mesopore surface areas were determined by the t-method.

The adsorption and desorption isotherms of the powder Ni-Ru based catalyst 200 times reused are displayed in Figure 6.1. The result shows that the N_2 isotherm shape are not of type IV, at least for $P/P_0<0.986$. Hence the validity of BJH method is discussable for this powder material. The plot on Figure 6.2 illustrates the pore size distribution. As shown, the pore radius peak shifts to a smaller size region, in the range 17-23 Å.

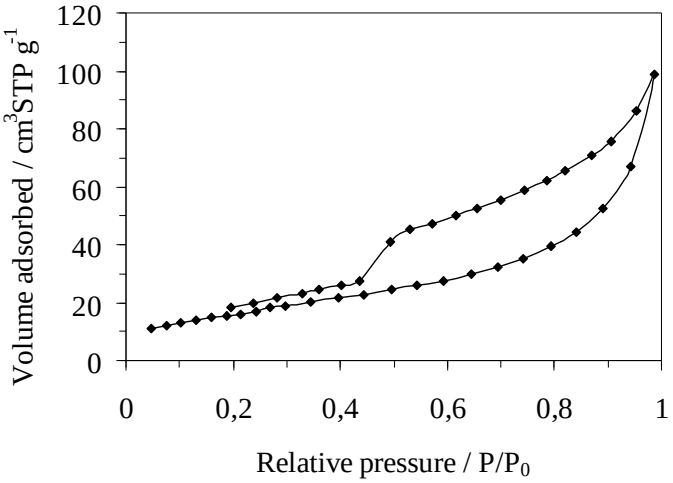

Figure 6.1. Nitrogen isotherms of powder Ni-Ru based catalyst 200 times reused.

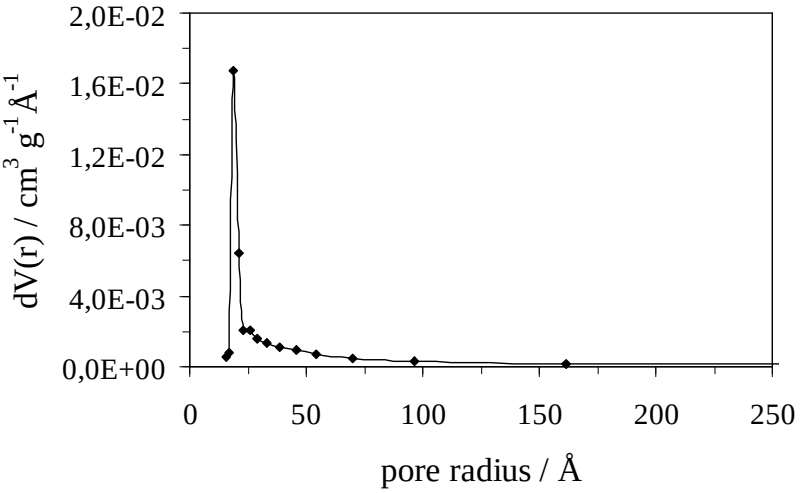

Figure 6.2. Pore size distributions of powder Ni-Ru based catalyst 200 times reused.

Table 6.1 summarizes the textural properties of powder Ni-Ru based catalyst 200 times reused.

Table 6.1 - Textural properties of powder Ni-Ru based catalyst 200 times reused sample.

S_{BET} / m^2g^{-1}	V_μ / cm^3 g^{-1}	S_{ext} / m^2 g^{-1}	V_p / cm^3 g^{-1}
58	0	58	0.15

S_{BET} = BET surface area;
V_μ = micropore volume by t-method;
S_{ext} = (mesopore + macropore) surface areas by t-method;
V_p = total pore volume, for P/P_0=0.986.

It should be noted that the rate of a catalytic reaction should be proportional to the surface area of the catalyst, provided that the transfer of reactants to or of products from the surface is not the slow step. It is therefore normally desirable to get as much surface area as possible into a given volume.

Analysing the data plotted in Fig. 6.2, we may conclude that the *pores* through the particles catalyst sample, assuming *microspheres* of *uniform size*, lies between 4 and 20 nm in diameter. This means that the pore size in our catalyst, after 200 reutilizations, belongs to the group of *mesopores*. Would pores below 2 nm in width, i.e., *micropores* be expectable?

If *micropores* existed, can they be *surface closed* by effects of particle agglomeration?

The values of surface areas, by BET and t methods, reveal 58 m^2/g; surprisingly, this is not a large surface area for a fine powder catalyst [6.4]. In fact $V_\mu = 0$ cm^3/g by t-method.

6.2.2 Morphology

Surface morphological observations were obtained at CEMUP (Centro de Materiais da Universidade do Porto). The Scanning Electron Microscopy (SEM imaging) coupled with EDS (analysis) spectroscopy was performed using a unit FEI Quanta 400 FEG ESEM / EDAX Genesis X4M operating at 15 kV in low vacuum mode (LVSEM for uncoated non conductive sample). The powder sample was prepared by simple dispersion over a double side adhesive carbon tape.

Figure 6.3 shows SEM micrographs of the powder Ni-Ru based catalyst 200 times reused, at magnifications up to 100 000X. SEM images at higher magnification showed distortions due to slight magnetic properties of the catalyst sample.

In the micrographs of Fig.6.3, from (a) to (b), the catalyst sample in the bulk form seems that can be broken-up into smaller particles until reaching a consistency similar to that of a fine dust. Image 6.3(b) show a Ni-Ru based particle that is about 100 μm in vertical length and a background of smaller ones of about 1-25 μm in diameter. Going from Fig.6.3 (b) to (e), the magnetic properties of Ni-Ru based appear to cause some agglomeration of the smaller particles. Therefore, closer examination of the particles surface in Fig.6.3 (c) shows a finer reticulated structure, interconnecting more or less spherical particles.

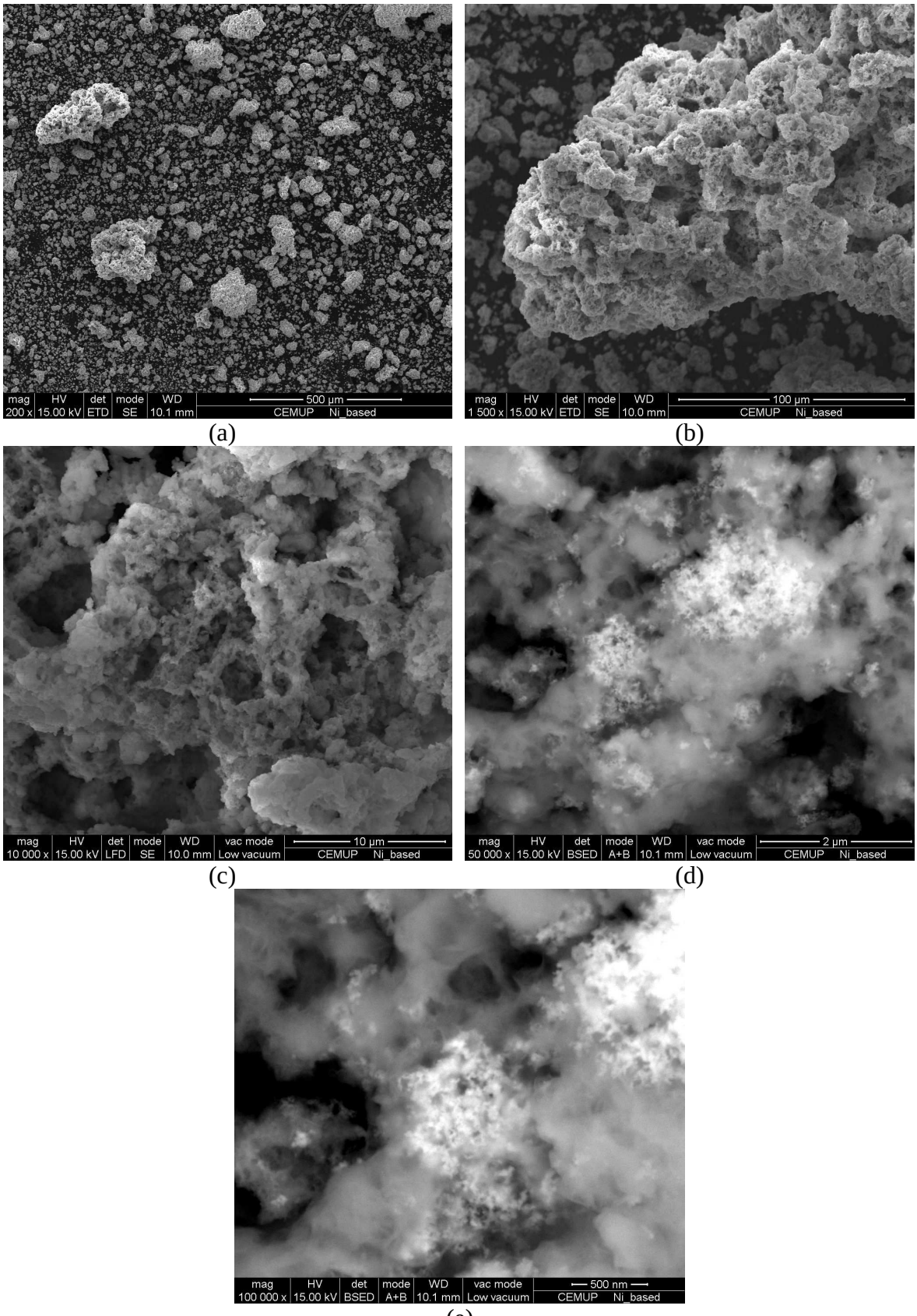

Figure 6.3. SEM micrographs of powder Ni-Ru based catalyst, 200 times reused. Magnifications between 200 and 100 000X, increasing from (a) to (e).

Going from Fig.6.3 (d) to (e), it may be assumed that mesopores (and macropores) exist between these 'microspheres', which form a three-dimensional structure.

EDS spectroscopy was used to analyse the chemical content of Ni-Ru based catalyst sample. Figures 6.4 – 6.6 shows the SEM image coupled with EDS spectrum of Ni-Ru based catalyst 200 times reused, at specific magnifications of 200X, 1 500X and 10 000X, respectively.

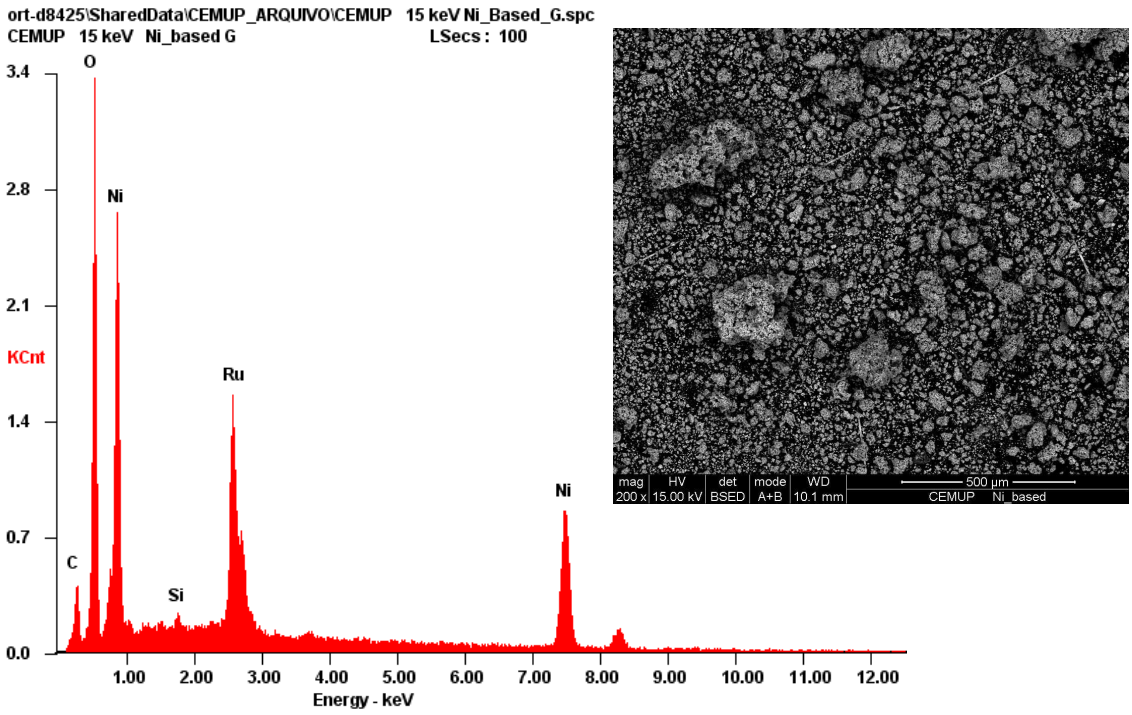

Figure 6.4. SEM image coupled with EDS spectrum of Ni-Ru based catalyst 200 times reused and a magnification of 200X.

The EDS spectra show that nickel (Ni) is the main constituent of the powder Ni-Ru based catalyst 200 times reused. Small portions of silicium (Si) and sodium (Na) were detectable in the catalyst sample at magnification of 1500X (see Fig.6.5).

In Figure 6.6, the amount (weight percentage) of ruthenium (Ru) element depends directly on the magnitude of the surface area selected to EDS analysis. In fact, for particular E2, E3 and E4 areas, the corresponding EDS spectra have shown different quantities of Ru.

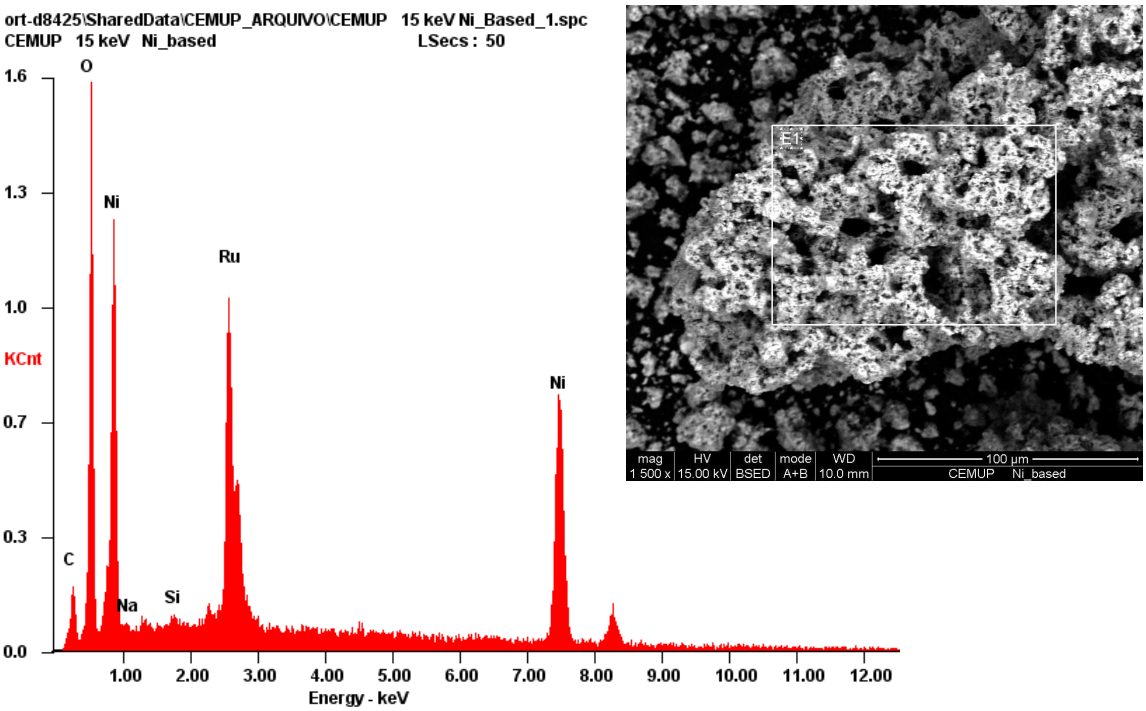

Figure 6.5. SEM image coupled with EDS spectrum of Ni-Ru based catalyst 200 times reused and a magnification of 1500X.

Therefore, the amount of Ru recorded on EDS spectrum is somewhat related with the more *brilliant* or *dense* area visualized on SEM micrographs, and this calls for a non homogeneous distribution of Ru element on the sample. Is this an added characteristic of Ru-Ni based catalyst after 200 times reused?

At this time, we may assume that the continuous reuse of Ni-Ru based catalyst enhance some loss of Ru from the initial metal matrix (Ru-Ni based, 0 times used). Hence, due to the magnetic properties of Ru-Ni based, the *natural* tendency of these *lost* Ru elements is to agglomerate and then form denser areas on the catalyst sample, which becomes richer in Ru element.

6.2.3 XPS analysis

In order to obtain additional information about the surface structure/composition of our 200 times reused catalyst, X-ray Photoelectron Spectra (XPS) analyses were performed at CEMUP (Centro de Materiais da Universidade do Porto) using a VG Scientific ESCALAB 200A spectrometer with PISCES software for data acquisition and analysis.

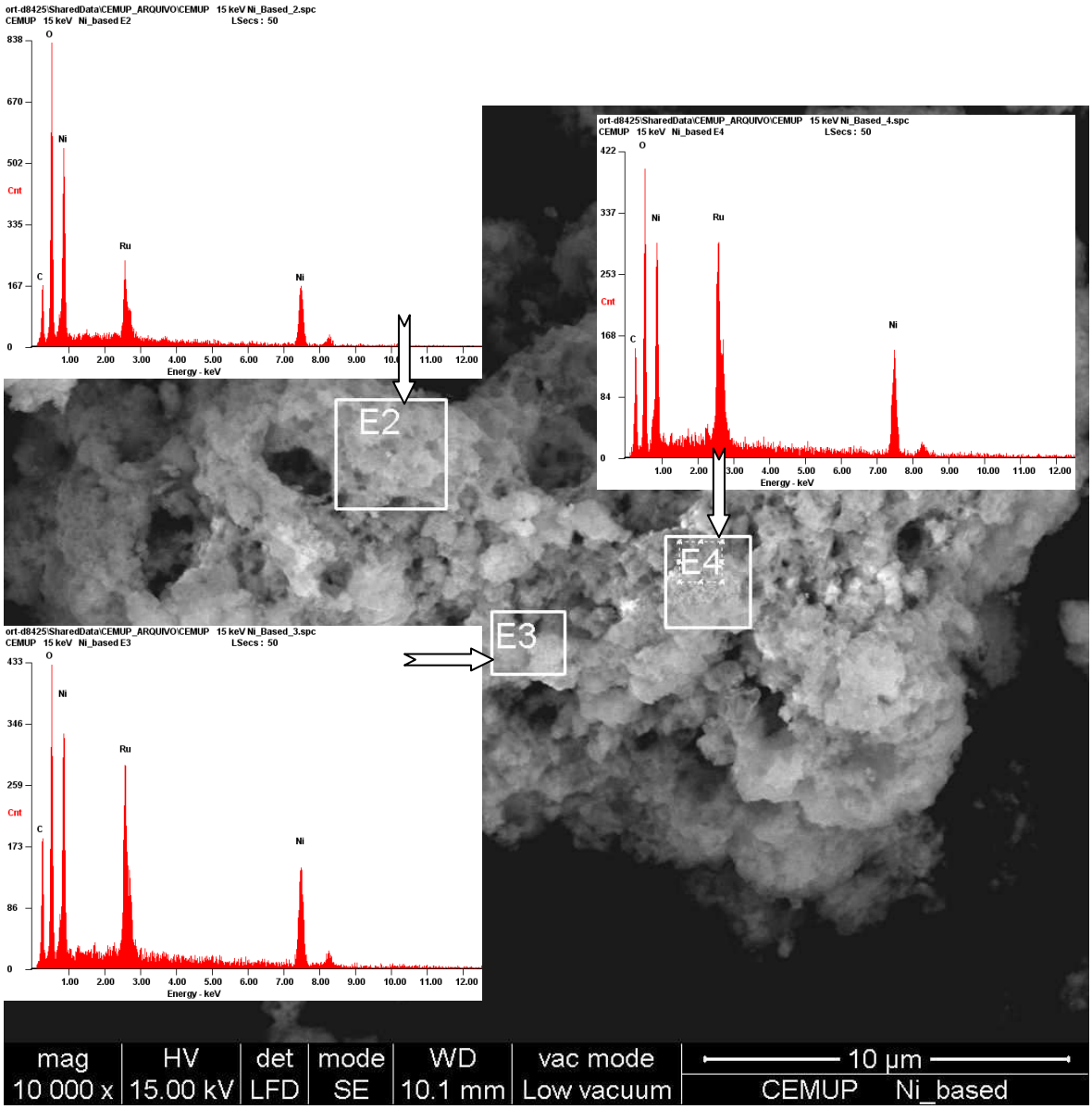

Figure 6.6. SEM image coupled with EDS spectrum, at three different selected areas, of Ni-Ru based catalyst 200 times reused and a magnification of 10 000X.

For the analysis, an achromatic Al (Kalfa) X-ray source operating at 15kV (300 W) was used, and the spectrometer, calibrated with reference to C1s (285 eV), was operated in CAE mode with 20 eV pass energy. Data acquisition was performed with a pressure lower than 1E-6 Pa. Spectra analysis was performed using peak fitting with Gaussian-Lorentzian peak shape and Shirley type background subtraction (or linear taking in account the data).

The powder sample, with a shape of 10 mm diameter pellet (see Fig.6.7), was appropriately fixed on a copper plate before inserting it in the spectrometer for XPS analysis.

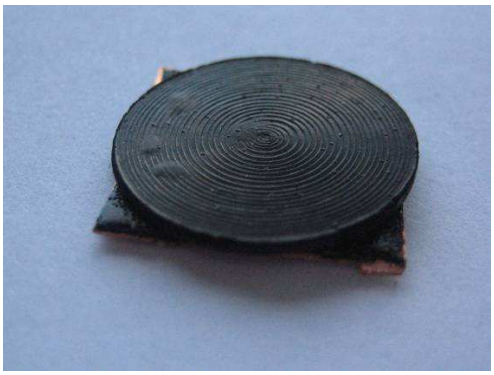

Figure 6.7. Photograph of Ni-Ru based catalyst 200 times reused pellet, with 10 mm in diameter, for use in XPS analysis.

Table 6.2 details the conditions in which XPS analysis was carried out.

Table 6.2 - Specific conditions for XPS analysis of Ni-Ru based catalyst 200 times reused.

Regions	Pass Energy	Step / eV	Dwell Time / ms
Survey	50	1	200
C 1s – Ru 3d	20	0.1	1000
O 1s	20	0.1	1000
Ni 2p	20	0.1	1000

Tilt=0 | Source: Al (Kalfa) X-ray | Eo = 15kV (300W) | Charge Corr = NA | Ref: C 1s=285 eV

Figure 6.8, shows a survey XPS spectrum of the studied sample. A small amount of Na was detected.

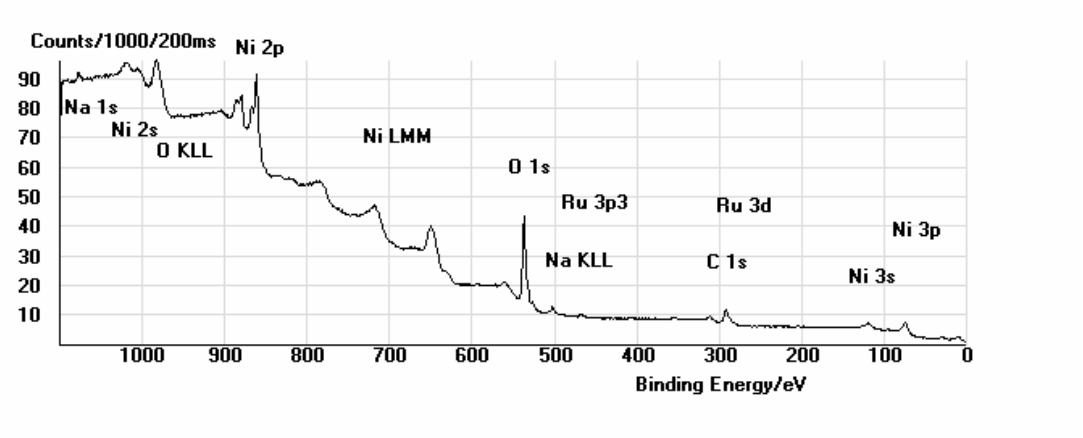

Figure 6.8. A survey XPS spectrum of Ni-Ru based catalyst 200 times reused.

Deconvolution XPS spectra are sequentially presented for C1s – Ru 3d, O1s and Ni 2p (2p1,2p3) in the plots of Figure 6.9. A common behaviour observed on these spectra is the presence of two dominant peaks. For the spectrum analysis, peak fitting with Gaussian-

Lorentzian peak shape and Shirley type background subtraction (or linear taking in account the data) were used. In the particular case of C1s - Ru 3d5 spectrum, the existence of two groups of Ru 3d5 peaks displaced by effects of differential electric charge was assumed.

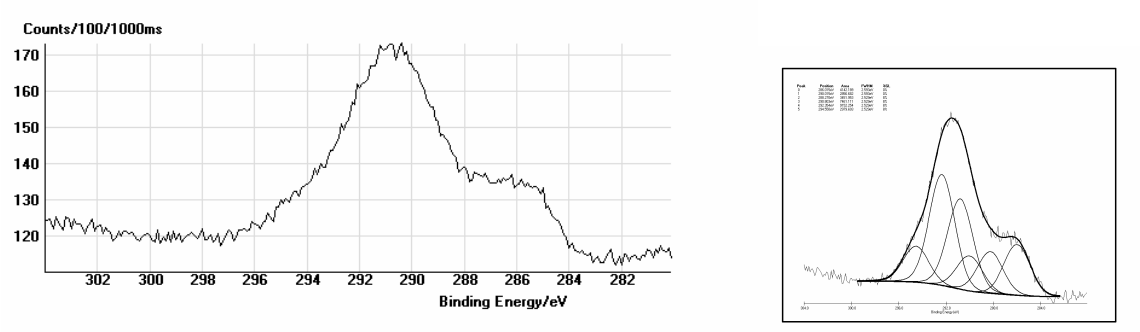

C 1s – Ru 3d

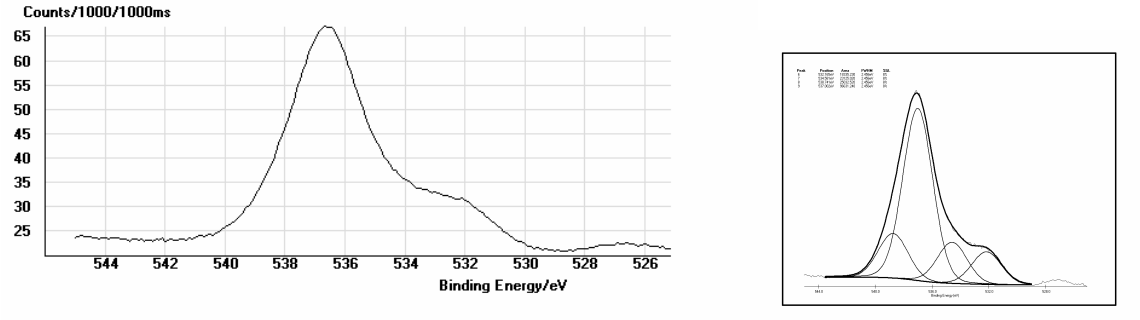

O 1s

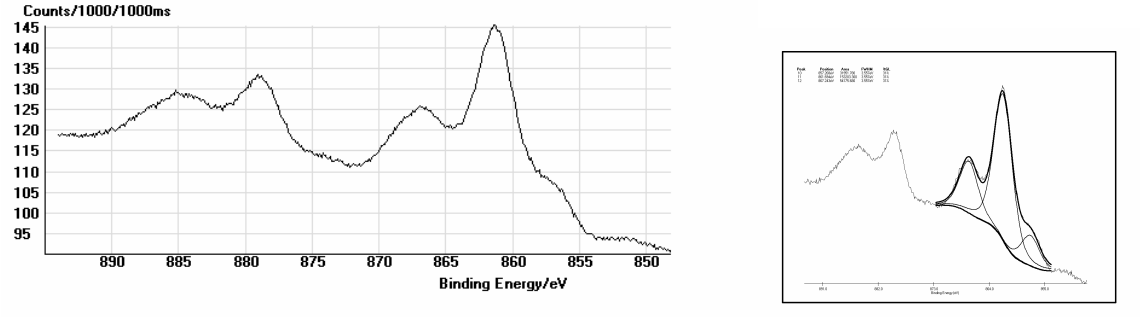

Ni 2p (2p1,2p3)

Figure 6.9. XPS spectra for Ni-Ru based powdered catalyst 200 times reused.

Table 6.3 summarises the XPS analysis results of the Ni-Ru based catalyst 200 times reused.

Table 6.3 - Results of XPS analysis of Ni-Ru based catalyst 200 times reused.

Element	*Peak range*	*Area*	*Sens. Factor*	**At** / %
C 1s	synthesis	13285	1	13.57
O1s	synthesis	187038	2.93	65.20
Ni 2p3	synthesis	283316	14.61	19.81
Ru 3d5	synthesis	10269.3	7.39	1.42

At = total surface area.

The XPS analysis showed that nickel (Ni 2p3) is the main metal surface constituent of our bimetallic powdered catalyst 200 times reused, 13.57 % At. Ruthenium (Ru 3d5) contribution is about 1.42 % At. The XPS data confirmed the increased in Ru concentration (Ru3d5) from 0.74 to 1.42 At %. A slight increase in area (At %) is suggested which is thought to be due to segregation of ruthenium as a result of the extensive use in the catalyzed hydrolysis.

6.3 CATALYST ACTIVITY ANALYSIS AFTER 200 REUTILIZATIONS

This section intends to characterize the catalyst after 200 reutilizations. The state of '*health*' of our Ni-Ru based powdered catalyst (200 times reused) is checked by evaluating its activity, in terms of yield, lag time and dP/dt slopes in the linear zone, at two different stages of reutilization. Two experiments, of the topic of *alkali* hydrolysis of $NaBH_4$, were chosen to illustrate our analysis.

Plots in Figure 6.10 shows the hydrogen generation of 10 mL of a reactant solution with concentration of 10 wt% $NaBH_4$ and 7 wt% NaOH by weight, performed in reactor LR (646 cm^3) with a proportion of Ni-Ru based catalyst/$NaBH_4$: 0.4 g/g (≈ 0.43 g), when the catalyst was 28 times and 200 times reused. No stirring was performed in the solutions inside the reactor. Both reactions were performed at room temperature, without temperature control: the reaction with catalyst reused 28 times was carried out in the summer of 2008 (at 27 ºC) and the reaction with catalyst reused 200 times in the middle of the spring of 2009 (25 ºC).

Table 6.4 shows the values of lag time and *dP/dt* obtained from the curves presented in Figure 6.10.

The results in Table 6.4 (and in Figure 6.10) revealed that our nickel-based bimetallic catalyst reused 200 times is '*healthy*', although some deterioration in terms of H_2 yield and rate is evident (note that the two reactions plotted in Figure 6.10 employ a catalyst separated by 172 uses).

Table 6.4 - Results for yield, lag time and dP/dt slope in hydrogen generation of 10 mL of 10wt% $NaBH_4$ and 7wt% NaOH solution, at two different stages of Ni-Ru based catalyst reutilization (for 28 and 200 times reused), in batch reactor LR (646 cm^3).

Ni-Ru based catalyst	*yield / %*	*lag time / s*	dP/dt slope* / bar/s
28 times reused	100	20	2.48E-02
200 times reused	91	21	7.59E-02

* calculated in the linear zone.

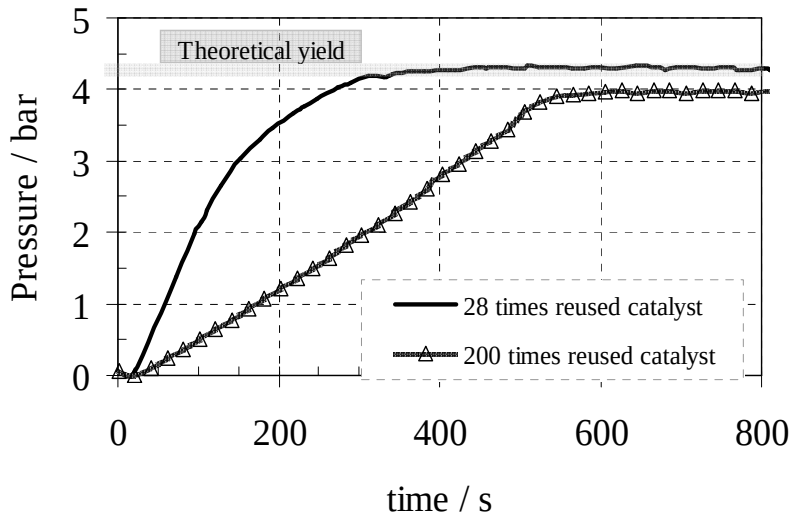

Figure 6.10. Hydrogen generation plots with a $NaBH_4$ concentration of 10%, an inhibitor concentration of 7%, for two different stages of catalyst reutilization (28 times reused and 200 times reused). The reactions, for 10 cm^3 of reactant solution, were performed in LR batch reactor (646 cm^3) with a proportion of Ni-Ru based catalyst/$NaBH_4$: 0.4 g/g, at room temperature of ≈ 25 ºC.

In terms of yield, the results found in Table 6.4 shows deterioration by a factor of 1.1, $\eta_{28X} = 1.1\eta_{200X}$, this means that the average loss in yield per each utilization of the catalyst is approximately 0.6 %. In terms of hydrogen generation rate, a larger factor was found in the universe of 172 reutilizations: 3.3, i.e., $(dP/dt)_{28X} = 3.3(dP/dt)_{200X}$ in the linear zone; hence a loss of 1.9% per reutilization can be estimated for the rate value. With respect to lag time, identical values were found in the two experiments, indicating that the catalyst can be reused several times without affecting lag time.

6.4 CONCLUSIONS

The study of catalyst durability on catalyzed hydrolysis of sodium borohydride is essential from an application point of view. Few works on this topic are available in the literature. In the present chapter, an effort was made to characterize the powder nickel-based bimetallic

catalyst, used in two different schemes of $NaBH_4$ hydrolyzing (*alkali* hydrolysis and *alkali free* hydrolysis) and after 200 reutilizations.

The textural characterization of the Ru-Ni based powdered catalyst (200 reused) showed an N_2 isotherm shape different from type IV, at least for $P/P_0<0.986$, evaluated by BJH method. The pore size distribution, obtained from the desorption branch of the isotherm, gave pore radius peak shifts in the range 17-23 Å, showing an abundant presence of *mesopores* in the catalyst. This corroborate with the values found for surface areas by BET and t methods of 58 m^2/g. The t-method also revealed the absence of micropores volume in the 200 times reused powder catalyst.

Surface morphology analysis by using scanning electron microscopy (SEM) coupled with EDS spectroscopy revealed that nickel is the main constituent of the powder Ni-Ru based catalyst 200 times reused. The XPS study showed that nickel (Ni 2p3) is the main metal surface element (13.57 % At.) and ruthenium (Ru 3d5) contributed with 1.4 % At.

The catalyst activity was checked by confronting the values of *yield*, *lag time* and dP/dt slopes (in the linear zone, of a graphical representation of reactor inside pressure as function of time). In two similar experiments for hydrogen generation by *alkali* hydrolysis of $NaBH_4$, but performed at two different stages of catalyst reutilization (which differ from each other in 172 times), the results revealed some deterioration of the catalyst activity (the dP/dt slopes are lower, as expected, after such a long time utilization).

Finally, we may conclude that the powder Ni-Ru based catalyst, after 200 applications for hydrolyzing $NaBH_4$, looses approximately 0.6 % in yield and 1.9% in rate, per reutilization, but still preserves the lag time required to observe an increase in H_2 pressure. For this reason, since no great major deterioration was found in the catalyst activity after it was used 200 times - in truth, it still works at very reasonable H_2 generation rates - we can conclude that its *durability* is rather long. A possible explanation for this active catalyst, comparing with similar work done by Pinto *el al.* [6.5], is the presence of 1.4 wt% of ruthenium, a noble Group VIII metal.

6.5 REFERENCES

[6.1] J.H. Wee, A comparison of sodium borohydride as a fuel for proton exchange membrane fuel cells and for direct borohydride fuel cells , J. Power Sources 155 (2006) 329-339.

[6.2] J.H. Kim, K.T. Kim, Y.M. Kang, H.S. Kim, M.S. Song, J.Y. Lee, Study on degradation of filamentary Ni catalyst on hydrolysis of sodium borohydride , J. Alloys Comp. 379 (2004) 222-227.

[6.3] U.S. Department of Energy Hydrogen Program. Available from: http://www.hydrogen.energy.gov/.

[6.4] G.C. Bond, "Heterogeneous catalysis: principles and applications", Oxford Chemistry Series, 1974.

[6.5] A.M.F.R. Pinto, D.S. Falcão, R.A. Silva, C.M. Rangel, Hydrogen generation and storage from hydrolysis of sodium borohydride in batch reactors, Int. J. Hydrogen Energy 31 (2006) 1341-1347.

CHAPTER 7

Conclusion

This chapter is devoted to conclusions and suggestions for future work.
Conclusions drawn from the results indicate that the reused ruthenium nickel based catalyst is capable of catalyzing the sodium borohydride solutions at a sufficient rates, in the two schemes presented in this dissertation for comparison – alkali hydrolysis and alkali free hydrolysis of sodium borohydride for hydrogen generation under pressure.

7.1 CONCLUSIONS

This section provides a summary of the primary research results. The sequence of appearance is the one of the body of the manuscript.

Experimental techniques and apparatus

Description of the materials used in all the experimental work, including the nickel based bimetallic catalyst, is given.

The plan for studied the catalytic hydrolysis of sodium borohydride under pressure, in three batch reactors, with different bottom geometries, is available.

To study the influence of reactor bottom shape on the hydrogen generation rates - this constitutes one of the *originalities* of the present dissertation, two different bottom geometries were designed – one flat and the other conical. The latter has the purpose of enabling non-dispersible effects during the contact of the catalyst with the reactant solution.

Alkali hydrolysis, for sodium borohydride kinetic experiments

An extensive experimental work was carried out with the objective of studying various effects in hydrogen generation rate, yield and lag time, by catalytic *alkali* hydrolysis of sodium borohydride. It was concluded that:

- increasing the temperature of the reaction medium, increases the rate of H_2 generation;
- the reaction rate increases with increasing the hydride concentration up to 20 wt% of $NaBH_4$. Above this value, a slight decrease on both H_2 and yield was found;
- the reaction rate is greatly enhanced by the increase of the NaOH concentration, ensuring good efficiency of hydrogen generation;
- the reactor bottom shape affects the course of hydrogen generation. It was found that the conical bottom geometry leads to an increase on reaction rate, in the absence of H_2 lag time;
- the Ni-Ru based catalyst has a good performance in refueling experiments. In fact, it was found that the catalyst tends to perform better, with a higher H_2 rate, after the first loading of reactant (the amount of catalyst remains the same from the first to the last loading);
- a vigorous stirring of the solution inside the batch reactor, during the experiments with successive fuel loadings, reveals minor reaction induction time and a slight higher yield in hydrogen generation. This indicates possible mass transfer limitations during the course of reaction between the fuel and the active sites of the catalyst.

The x-ray diffractions analyses reveal a sodium metaborate dehydrated, $NaBO_2.2H_2O$, as the main by-product.

Alkali free hydrolysis, for sodium borohydride kinetic experiments

Chemical hydrides have the potential to meet certain H_2 storage targets only if the water consumption is minimized. The main purpose of the *alkali free* hydrolysis of $NaBH_4$ experiments reported in this dissertation was to produce pure hydrogen gas with very high gravimetric and volumetric densities.

The *alkali free* hydrolysis under pressure, when the operating pressure is > 1 MPa, for a system with $H_2O/NaBH_4$: 4 mol/mol and Ni-Ru based/$NaBH_4$: 0.4 g/g, performed in a batch reactor with conical bottom shape (229 cm^3), produced H_2 almost at 100% conversion of $NaBH_4$, and hydrogen was delivered at a fast rate without significant lag time. In terms of gravimetric hydrogen density a value of 6.3% was found (this value does not take into account the *hardware* of the system).

lPOPS hydrolysis, for sodium borohydride kinetic experiments

The capability of the liquid by-product ($NaBO_2.2H_2O$, metaborate dehydrate) to store hydrogen gas by its dissolution was tested in this dissertation section. With that goal, small amounts of an organic polymer, Carboxyl Methyl Cellulose (CMC), and a surfactant,

Sodium Dodecyl Sulphate (SDS), both in the form of fine powder, were added to the reactant solution before its injection in the reactor. The results obtained show that the gas dissolution in the liquid phase and the gravimetric hydrogen density increase with high H_2 pressures, and are additionally enhanced by the polarity change (measured by conductivimetry) of the remaining solution inside the reactor. As a consequence, anhydrous borates were produced in the presence of these additives (CMC or SDS). We believe that this finding may be the key to increase the overall storage density of systems based on $NaBH_4$ as hydrogen carrier. However, the eventual success of this *new* approach will depend upon the development of a simple method of converting borates (BO_2, BO_3, BO_4 groups) into tetrahydroborate.

Nickel based bimetallic catalyst characterization after 200 times reuse

Catalyst durability on catalyzed hydrolysis of sodium borohydride is essential from an application point of view.

The textural characterization of the Ru-Ni based powdered catalyst (200 reused) showed an N_2 isotherm shape different from type IV, at least for $P/P_0<0.986$, evaluated by BJH method. The pore size distribution, obtained from the desorption branch of the isotherm, gave pore radius peak shifts in the range 17-23 Å, showing an abundant presence of *mesopores* in the catalyst. This corroborates with the values found for surface areas by BET and t methods of 58 m^2/g. The t-method also revealed the absence of micropores volume in the 200 times reused powder catalyst.

Surface morphology analysis by using scanning electron microscopy (SEM) coupled with EDS spectroscopy revealed that nickel is the main constituent of the powder Ru-Ni based catalyst 200 times reused. The XPS study showed that nickel (Ni 2p3) is the main metal surface element (13.57 % At.) and ruthenium (Ru 3d5) contributed with 1.4 % At.

The catalyst activity was checked by confronting the values of *yield*, *lag time* and dP/dt slopes (in the linear zone, of a graphical representation of reactor inside pressure as function of time). In two similar experiments for hydrogen generation by *alkali* hydrolysis of $NaBH_4$, but performed at two different stages of catalyst reutilization (which differ from each other in 172 times), the results revealed some deterioration of the catalyst activity (the dP/dt slopes are lower, as expected, after such a long time utilization).

Finally, we may conclude that the powder Ni-Ru based catalyst, after 200 applications for hydrolyzing $NaBH_4$, looses approximately 0.6 % in yield and 1.9% in rate, per reutilization, but still preserves the lag time required to observe an increase in H_2 pressure.

For this reason, since no great major deterioration was found in the catalyst activity after it was used 200 times - in truth, it still works at very reasonable H_2 generation rates - we can conclude that its *durability* is rather long. A possible explanation for this activity of the catalyst is the presence of 1.4 wt% of ruthenium, a noble Group VIII metal.

7.2 SUGGESTIONS FOR FUTURE WORK

The following is a list of the objectives that would, perhaps, be most significant as further development of the present research:

I – Development of a reaction model that reflects the reaction rate as a function of concentration, pressure, and temperature, model which is currently not available in the literature. In fact, a model capable of predicting the hydrolysis rate for hydrolyzing systems under increasing pressure, would be worthwhile principally for systems similar to that developed in this dissertation;

II - Rate data is needed for $NaBH_4$ concentrations greater than 30 wt%. Systems intended to exceed the DOE 2010/2015 objective will require information about how solutions behave at high $NaBH_4$ concentrations. Additional information is also needed at low temperatures, less than 20 ºC, to address start-up issues associated with hydrogen generators or fuel cells operating in cold environments;

III – Data on solubility of H_2 in aqueous borate systems is needed for storage molecular hydrogen in liquid phase. Working at high H_2 pressures, where the hydrogen generated is allowed to build up within the closed system, facilitate dissolution of hydrogen by solubility effects. Hence, it is possible envisage a system that generates and simultaneously stores molecular hydrogen in the reminiscent liquid phase inside the reactor. Indeed information about the amount of hydrogen dissolved in the solution with several concentrations of hydride and of inhibitor, which can be estimated trough Henry's Law for the range of pressure and temperatures of operation, is necessary to carry out.

IV – Knowing materials (chemicals) which enhance the solubility of hydrogen gas in liquid phase, under moderate pressures, is of great value for hydrogen storage in liquid phase.